The Influence of Lake Surface Temperature on Atmospheric Circulations in the Great Lakes Region

by

David M. Wright

A dissertation submitted in partial fulfillment
of the requirements for the degree of
Doctor of Philosophy
(Atmospheric, Oceanic, and Space Sciences)
in the University of Michigan
2016

Doctoral Committee:

Associate Professor Derek J. Posselt, Chair
Associate Professor Valeriy Y. Ivanov
Assistant Professor Gretchen Keppel-Aleks
Greg E. Mann, National Weather Service
Associate Professor Allison L. Steiner

For Erin, Oliver, Mom, and Dad.

ACKNOWLEDGMENTS

First, I would like to thank Dr. Derek Posselt for his guidance through this entire process. The knowledge and eternal optimism you have provided has been the key in getting me to this point. I would also like to thank the rest of my committee, Valeriy Ivanov, Gretchen Keppel-Aleks, Greg Mann, and Allison Steiner. Your knowledge, dedication, and patience during the completion of this thesis cannot be overstated.

I would also like to thank the other members of the research lab and department who have helped me in a variety of ways. Greg, Sam, Fei, Juan, Annareli, Stacey, and Jared, without our discussions about anything and everything ("Are thunderstorms like chocolate chip cookies?"), I would have never been able to fully understand my research as I do now.

Most importantly, I would like to thank my family. Mom and Dad, you have taught me the value of education and given me the foundation needed to create this dissertation. To my wife, Erin, and son, Oliver, who have helped me emotionally and motivated me to attempt and complete this endeavor, I thank you. I could not have done this without you. Finally, to my cat/ghostwriter Rocky, please stop chewing on this page.

PREFACE

This thesis is a collection of work that has or will be submitted to appear in other scholarly journals. Chapter 2 has been published in *Monthly Weather Review* (Wright et al. 2013) and is used here with permission from the American Meteorological Society. Chapters 3 and 4 are being prepared for submission to peer-reviewed journals when this thesis is to be submitted. Chapter 1 is loosely based on an article published in *Physics Today* (Wright 2015).

TABLE OF CONTENTS

LIST OF FIGURES

LIST OF TABLES

LIST OF APPENDICES

ABSTRACT

The Influence of Lake Surface Temperature on Atmospheric Circulations in the Great Lakes Region

by

David Wright

Chair: Dr. Derek J. Posselt

Recently, media coverage of extreme weather events has come with the question "Was this storm caused by climate change?" The scientific community has started to develop statistical measures to try to answer this question, but these studies do not gain insight into the physical causes leading to the storm. This thesis will directly look at some of the physical processes within weather systems in the Laurentian Great Lakes region that could be altered in a future climate through a series of convective allowing simulations using the Weather Research and Forecasting Model (WRF).

In the Laurentian Great Lakes region, located at the border of Canada and the United States, the existence of the lakes and the lake surface temperature play a key role in the weather and climate of the region. While it is projected that lake temperatures will increase in a future climate, it is still relatively unknown what this change could mean to atmospheric circulations in the region. The case studies presented look at the direct role

the lake surface temperature has on these circulations during the cold and warm seasons to understand the sensitivity of these circulations to future climate conditions.

For a lake-effect snowfall simulation, it is shown that the lake temperature influences the extent and intensity of the snowfall downwind of the lake, while interactions with the topography downwind of the lakes still have a critical role. Warm season simulations showed little influence from the lake temperature on precipitation amounts. However, various degrees of change were seen in atmospheric circulations, from little to no change in the convective initiation along Lake Michigan due to the passing of a potential vorticity feature, to larger changes over Lake Superior to the structure of the barrier jet and a mesoscale convective system. Collectively, these simulations show the importance of resolving the lakes in climate simulations and feedbacks that may not be resolved at lower horizontal resolutions, especially in winter. These simulations also give a baseline for future work testing the sensitivity of storm systems over the region to other components.

CHAPTER 1. INTRODUCTION

1.1 Motivation

Extreme weather events can create substantial damage and fatalities. For example, Hurricane Sandy created nearly $50 billion of damage along the eastern coast of the United States from October 22-29, 2012 (Blake et al. 2013). In 2014, during a lake-effect snow event, 7 feet of snow fell on areas of Buffalo, NY leading to the deaths of 13 people (Vogel et al. 2014). After both storms, the question of "Was this storm caused by climate change?" was asked or hinted at by media outlets (e.g., Kershner 2012, Zremski 2014). This question points to both a belief that these extreme weather events are caused by climate change and that there is a physical connection between climate and weather.

To start, it is important to define the difference between weather and climate. Weather, as defined in the American Meteorological Society Glossary (2016), is "the short-term variations in atmospheric conditions", typically on the order of minutes to several days. Climate, on the other hand, is "the slowly changing aspects of the atmosphere", which are statistically represented over months to years (American Meteorological Society 2016). In other words, weather events over a period of time create the climate of a region. But can climate and changes taking place on a climate timescale influence the weather, and if so, how? These questions are the basis of attempting to attribute extreme weather events to climate change.

The ability to attribute weather events to changes in climate has gained considerable attention from the scientific community. The National Academies of Sciences,

Engineering, and Medicine (2016) created an overview of the current state of the science and proposed a methodology on how to attribute events to climate forcing. The authors discuss the use of causal theory to begin to attribute extreme events to climate change, in particular necessary and sufficient causality. Hannart et al. (2016; hereinafter referred to as H2016) expanded on the subject of causal theory and created a framework for the atmospheric science community to create a series of standard definitions. First, the authors argue that a standard definition of "cause" is needed to keep a consistent definition across case studies. They cite Trenberth (2012), who argued that since single weather events have multiple factors then an event cannot be caused by simply a single forcing (e.g. carbon dioxide), which H2016 believed to be misleading.

H2016 defined the probabilities of necessary causality and sufficient causality to define the probability of a single event being caused by a particular forcing. Necessary causality is defined as the probability of an event to not have happened given a forcing factor was missing. This means the event requires the forcing to be present, but other factors might also be required. Sufficient causality is defined as a particular forcing always triggers the event but the event can also occur due to other forcing mechanisms. H2016 then apply these definitions to Trenberth's (2012) argument to state that while carbon dioxide might not be a necessary condition for causality, it could be a sufficient condition.

A common practice to attempt to connect weather events to climate change is through sea surface temperatures (SST) (Pall et al. 2011, Christdis et al. 2013**,** Stott et al. 2015). Pall et al. (2011) used a series of climate simulations to explore how greenhouse gas emissions changed the probability of flooding to occur in England during the fall of 2000.

In it, they compared simulations created to represent the real world with altered simulations that removed the greenhouse gas emissions and lowered SST. They found that in most cases, the risk of flooding in England increased with the inclusion of anthropogenic warming. Christdis et al. (2013) attempted a similar study, using both observed and reduced SST values to look at the influence of warmer SST on several high impact events around the world in 2010. The authors found that their reduced SST simulations increased the probability for winters to be colder than the 2009-10 winter in England and for the likelihood of heat waves in Moscow to be reduced.

A theme through these studies, as well as in H2016, is that the attribution of these events to a climate forcing is purely a statistical relationship. Little is mentioned regarding physical processes on a weather timescale that are altered from changes in the climate system. Some work has been done to connect physical processes with changes in the climate (e.g. Francis and Vavrus 2015), but more research is needed to explore the sensitivity of atmospheric circulations on weather timescales to different components of the system. The authors of the National Academies of Sciences, Engineering, and Medicine (2016) specifically call out the need to for a better understanding of the physical processes, both thermodynamic and dynamic, needed for extreme weather events and how these events are influenced by changes in these physical processes. For example, how changes in SST specifically create extreme events through increases in latent and sensible heat flux off the water surface, changes in local thermodynamic gradients, and/or changes in large-scale flow and dynamics.

The goal of this dissertation is to begin to explore the changes in atmospheric circulations generated from changes in lake surface temperature in the Great Lakes

region. This will begin to hint at how storm systems generated or influenced by the Great Lakes may be altered in a changing climate.

1.2 Climate of the Great Lakes

The Laurentian Great Lakes, located in North American on the border between the United States and Canada, are a series of fresh water lakes. These lakes contain approximately 18% of the world's liquid fresh water, and are the largest system of fresh water lakes in the world. With over 30 million people living in the basin and a portion of the region's economy relying on the industrial and recreational use of the lakes, it is important to fully understand the role the lakes have in the hydrology of the region (US Environmental Protection Agency and Government of Canada 1995). This includes the distribution and direct creation, enhancement, or suppression of precipitation around the region due to the presence of the lakes.

The influence of the Great Lakes on the region's weather and climate has been studied in the past. For example, Scott and Huff (1996) explored the role of the lakes on the climate of the region, comparing surface observations from stations within 80 km of the lake (lake influenced) and 300 km away from the lake (background). It was found that the lakes have a stronger influence on regional precipitation downwind of the lakes during the winter than the summer. They also concluded that the lakes had a strong influence in warming the mean minimum temperature in the winter while cooling the mean maximum temperature in the summer.

1.2.1 Global and Regional Modeling

To test the existence of the lakes on region's weather and climate, studies have run experiments either including the lakes in global simulations that did not include them or

remove them from regional climate model (Sousounis and Fritsch 1994, Lofgren 1997). Lofgren (1997) looked at the influence of the lakes on the region's climate and hydrology through a general circulation model run without lakes, with lakes, and with swamps instead of lakes. The swamps represented an unlimited amount of soil moisture for evaporation while still interacting with the environment as a land surface. These results showed reduced evaporation over the lakes when present during the spring and early summer, while enhanced in the fall and winter. This change in evaporation, coupled with an increase in fall and winter precipitation with the lakes, resulted in a net gain (precipitation minus evaporation) of .049 mm per day with the inclusion of the lakes. The difference between the swamp and no lakes showed little influence on the temperature but an increase in precipitation throughout the year. Bryan et al. (2015) showed through a series of climate simulations that the lakes provide up to 30% of the moisture over the region during the summer and 12% during the winter through evaporation off of the lakes. Sousounis and Fritsch (1994) used a regional model to simulate the lake aggregate influence on a winter storm passing through the Great Lakes region by removing the lakes and replacing them with land. The authors showed that the lakes could split high-pressure systems around the lakes as they move into the region while also deepening and accelerating low-pressure systems moving into the region. Angel and Isard (1997) also found that cyclones accelerated and intensified while over the lakes during the ice-free fall and early winter, when the air above the lake is relatively unstable, as well as during the late spring and early summer when the air above the lakes is relatively stable. This acceleration and intensification was reduced once ice formed on the lake in the late winter.

Grover and Sousounis (2002) found that from 1935-95, there was an increase of about 15% in fall precipitation amounts across the Great Lakes basin. Most of this increase in precipitation was found to be associated with increased warm, stationary, and occluded fronts passing over the region that used to be dominated by cold and low-pressure systems. The authors concluded that there was a change in large-scale flow over the region, but the physical reasons for this happening were unknown. The authors continued this work looking at the projection of future weather around the region (Sousounis and Grover 2002**)**, using Canadian and Hadley Climate models to evaluate the synoptic scale conditions for a future climate scenario over the region. They found that by the end of the century there is an increase of about 4 days of precipitation per year, with a greater number of heavy events (>25 mm per day) resulting in an overall increase in precipitation over the region for the Canadian General Circulation Model. The Hadley Climate Model had fewer precipitation days, but an increase in number of moderate to heavy rainfall events (>12.5 mm per day) resulting in an overall increase in accumulated precipitation. Both models also showed fewer cold air outbreaks during the winter and more heat waves in the summer.

1.2.2 Mesoscale Resolving Simulations and Local Influences

The previously described studies typically utilized global or regional models that have poor horizontal resolution, meaning the lakes are only represented by a few grid points, if at all. Gula and Peltier (2012) used the Weather Research and Forecasting Model (WRF) to dynamically downscale global climate model projections onto a 10km horizontal grid to explore the direct influence of the lakes in a future environment. It was found that the 10km resolution did show an improvement in recreating the instrumental

period (1979-2001) over the global models. They also found large differences in the January-February timeframe between 2050-60 and 1979-2001, with increased 2m temperature, fewer ice covered days over the lake, and irregular changes to snowfall, precipitation, and heat fluxes (sensible and latent) over the region.

On a local scale, several studies have looked at the changes in over-lake characteristics. Austin and Colman (2007) found that the water temperature over Lake Superior has increased more rapidly than air temperature over the surrounding land region, increasing on the order of 2.5 degrees Celsius from 1979-2006. They attribute this warming to the change in length of the ice cover season on the lake, which changes the start date of stratification in the lake. When the stratification occurs sooner in the season, the surface water is able to interact with sunlight for a longer period of time, without overturning, to increase the temperature. A portion of this warming is also due to warmer air temperatures. The warming of the lake has shown an increase in wind speed over Lake Superior by 12% (.2 m/s) since 1985 (Desai et al. 2009).

Trumpickas et al. (2009) used a series of empirical relationships between surface water temperature and air temperature to predict surface water temperature changes by the year 2100 in the Great Lakes during the water stratification period of the year (spring through fall). Using future air temperature projections, the authors found temperature increases of 4.6 and 6.7 degrees Celsius for Lake Superior, depending on the future climate scenario, and increases of 2.4 and 3.3 degrees Celsius for Lake Erie. Lakes Huron and Ontario were projected to be slightly warmer than Lake Erie.

1.3 Outline of Thesis

The previous studies help to highlight the current state of knowledge from around the Great Lakes in terms of climate change and influence on the region. One area that is still poorly understood is the direct role the lakes have on atmospheric circulation and precipitation processes, and as an extension how variations in the temperature of the lakes can influence these circulations. This thesis examines interactions between the atmosphere and lake surface temperature to inform the sensitivity of atmospheric circulations associated with precipitation in the Great Lakes region to changes in lake surface temperature. From this, the physical feedbacks between a warming lake surface in a changing climate and weather circulations can begin to be determined.

This will be accomplished through three studies looking at different atmospheric circulation types. Chapter 2 will examine the role lake ice and temperature has in the direct creation of lake-effect snowfall. Chapter 3 will explore the combined roles of upper level vorticity advection and changes in lake temperature and lake surface in the creation of a thunderstorm in the springtime. Chapter 4 will examine how the lake temperature and the stable boundary layer, located above the lake surface in the summer, influence the passing of a mesoscale convective system over Lake Superior. Conclusions drawn from the three case studies will be presented in Chapter 5.

CHAPTER 2. SENSITIVITY OF LAKE-EFFECT SNOWFALL TO LAKE ICE COVER AND TEMPERATURE IN THE GREAT LAKES REGION

2.1 Introduction

Lake-effect snow (LES) is a common meteorological phenomenon downwind of the Great Lakes during late fall and winter, and is caused by the horizontal collocation of cold polar air with a relatively warm lake surface. The associated temperature contrasts between lake, land, and air lead to steep atmospheric temperature lapse rates and significant thermal energy and water vapor fluxes from the lake surface. Together, large surface-to-air temperature gradients and moisture fluxes destabilize the atmospheric boundary layer and, in some cases, initiate shallow convection. Advection of the unstable air mass downstream over and downwind of the lee shore, and the consequent friction-induced convergence over land, can enhance the lake-induced convection, or produce precipitation solely due to the increased mechanical shear. On average Great Lakes LES contributes between 10 and 50% of the total regional winter precipitation (Scott and Huff 1996).

In observational studies, LES events have been classified into four morphological types: widespread coverage, shoreline bands, mid-lake bands, and mesoscale vortices (Kelly 1986; Schoenberger 1986; Kristovich et al. 1999, 2003; Laird 1999; Liu et al. 2004). Widespread coverage occurs over a large area, and is also commonly associated with boundary layer rolls, cellular convection, or a combination of the two. Shoreline bands occur when winds travel a short distance over the lake, and produce small linear patterns of snowfall perpendicular to the lakeshore with band-to-band spacing on the

order of approximately 2-5 km. Observations and numerical simulations of these bands exhibit strong narrow updrafts, surrounded by broad regions of weaker descent (Liu et al. 2004). Mid-lake bands form parallel to the major axis in the middle of the lake, with the major axis being defined as the longer diameter of the elliptical lakes. These single bands can produce copious snowfall due to the long fetch over water, and are often enhanced by land-lake breezes on either side of the band which lead to increased mid-lake convergence and enhanced vertical velocities (Schroenberger 1986). Mesoscale vortices are rare, and only occur under light wind conditions. Vortices form in a region of land-breeze convergence at the center of the lake and are typically associated with narrow snow bands. After formation, the entire vortex is subsequently advected over land (Laird 1999).

Variations in wind speed and direction, and consequent changes in residence time of air over open water, can lead to changes in LES morphology during a single LES event. Studies using idealized lake coastlines have shown LES morphology to be dependent upon the ratio of wind speed to fetch over open water. This ratio represents the residence time of the air parcel over open water, which in turn determines the extent of destabilization and water vapor added to the air (Laird et al. 2003a,b). The wind speed to fetch ratio is limited in its predictive ability, as it does not account for transition zones in which multiple types of morphology may be present simultaneously (Laird et al. 2003b). Its ability to predict morphology in observed conditions is generally limited due to complex interactions between coastlines, local and large-scale circulations (Laird and Kristovich 2004; Laird et al. 2003b).

The large-scale conditions necessary for the formation of LES have been studied extensively with a variety of models and observations, and the role of lake-atmosphere temperature gradients, wind speeds and shear, lake orientation and bulk lake ice coverage in LES formation are now relatively well understood (Wiggin 1950; Eichenlaub 1970, 1979; Niziol 1987; Niziol et al. 1995; Ballentine et al. 1998; Kristovich and Laird 1998; Liu et al. 2006). Specifically, lake surface latent heat flux decreases linearly with increasing lake ice areal coverage, while sensible heat fluxes are relatively constant below 70% ice area fraction, rapidly decreasing with increasing ice coverage (Gerbush et al. 2008). Changes in lake ice coverage have also been shown to produce significant modifications not only to LES amount, but also precipitation morphology (Cordeira and Laird 2008). Ice thickness also modulates the water-to-air fluxes of thermal energy and water vapor, leading in some cases to relatively large fluxes even in cases with large fractional ice cover (e.g., Zulauf and Krueger 2003). As such, while relatively large ice-free surfaces are generally required for the generation of LES, a few studies have noted large fluxes in the presence of relatively high ice concentration. Specifically, cases of LES over lakes with significant (greater than 80%) ice cover concentration over the entire lake have been observed (Laird and Kristovich 2004; Cordeira and Laird 2008). Studies conducted on decadal time scales indicate such events are rare (Notaro et al. 2013; Vavrus et al. 2013).

The magnitude of LES is to a large extent dependent on the thermal gradient between lake surface and atmosphere, and global warming-induced changes in the spatial distribution of lake ice may therefore cause changes in the characteristics of future LES events. Observed trends indicate a general decrease in lake ice coverage and thickness

over the past few decades (Assel et al. 2003; Assel 2005), though there are occasionally anomalous years with larger ice extent associated with variability in the atmospheric circulation related to changes in the phase of the Arctic Oscillation and the El Niño-Southern Oscillation (ENSO; Wang et al. 2010). In addition to decreases in lake ice coverage, several studies suggest an increase in the frequency and intensity of LES events as lake temperatures warm. Hjelmfelt and Braham (1983) found that while the distribution of lake temperature did not change the intensity of precipitation, differences in mean lake temperature could significantly alter total precipitation amounts. Theeuwes et al. (2010) showed that changes in lake temperature alter the precipitation totals for a case study over Lake Erie using 9km horizontal grid spacing. They found that with an increase of 10 Kelvin the precipitation downwind of the lake could be doubled. Kunkel et al. (2009) examined measurements taken during 1930-2004 at 19 National Weather Service cooperative observing stations and found a robust upward trend in observed LES depth and liquid equivalent downwind of Lakes Superior and Michigan, while results for Lakes Erie and Ontario were mixed and dependent on the period of analysis. Burnett et al. (2003) found that the frequency of LES events increased over all lakes during the 1990s and associated this increase with a rise in Great Lakes average LSTs of approximately 1 degree Celsius from 1995-2000. The frequency and intensity of cold air outbreaks did not change during this time period (Walsh et al. 2001), even under conditions of strong surface warming. Bard and Kristovich (2012) found that the contribution from Lake Michigan to the regional snowfall increased from the middle to the late 20th century, but began to decrease afterwards. Trumpickas et al. (2009), using various Intergovernmental Panel on Climate Change (IPCC) emissions scenarios project

increases of 2.5 to 7.0 degrees Celsius in LST over the Great Lakes by the year 2100 in summertime lake temperatures and the warmer lake temperature extending further into the fall and winter season before lake overturn, but it is unclear if changes in temperature will be accompanied by increases in the frequency or intensity of LES. Kunkel et al. (2002) examined output from two global climate model (GCM) simulations and found that intense LES events (those that produce greater than 35 cm of snow) decrease in frequency in the latter part of the 21st century, likely due to a decrease in the projected number of cold-air outbreaks (Vavrus et al. 2006).

While the literature indicates a general increase in the intensity of LES in a warming climate, determination of the local-scale distribution of LES is complicated by the interaction between the large-scale flow and the lakeshore geography and topography. Hjelmfelt (1992) found that even downwind of Lake Michigan, which has minimal orography, changes in wind direction resulted in local changes in snowfall intensity through interactions between the wind and orography. Veals and Steenburgh (2015) found the generation or intensification of LES over Tug Hill Plateau were present even when LES features were south of the plateau. This interaction with the Tug Hill Plateau is still under investigation, as Minder et al. (2015) recently discovered that the convective intensification over the region could be due to a transition from convective to stratiform precipitation. With these complex interactions, the mechanistic details of how the distribution and intensity of LES might change in a warming climate are not yet clear. Studies of the morphology and intensity of LES (e.g., Kristovich et al. 2003a) reveal a high degree of event-to-event diversity in fine scale precipitation structure, requiring models that account for the response of mesoscale dynamics and cloud system properties

to changes in the large-scale environment. The goal of this study is to examine the mesoscale and cloud scale changes to precipitation structure over-lake and downwind that arise from changes to Great Lakes ice coverage and lake temperature consistent with future climate conditions. Specifically, we use a set of control and sensitivity simulations to determine whether changes in LES in a warming climate can be described simply as a response to changes in the over-lake fluxes, or whether these changes are modulated by interaction with the local-scale topography and shore geometry. To understand local- and regional-scale interactions at the process level, we focus on a specific event that occurred during 14-17 January 2009, and employ high-resolution Weather Research and Forecasting (WRF) model simulations with differing lake ice coverage and LSTs (LST) consistent with conditions projected for the latter half of the 21st century. We first examine the regional scale snowfall response and then perform a more detailed analysis of the fine-scale precipitation structures.

The remainder of this chapter is organized as follows. Section 2.2 contains an overview of the WRF model configuration and physical parameterizations, a description of the modifications used to test the sensitivity of the event to lake conditions, and an overview of our selected case. Section 2.3 reports the results of each experiment, and a summary and conclusions are presented in section 2.4.

2.2 Model Setup and Description of the January 2009 Case

2.2.1 Model Configuration

The Advanced Research Weather and Forecasting Model (WRF-ARW) version 3.2.1 is utilized to simulate LES over the Great Lakes region. The model is run on two domains, including 1) a 3 km horizontal grid spacing with 35 terrain-following vertical

levels on the outer domain and 2) a 1 km grid spacing with 69 vertical levels on the inner nest (Figure 2.1). One-way nesting is used to transfer information between outer and inner nests. Initial and lateral boundary conditions for the 3 km nest are obtained from the North American Regional Reanalysis (NARR) dataset (Mesinger et al. 2006, Rutledge et al. 2006), and lateral boundary conditions are updated every three hours. Each simulation is run for a total of 60 hours starting at 1200 UTC 14 January and ending at 0000 UTC on 17 January 2009. LES initiation occurred at approximately 0000 UTC 15 January, and the model was started 12 hours previous to allow sufficient time for initialization and spin up.

All simulations employ the Goddard microphysics and Mellor-Yamada-Janic planetary boundary layer schemes, as these parameterizations have demonstrated success in modeling LES events in previous studies (Shi et al. 2010; APPENDIX D). See Table 2.1 for the complete suite of physics schemes used. The fine horizontal grid spacing used in our simulations obviated the need for a deep convective parameterization. While the horizontal grid spacing used on both model domains is too coarse to resolve individual shallow convective elements, as of yet there is no shallow convective parameterization appropriate for the simulation of LES. If, in general, a minimum of 4-6 model grid points are required to resolve a physical structure (Durran 2000; Grasso 2000), simulation of individual 1 km in width LES bands would require horizontal grid spacing less than 250 meters. Computational limitations restricted the simulations used in this study to a horizontal grid spacing of 1 km in length and larger. Comparison between simulated snow bands and those observed indicates the grid spacing was sufficient to reproduce the observed mesoscale cloud structure and precipitation distribution.

Microphysics	Goddard Microphysics Scheme
Planetary Boundary Layer	Mellor-Yamada-Janjic Scheme
Land Surface Model	Noah Land Surface Model
Shortwave Radiation Physics	Dudhia scheme
Longwave Radiation Physics	Rapid Radiative Transfer Model
Cumulus Scheme	None
Surface Layer Physics	Eta Similarity

Table 2.1. Parameterization schemes used in the setup of the WRF model.

The NOAH land surface model is used to simulate subsurface temperature and soil moisture. LST and sea surface temperatures (SST) are initialized using satellite-derived surface skin temperature in the NARR dataset, with lake ice grid cells defined as any inland water points with LST at or below 271 K. Lake ice grid cells (Figure 2.1) are treated as bare land, with the subsurface treated as saturated frozen soil. Temperatures of ice grid points decrease linearly to 270 K at a depth of 1.5 m below the surface, while water points with temperatures greater than 271 K are isothermal through this depth.

In addition to the control simulation (hereafter CTRL), three test cases are used to explore the impacts of ice coverage and lake surface temperature on the formation of lake-effect precipitation. These employ the following surface boundary conditions (APPENDIX A): 1) all lakes are assumed to be completely ice covered (ALLICE) by setting initial skin temperatures over lakes to 265 K (the average NARR skin temperature for all ice covered lake points), 2) all lakes are assumed to be ice free (NOICE) by setting any lake point temperatures below 273.15 K to 273.2 K and 3) all lakes are assumed ice free and with a surface temperature uniformly 3 degrees Kelvin greater than the ice-free case (LST3K). Changes to the surface boundary conditions are only applied to continental water points, and points over the Atlantic Ocean are left unmodified. Our focus is restricted to the areas immediately surrounding the Great Lakes. With the exception of changes in the lake ice, all other initialization remains the same and the

simulations are otherwise identical with respect to length of simulation, resolution, parameterizations, and boundary conditions.

2.2.2 January 14-17, 2009 Case Study

Here we provide a brief overview of the synoptic-scale conditions observed during the January 2009 cold-air outbreak case using NARR temperature, geopotential height, and wind data at 850 hPa. At 1200 UTC 15 January 2009, a high amplitude ridge-trough system was located over North America with a trough that stretched from Ontario south along the Atlantic coastline (Figure 2.2a). Temperatures over the Great Lakes region were uniformly lower than -20 °C, and winds over the lakes were oriented primarily from northwest to southeast at this time. The surface cyclone (indicated by the "L" in Figure 2.2a and b) was located over the Atlantic Ocean just east of the mid-Atlantic states. By 0000 UTC 16 January, the surface cyclone had moved farther off shore and winds over the Great Lakes had acquired a more westerly component. At 1200 UTC 16 January, winds over the lakes were oriented primarily from west to east, and while 850-hPa temperatures had increased over the preceding 12 hours, the air over the Great Lakes region remained colder than -15 °C. With open water temperature >= 0 °C, all lakes satisfy the Holroyd (1971) criterion of 13 degree Celsius difference between 850mb and LST for the formation of LES.

To evaluate the control simulation of LES for this event, we compare simulated versus observed composite radar reflectivity, as liquid equivalent precipitation is difficult to measure accurately over broad spatial scales with either in situ or radar observations. Simulated reflectivity was generated using the Advanced Research WRF post-processing package (ARWpost), which computes equivalent reflectivity factor from the mass and

particle size distribution of all precipitating hydrometeors (rain, snow, and graupel). Bright-band effects are simulated by scaling the equivalent reflectivity factor of snow and graupel at temperatures greater than freezing. The combined reflectivity factors from all precipitating hydrometeors are then summed and converted to reflectivity in dBZ. Although simulated radar reflectivity is not an exact analogue to the precipitation rate at the surface, it does facilitate comparison of the simulated and observed precipitation spatial scale and cloud hydrometeor content. At 1200 UTC 15 January (Figure 2.3a), the model produces lake effect snowfall over and downwind of each of the Great Lakes. Comparison with the observed radar reflectivity (Figure 2.3b) indicates the model is producing precipitation in close proximity to most of the observed locations, with particularly good agreement downwind of Lake Michigan. Note that there are modeled LES bands over Lake Huron and downwind of Lake Erie that are not seen in the observed radar imagery. The bands over Lake Huron appear in geostationary satellite imagery (not shown). They do not appear in the current images due to NWS NEXRAD radar coverage not extending past Lake Huron, and radar overshooting the tops of the shallow convection, although we note these bands are observed in Canadian-based radar sites (not shown). The modeled bands downwind of Lake Erie that are not observed in the radar observations form in close proximity to the region of open water over the lake (see ice extent depicted in Figure 2.1), and it is possible that local-scale convergence features around the ice edge may be enhancing the precipitation in the model at this time. The model produces precipitation features over and downwind of the lakes that are very consistent with those observed at 0000 and 1200 UTC on the 16th of January (Figure 2.3b-d and Figure 2.3e and f, respectively), though the mid-lake band over Lake Ontario

is slower to develop in the model than in reality. The broad region containing large reflectivity values over southern Wisconsin and northern Illinois at 1200 UTC on the 16th of January (Figure 2.3e) is not produced by the model (Figure 2.3f). Surface observing stations and satellite images over this region (not shown) report uniformly clear skies at this time. The relatively large observed reflectivities may be caused by downward refraction of the radar beam (and subsequent intersection with the surface) in the presence of extremely cold air in this region (approximately -30 °C at this time).

As mentioned in Section 2.1, LES differs in morphology according to the details of the large-scale wind flow, fetch, and lake surface-air temperature difference. Examination of the simulated reflectivity output from the model reveals evidence of each of the observed types of LES with the exception of mesoscale vortices, which are prevented by the persistence of strong winds over the lakes for the duration of the event. Shoreline bands are evident south of Lake Ontario at 1200 UTC 15 January and south of Lake Erie at 0000 and 1200 UTC 16 January. Mid-lake bands can be seen over Lakes Superior and Huron at 0000 and 1200 UTC 16 January and over Lake Ontario at 1200 UTC 16 January.

Comparison with the ice concentration analysis from the NOAA/National Ice Center (1995) over the Great Lakes shows a close agreement in the location of ice between observations and the WRF (not shown). The most notable error occurs over central Lake Huron, where WRF includes an isolated region of ice that is not seen in the satellite observations. All other lakes show reasonable agreement with observations, with minor errors in extent of ice coverage over lakes Erie, Ontario, and Superior. Note that ice location and thickness is not updated during our WRF simulations. Ice concentration is

observed to change during 15-17 January, in particular associated with formation of thin new ice over Lake Erie and south-central Lake Superior. However, the maximum ice depth observed during the simulated time period is 30-70 cm over small portions of Lake Erie's western basin, Green Bay in northwest Lake Michigan, off the coast of Manitoulin Island in northeastern Lake Huron, Saginaw Bay in Lake Huron, and off the coast of Thunder Bay, Ontario in the northern part of Lake Superior. Other ice covered areas range in thickness from new ice to 10-30 cm. Since the changes in ice cover are small, we expect the discrepancies due to the lack of an ice cover update in our model to be negligible.

2.3 Results from Lake Surface Sensitivity Tests

2.3.1 Changes in Regional Precipitation Distribution

As mentioned in the Introduction, we begin with an analysis of changes in the regional distribution of LES and then proceed to a detailed examination of cloud and precipitation structure. We base our analysis on the area downwind of the Great Lakes with output from the larger region encompassed by the 3 km nest, and utilize the higher resolution 1 km nest to explore the interaction between LES, topography, and shoreline geography in Section 3.3. Figure 2.4 displays the cumulative liquid equivalent precipitation in the CTRL (Figure 2.4a), ALLICE (Figure 2.4b), NOICE (Figure 2.4c), and LST3K (Figure 2.4d) cases, along with difference plots (Figure 2.4e-g) for the time period spanning 0000 UTC 15 January through 0000 UTC 17 January 2009. Precipitation in CTRL (Figure 2.4a) is due both to the frontal and synoptic scale forcing for vertical motion associated with the passage of the mid latitude cyclone as well as the effect of the lakes on the formation of LES. Each of the Great Lakes is producing lake effect

precipitation both over and downwind of the lake, with precipitation maxima located primarily along the downwind (southern and eastern) shores. Local precipitation minima along the northwest shore of Lake Superior, as well as the southwestern and southeastern shore of Lake Erie are associated with ice cover in these regions.

Comparison of the results for CTRL (Figure 2.4a) and ALLICE (Figure 2.4b), as well as the difference plot in Figure 2.4e, illustrates the influence of lake ice on the generation of lake effect precipitation. Less than 3 mm of total precipitation is produced in the ALLICE simulation over or downwind of the lakes (Figure 2.4b). The reduction in precipitation is most notable in the western portion of Michigan's lower peninsula, throughout Michigan's upper peninsula and along the southern and western shores of Lake Erie. In the absence of LES, all accumulated precipitation in the ALLICE case is associated with the passage of the mid-latitude cyclone. The small amount of accumulated precipitation over southern Michigan and northwestern Ontario is likely due to convective instability in the cold air to the northwest of the surface cyclone. The simulation of complete ice coverage not only removes the lake effect precipitation over and immediately downwind of the lakes, it also has the effect of removing all accumulated precipitation over southern Michigan and most of Indiana and Ohio (Figure 2.4e). The lakes are too far removed to directly contribute to the formation of precipitation in these regions, but the absence of water vapor from over-lake evaporation in the ice-covered case leads to a drier atmosphere, and hence to the suppression of synoptically forced precipitation in these regions.

The precipitation distribution in NOICE (Figure 2.4c) is similar to the pattern seen in CTRL (Figure 2.4a), with the most intense areas of precipitation located along the

southern shores of Lakes Superior and Erie, the east coast of Lake Ontario, and the eastern shores of Lakes Michigan and Huron. Though the patterns of precipitation are similar between CTRL and NOICE, areas receiving relatively small (≥ 2 mm) and large (≥ 10 mm) amounts of precipitation increase 28 and 93%, respectively, over the CTRL case (Table 2.2). The NOICE – CTRL difference plot (Figure 2.4f) reveals a general increase in precipitation downwind of each of the lakes. Decreases in precipitation over each of the lakes is primarily due to a shift in the position of the mid-lake band(s) caused by the removal of ice, while decreases farther to the south and east of Lakes Michigan, Erie, and Ontario are associated with small shifts in the position of downwind snow bands.

When LST is increased by 3 K over the no ice case (Figure 2.4d), the spatial structure of the accumulated precipitation changes little compared with NOICE (Figure 2.4c), however, the total area that encompasses all accumulated snowfall increases. In addition, the overall intensity of precipitation increases substantially, with areas that experience relatively large precipitation (≥ 10 mm) increasing by 63.3% over the no ice case (Table 2.2; Figure 2.5). The plot of the difference between LST3K and CTRL (Figure 2.4f) indicates precipitation is not only more intense along the downwind lakeshores, but also exhibits deeper inland propagation. A comparison of our results to the climatological precipitation in the Great Lakes region (e.g., Scott and Huff 1996) reveals the accumulated precipitation in our simulations of this single case is equivalent to approximately 3-7%, 4-9%, and 5-17% of the total average wintertime precipitation in the CTRL, NOICE, and LST3K cases, respectively.

The change in LES coverage between CTRL, NOICE, and LST3K is evident when masking the 36-hour precipitation amounts ≥ 2 mm (Figure 2.5a), ≥ 5 mm (Figure 2.5b), and ≥ 10 mm (Figure 2.5c). The 36-hour time period ending at 0000 UTC 17 January is chosen to isolate the signal of lake effect snow and minimize the contribution from precipitation produced by the surface cyclone to the east. For each threshold value, the area of LES expands with a decrease in ice fraction and increase in LST. The largest increases in area covered by LES at each threshold occur when all ice is removed from the lakes with more modest areal increases in LES with an increase in LST. The expansion of LES with a transition to NOICE and LST3K does not solely occur in the downwind direction, but expansion is also evident in the upstream direction, and perpendicular to the flow.

48 Hour Accumulation Greater than or Equal to **2mm**			
	CTRL	NOICE	LST3K
Number of Grid Cells	45060	57455	62935
% Change from CTRL		27.5 %	39.7 %
% Change from NOICE			9.5 %
48 Hour Accumulation Greater than or Equal to **10mm**			
Number of Grid Cells	4133	7954	12986
% Change from CTRL		92.5 %	214.2 %
% Change from NOICE			63.3 %

Table 2.2. Number of grid cells in the Great Lakes region reporting 2mm or more and 10mm or more of precipitation.

We further investigate changes in the intensity and inland propagation of precipitation by examining precipitation transects across several of the lakes, where precipitation is averaged perpendicular to the transect over the gray shaded areas in Figure 2.1. For the transect across Lakes Michigan and Erie (Figure 2.6a), the removal of ice cover and increase in LST triggers little change in precipitation over Lake Michigan, while precipitation downwind of the lake increases by approximately 50%. In contrast, the removal of ice increases precipitation at the lakeshore both over and downwind of Lake Erie. The location of the precipitation maximum is unchanged for both lakes in all three simulations but LST3K, for which the maximum in precipitation moves downwind of Lake Michigan. In the transect across Lakes Michigan, Huron, and Ontario (Figure 2.6b), removal of lake ice and increase in LST result in an approximately 30% increase in LES downwind of Lakes Michigan and Huron. The removal of ice over Saginaw Bay (approximately 83.5°W; see Figure 2.1 for a map of ice cover) also causes an increase in

LES over the western portion of Lake Huron and Michigan's northeast Lower Peninsula in the NOICE simulation. LES magnitude over Lake Ontario increases by less than 10 % with the removal of ice, but increases by approximately 500% downwind over land in areas originally experiencing minimal precipitation. In contrast to the southern transect, the location of the precipitation maximum shifts downstream of Lakes Michigan and Ontario while remaining nearly stationary over Lake Huron.

In the northern west-east transect across the upper peninsula of Michigan and portions of Lake Superior (Figure 2.6c), when ice is removed (NOICE) and LSTs increased (LST3K), precipitation amounts increase downwind of the lake from 40% over the eastern portion to 150% over the western edge. This variability in the increase of precipitation is mainly due to the spatial pattern of ice coverage, as well as the morphology of the shoreline (Figure 2.1). The largest fractional ice coverage in CTRL is located in the western basin of Lake Superior, and removal of ice lengthens the open water fetch in this region. Increased fetch, and consequent increases in latent and sensible heat fluxes, lead to increases in the areal extent of precipitation over land (e.g., west of 90°), but minimal change in location and magnitude of the precipitation maximum downwind of the lake (near 85°W). When LSTs are increased, the location of the precipitation maximum changes little, but there is a 40% increase in liquid equivalent snowfall. In this case, there is little to no increase in open-water fetch. Instead, increases in snowfall between NOICE and LST3K are due to a surface-warming-induced increase in the magnitude of surface sensible and latent heat fluxes (Figure 2.2).

The precipitation mask (Figure 2.5) and transects (Figure 2.6a-c) show an increase in the intensity of the precipitation downwind of each of the lakes in NOICE and LST3K.

The location of the precipitation maximum also shifts inland of Lake Michigan in both the NOICE and LST3K experiments, whereas the position of peak precipitation downwind of all of the other lakes shifts very little (typically less than 10 km). Over most lakes, the increase in precipitation associated with removal of lake ice is of the same order of magnitude as the additional increase due to lake surface warming. The exceptions are those regions more than 50 km downwind of Lakes Erie and Ontario, which do not experience an increase in precipitation with increases in LST (Figure 2.6a and b). This distinguishes the precipitation response between east-west oriented lakes and north-south oriented lakes, with increases in LST causing an increase in precipitation upwind for east-west lakes (Erie and Ontario) and downwind for north-south lakes (Michigan and Huron). This is consistent with the known contribution of north-south oriented lakes to increased precipitation downwind of downstream lakes (so-called "lake-to-lake" snowfall events; e.g., Rodriquez et al. 2007).

Both the precipitation mask plots (Figure 2.5) and transects (Figure 2.6) suggest that removal of ice (and consequent increases in over-water fetch) expands the total area affected by LES more than increases in LST. Warming of the lake surface leads to a modest expansion in LES area, but serves primarily to increase the area over which heavy precipitation (accumulated liquid amounts $\geq$ 10 mm) falls. This is because the ice cover in CTRL is not uniformly distributed over the lakes; when ice is removed, the lake surface fluxes increase, but not in a spatially uniform fashion. As such, there are regions downstream of the lakes in CTRL that do not exhibit any lake effect snowfall. When ice is removed and over-water fetch increases, the area of influence of lake effect precipitation expands. Increases in precipitation amount and intensity downwind of the

lakes are likely due to larger total latent and sensible heat fluxes from the lake surface, which in turn lead to increased destabilization of the lower atmosphere and to stronger convective updrafts. These mechanisms are discussed in Section 3.2.

2.3.2 Mechanisms

Both sensible and latent heat fluxes increase over each of the lakes with the removal of ice and increase in LST, and the largest changes occur over areas previously covered by ice (Figure 2.7a and b, respectively). Daytime sensible heat fluxes increase 100-400 W m^{-2} over areas previously covered by ice, with the largest increases occurring over western Lake Michigan and northern Lake Superior. Removal of lake ice increases the daytime latent heat fluxes 100-200 W m^{-2}. An increase in LST leads to a smaller increase in fluxes from the lake surface compared with removal of lake ice; surface fluxes in LST3K are at most 10 W m^{-2} larger than those in the NOICE case (not shown). While the magnitude of the increases due to warming LST are smaller, they occur over a far greater area. The temporally averaged total energy flux increase from all of the lakes combined is 2.86 x 10^{13} W between CTRL and NOICE and 2.61 x 10^{13} W between NOICE and LST3K; a difference of 8%. Note that the increase in surface heat flux would have been greater (less) than in our simulations if the control ice coverage had been larger (smaller). Cordeira and Laird (2008) observed a reduction of 85% and 95% of total energy flux off of Lake Erie from open water to ice covered conditions in two separate LES cases.

Next, we examine how changes in sensible and latent heat fluxes affect the stability and height of the planetary boundary layer. We focus our analysis on Lake Erie, which exhibits large fractional ice coverage in CTRL and is thus strongly influenced by the removal of ice. Figure 8 depicts the modeled vertical temperature and dew point

temperature profile at 1200 UTC 16 January averaged over a 6x6 grid in central Lake Erie as compared with another 6x6 region over southern Michigan ("X"s in Figure 2.1). A strong LES band was located along the southeastern shore of Lake Erie at this time (Figure 2.3f).

Increases in open water area and in lake surface temperature result in nearly equivalent precipitable water vapor (PW) increases between CTRL and NOICE (Figure 2.8d and e), and between NOICE and LST3K (Figure 2.8e and f) over Lake Erie. In contrast, while there is a monotonic increase in PW between CTRL, NOICE, and LST3K over land (Figure 2.8a-c), the largest increase occurs for the transition between NOICE and LST3K (Figure 2.8b and Figure 2.8c, respectively). The increase in PW from CTRL to NOICE in both locations is due to removal of lake ice and increase in open-water fetch; because there is relatively smaller initial ice cover on Lake Michigan upstream (Figure 2.2c) of the inland point, the increase in PW is smaller than it is over Lake Erie. In contrast, the increase in PW produced by increases in surface heat fluxes associated with surface warming is comparable for the over-land and over-lake points.

In the CTRL case (Figure 2.8d), convective available potential energy (CAPE) calculated from a surface based parcel is minimal at 9 J/kg. The NOICE and LST3K cases exhibit greater buoyant instability with CAPE values of 63 and 93 J/kg, respectively (Figure 2.8e and f). While values of CAPE are relatively low in all simulations, observations have shown that large positive CAPE values are not necessary for LES formation (Schultz 1999). The near-zero CAPE values in CTRL are the result of a near-isothermal stable layer located approximately 500 meters above the surface (Figure 2.8d). Examination of the time evolution of the upstream low-level

temperature distribution reveals this layer to be created over land and partially frozen lakes through overnight radiative cooling. The result is a strong (4 K (500 m)$^{-1}$) low-level temperature inversion (Figure 2.8a). In CTRL, the Lake Erie sounding is located just downstream of the ice edge (Figure 2.1), and in this case there has not been sufficient sensible heat transfer from the lake to the atmosphere to entirely remove the stable layer. The temperature inversion upstream of Lake Erie in NOICE and LST3K (Figure 2.8b and c) is of similar magnitude and depth to CTRL, but in these cases surface sensible heat flux from the longer open water fetch over the ice-free western end of Lake Erie has sufficient mixing to eliminate the inversion. While the properties of the low-level temperature inversion are similar in all three cases, the depth and water vapor content of the boundary layer increase in both NOICE and LST3K. The fact that qualitatively similar changes are observed both over and upstream of Lake Erie indicates the importance of the upstream lakes in modifying the thermodynamic environment. The influence of the upwind lakes on downwind LES has been observed in previous studies (Sousounis and Mann 2000; Mann et al. 2002; Rodriguez et al. 2007). In this case, warming over the upwind lakes helps to "prime" the atmosphere by warming the boundary layer and reducing the stability of the lower troposphere. This in turn leads to greater instability over the lake as the low-level inversion mixes out, giving the potential for deeper updrafts and more intense precipitation.

2.3.3 Precipitation Structure

The deeper and more well-mixed boundary layers exhibited by NOICE and LST3K allow for consequent increases in column integrated water vapor, larger buoyant instability, and the possibility of deeper vertical circulations, and it is likely this that

contributes to the observed increases in precipitation amount and areal extent (Figure 2.4-6). We now examine the impact of lake ice changes on the cloud scale structure of the LES snow bands, focusing our analysis on Lakes Erie and Ontario. Lake Erie is selected because it has the largest fractional ice cover of the five major Great Lakes in the CTRL case and exhibits marked changes in precipitation morphology over the lifetime of the case, while Lake Ontario exhibits a well-defined mid-lake snow band. We utilize the 1 km grid-spacing nest in this analysis as it facilitates a more realistic representation of local-scale topography and precipitation features. One-hour accumulated liquid equivalent precipitation is used to depict the structure of the lake-effect snow features around Lakes Erie and Ontario (Figure 2.9). As the synoptic scale flow evolves, the air temperature and over-lake fetch change, leading to distinctly different precipitation regimes. We select three representative times that each illustrates different precipitation morphology.

At 1200 UTC 15 January, lower tropospheric winds over the Great Lakes were primarily northerly (Figure 2.2a), resulting in relatively short fetch over Lake Erie and the development of a shoreline snow band along the southern shore (Figure 2.9a-c). Though ice cover limited the horizontal extent of this band in CTRL (Figure 2.9a), increases in wind speed with transition from ice to water serve to enhance a mid-lake convergence zone and the associated precipitation over the lake. Removal of the lake ice and increase in LST (Figure 2.9b and c) result in the expansion of LES along the southern Lake Erie shoreline, as well as a general increase in LES magnitude. In a manner similar to the influence of the ice edge geometry in CTRL, the concave northern shore (to the south) produces mid-lake convergence in the ice-free cases; however, the convergence is

weaker and the north-south oriented mid-lake band is diminished in intensity. Precipitation in LST3K develops farther upwind of the lake shore than in NOICE, perhaps due to more rapid boundary layer destabilization caused by greater surface heat fluxes.

By 2100 UTC 15 January, the synoptic scale flow was directed from northwest to southeast over the Great Lakes (Figure 2.2a and b), leading to a change in the precipitation morphology from relatively widespread with embedded shoreline bands (Figure 2.9a – c) to widely separated flow-parallel bands (Figure 2.9d – f). This transition happens due to changes in fetch over the lake, and is broadly consistent with Laird et al.'s (2003a) idealized simulations, which showed a morphological transition from widespread coverage toward shoreline bands as the ambient flow direction changed from across to along the major (longer) lake axis. Close examination of the flow pattern to the south and east of Lake Erie reveals a complex interaction with the western side of the Allegheny Plateau (circled in red in Figure 2.9d–f; see also the terrain height map in Figure 2.10). Divergent flow around the Allegheny Plateau leads to local convergence on the southwest side in all cases, and to enhancement of the upstream mid-lake band in NOICE and LST3K (Figure 2.9e and f). Precipitation is likely limited over the Allegheny Plateau at this time because the over-lake fetch is short.

At 1200 UTC on the 16th of January, winds were oriented from west to east across Lake Erie and most of the rest of the Great Lakes region (Figure 2.2c). In the CTRL case (Figure 2.9g), extensive ice cover inhibits the development of precipitation, with snowfall restricted to a single band downstream of the largest patch of open water. When all ice is removed from the lake (Figure 2.9h), lee-side snowfall becomes more widespread.

Increasing the lake temperature (Figure 2.9i) results in expansion of LES downstream, but little change to the precipitation amount. Note that the upstream edge of the region of precipitation does not change between NOICE and LST3K, nor do the positions of the downstream snow bands. This indicates that, while the amount of precipitation is dictated by the surface properties and air temperature, the location is governed by the local geography.

The final row of Figure 2.9 depicts a mid-lake band over Lake Ontario at 1200 UTC on 16th of January. In the CTRL case (Figure 2.9j), 10m wind vectors show low-level convergence occurring near the center of the lake, creating the mid-lake band. In the NOICE case (Figure 2.9k), increases in over-lake fluxes lead to greater boundary layer destabilization, an increase in updraft velocity, and consequent increases in mid-lake convergence. Removal of ice from the northern portion of the lake causes the band and convergence zone to shift to the north. Preferential movement of the band to the north is likely due to the removal of the ice cover in the north central portion of the lake. The resulting decrease in roughness length from ice cover to open water allows for the development of a more southerly low-level flow. Decreases in precipitation intensity over the eastern end of Lake Ontario are due to changes in the interaction between the snow band and topography. In the control case, the flow and band impinge directly on the Tug Hill Plateau (indicated in the red circle in Figure 2.9j – l; see also Figure 2.10), an elevated region just east of the eastern end of Lake Ontario that rises to a height of just over 600 meters above sea level. The northward shift in the mid-lake band induced by removal of ice causes the band to be positioned to the north of the Tug Hill Plateau in a region with less potential orographic enhancement of precipitation. Snowfall in the

LST3K case (Figure 2.9l) develops further upstream of the lake shore, likely due to more rapid destabilization of the boundary layer over the warmer lake waters. This interaction with the Tug Hill Plateau has recently come into question whether it is due to orographic lift intensifying the existing convection or if it is due to a convective to stratratiform transition (Minder et al. 2015). Further examination is needed to understand if the convective to stratiform transition is the dominant mechanism or if a combination of the transition and interactions with orography are present.

Examination of hourly precipitation suggests that changes in lake surface properties produce local increases in magnitude and expansion in the areal extent of precipitation. It is clear, however, that these changes also interact strongly with the local topography and lakeshore geometry. To further explore these interactions, and to obtain a more detailed process level perspective on the boundary layer and cloud vertical structure, we examine cross-sections at 1200 UTC on the 16th of January located at distances of approximately 0 km, 30 km, and 60 km from the southeastern Lake Erie shoreline (Figure 2.10). The orientation is chosen to strike a balance between cross-sections that are parallel to the shoreline and also as close to perpendicular to the flow-parallel precipitation features as possible.

The cross-section nearest the lakeshore includes land to the southwest and water to the northeast, with the transition between land and lake located at approximately -79.8 degrees west longitude. Examination of the vertical distribution of water vapor (Figure 2.11 a, c, and e) indicates the top of the boundary layer (as determined by the mean height of the tops of shallow convective plumes) is approximately 600-800 meters higher over land vs. over the lake. The height of the 0.2 g/kg water vapor mixing ratio contour is

relatively constant over the land, and there is a monotonic increase in near-surface water vapor content in NOICE and LST3K. Over the lake, the 0.2 g/kg contour lowers with removal of ice and increase in LST (Figure 2.11 c and e). This is possibly due to (1) more vigorous mixing between shallow convection in the boundary layer and the free troposphere above, and (2) localized surface level divergence (and consequent subsidence above it) along the upwind shore as the reduction in surface friction causes low-level air to accelerate as it flows from land over the open lake water. No such increase is exhibited with transition from land to ice in CTRL, largely because the surface roughness of ice in the model is set equivalent to that of dry frozen soil. CTRL exhibits a single snow band, located at the boundary between land and lake (Figure 2.11 a and b); this is the band associated with mid-lake convergence noted above in Figure 2.9a. The presence of ice on the lake reduces the available water vapor, and there is no cloud over the lake or land to the east or west of this band. Removal of ice (Figure 2.11 c and d) leads to the appearance of shallow narrow updrafts over the lake with broader and deeper regions of snowfall over the land. Clouds over both the lake and land increase in depth with an increase in LST (Figure 2.11f), though increases are larger over land (~400-600 m) than over the lake (~200 m). Mean vertical velocity in updrafts changes little across the three cases, though detailed examination of the simulated vertical velocity field indicates the maximum updraft speed increases with transition from CTRL to NOICE and from NOICE to LST3K. Comparison of ice mass mixing ratio in each of the three cases reveals little consistency in the location of clouds over water or land in CTRL, NOICE and LST3K, with the exception of the land-lake boundary, which is a locus of snowfall in each case.

Thirty km downwind of the lake-shore transect (Figure 2.12), the single snow band in the CTRL case is shallow and contains approximately 0.16 g/kg less mass mixing ratio compared to locations along the lake shore. Upward vertical velocity and boundary layer water vapor content in all three cases is much smaller than in the along-shore transect, but there is little reduction in snow mass content in NOICE and LST3K. In contrast to the along-lake transect, cloud features appear in approximately the same locations in NOICE and LST3K. Close examination of the cross-section location relative to the terrain height (Figure 2.10) indicates several north-south oriented spurs of the Allegheny Plateau extend into the cross-section. While the influence of topography certainly also extends downstream, it appears that flow impinging on these spurs may serve to concentrate precipitation via local orographic enhancement. Locations to the north of the Allegheny Plateau (east of -79 deg. east longitude) experience less orographic enhancement, and the boundary layer remains relatively shallow and precipitation concentrated in narrower bands. In contrast, updrafts over the Allegheny Plateau are approximately two times deeper and clouds are significantly wider.

At locations 60 km downwind of the Lake Erie shore line (Fig. 13), clouds are nearly nonexistent in CTRL. Clouds persist in NOICE and LST3K, though cloud top heights are 400-1000 meters lower in comparison to locations nearer the lakeshore. The cross section is located almost entirely over the Allegheny Plateau, and many of the cloud features are associated with gradients in topography. This is particularly true of the elevated regions around -79.0 and -78.2 degrees west longitude. While changes in over-lake fetch can produce spatially consistent patterns in downstream snowband location and intensity, the fetch over Lake Erie upstream of each of the cross-sections changes little in the west-east

direction. Examination of the terrain height map (Figure 2.10) indicates the topographic gradients seen in Figure 2.13 extend both upstream and downstream of the cross-section, and it is reasonable to conclude that the snow band location is being influenced by flow along a local topographic feature.

The cross-section analysis suggests that the bulk surface fluxes determine the boundary layer water vapor content and by extension the amount of cloud mass that can be produced in each LES band. However, it appears that two sets of processes serve to generate snowfall at and downstream of the lakeshore. Frictional convergence at the land-lake boundary generates a significant amount of cloud mass, and greater amounts are found in cases with larger surface sensible and latent heat flux. Cloud mass generated at and near the lake shore is advected downstream, and advection of larger cloud amounts in the NOICE and LST3K cases leads to expansion in the LES region. However, in addition to the regional scale bulk thermodynamic response, small-scale horizontal gradients in topography serve to focus the snow bands and locally enhance snowfall amounts.

2.4 Summary and Conclusions

In this study, we have used the Weather Research and Forecasting model to examine how changes to lake surface properties affect snowfall distribution and amount for a case of lake effect snowfall in the Great Lakes region. Four cases were simulated: (1) a control case in which lakes were initialized with NARR-analyzed ice cover, (2) an all-ice case in which lakes were completely ice covered, (3) a no-ice case in which lakes were completely ice-free and (4) an ice-free case with 3 K increase in LST. This case study approach to understanding lake-land-atmosphere interactions is advantageous in that the WRF model configuration we have chosen is capable of simulating the meso-gamma

scale features associated with the development of intense lake effect snowfall. Our simulations have the appropriate resolution to capture the complex geography in the Great Lakes region.

The major conclusions of our study include the following:

1. As has been reported in previous studies, the location and extent of lake ice places a severe constraint on the location and intensity of LES. Our simulations indicate ice cover can, via changes in surface roughness around the ice edge, serve to focus and enhance precipitation in some cases.
2. With removal of lake ice and warming of the surface, lakes with short over-water fetch exhibit increases in the downstream extent of LES. By contrast, once ice is removed, lakes with relatively large over-water fetch show little additional downwind propagation of LES with increases in lake temperature.
3. Consistent with findings from prior LES research, fetch, wind speed, and wind direction determine the precipitation morphology. We find that the pattern of low-level flow, and the interaction between wind and the lakeshore geography and downstream topography, exerts a strong influence on the location of precipitation at the surface. For shoreline bands and widespread coverage, topography and lakeshore geography largely determine the spatial pattern of precipitation. Increases in LST serve primarily to increase the downwind extent of the heaviest precipitation. In contrast, the position of mid-lake bands (e.g., over Lake Ontario) is found to be sensitive to increases in LST, largely through the influence of lake surface fluxes on the strength of convection and mid-lake convergence.

4. Upslope enhancement of precipitation due to elevated topography downwind of the lakes is critical in determining the response of precipitation to changes in lake surface properties. In regions with complex downstream terrain, LES is generated both via lake shore convergence, and by local orographic enhancement.
5. Finally, examination of cross-sections through flow parallel bands (Figs. 11-13) indicates that an increase in LST does not significantly change the mean snow band updraft strength, but does lead to a narrowing and deepening of each band consistent with increases in boundary layer depth and buoyant instability. This suggests that the extended downwind propagation observed in the accumulated precipitation is due to a complex interaction between destabilization of air over the warmer waters and the location of regions of convergence and complex topography created along the shore.

These results have the following implications for the study of future climate in the Great Lakes region:

1. With reductions in lake ice, a greater area along the downwind shores of the Great Lakes may be exposed to increases in intense LES events.
2. With increases in LST, intensity of LES events increases along with the propagation downwind of LES.
3. The formation of LES is strongly coupled to the open water characteristics, as well as shoreline geography and topography. While LES events may become more intense, the spatial distribution of precipitation is strongly influenced by the location of topographic features, suggesting models that do not realistically

represent the interaction between precipitation and orography may have difficulty capturing the local scale distribution of snowfall.

Sensitivity of the LES distribution and intensity to lake surface conditions in our simulations is consistent with detailed observation-based studies of the ice cover-LES relationship (e.g., Cordeira and Laird 2008). Though applicability of our conclusions to future climate states is limited by the examination of a single LES event, the analysis presented here exhibits a wide range of observed LES morphology including widespread snow, shoreline bands, and mid-lake bands. The suite of simulations performed illustrates the various mechanisms that trigger LES in the Great Lakes region, and lends insight into a broader spectrum of cases in which LES is generated by cold-air outbreaks.

Ultimately, the long-term effects of changes to Great Lakes surface properties must be studied using simulations that span time scales of decades or longer, and can accurately capture the interannual variability of lake ice coverage (e.g., Notaro et al. 2013). The fact that ice cover concentration critically controls the amount and location of lake effect precipitation downwind of each of the Great Lakes has important implications for the design of decadal experiments. Specifically, accurate and realistic prediction of the timing of lake ice onset and melt, as well as the extent of cold season ice coverage and thickness, are critical for determining the timing and amount of lake effect (and by extension lake-enhanced) precipitation in future climate states. Fine-scale numerical experiments can be used to anchor coarser resolution simulations and may aid in the production of more accurate predictions of Great Lakes climate.

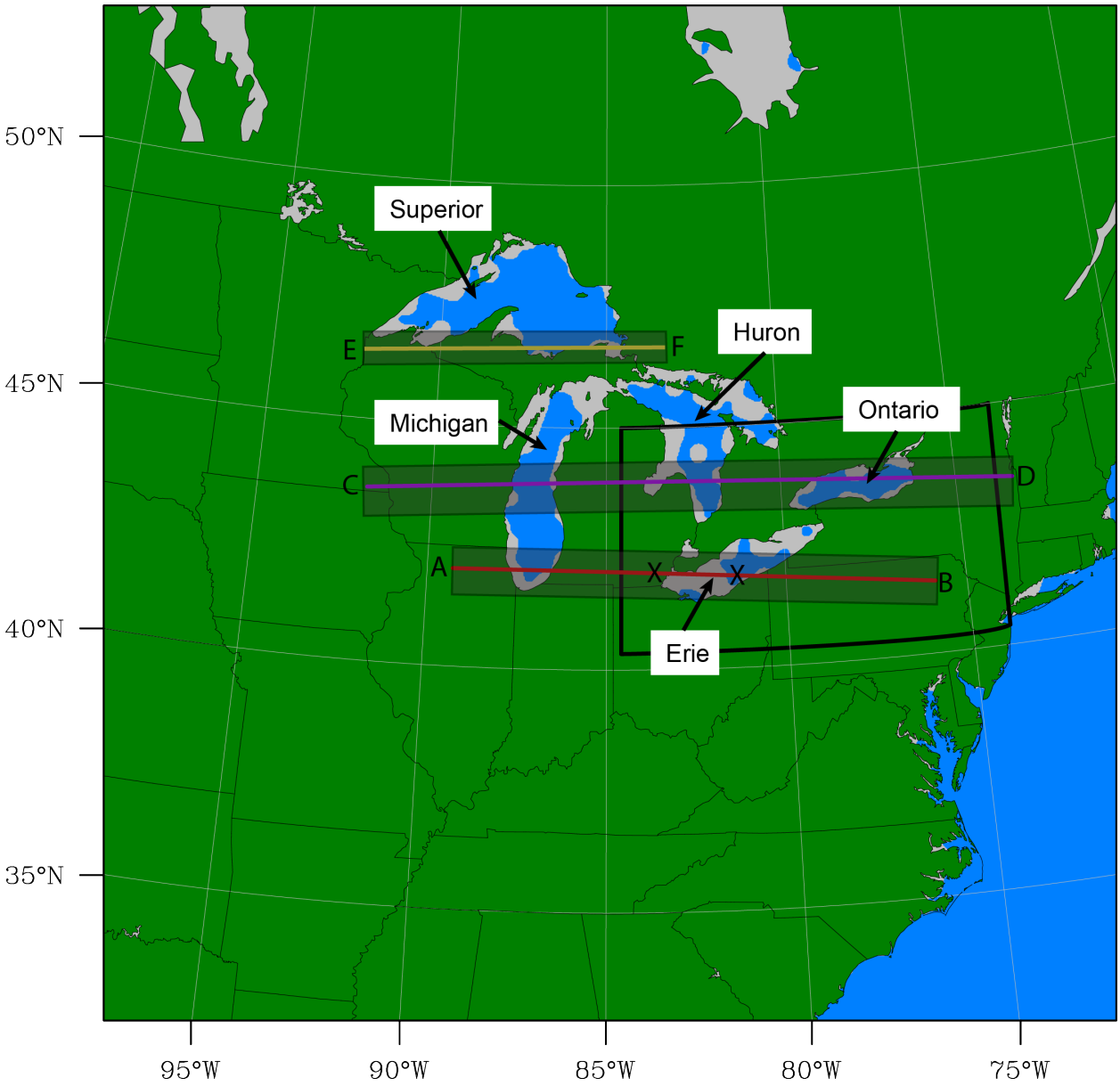

Figure 2.1. Geographic extent of the WRF model domain. Light gray shading over the lakes depicts the lake ice coverage as initialized by the model. Dark gray shading delineates the area average for precipitation transects analyzed in Section 2.3.1, while the "X"s mark the locations of the soundings plotted in Fig. 8. The location of the inner (1 km grid spacing) nest is depicted in the black box.

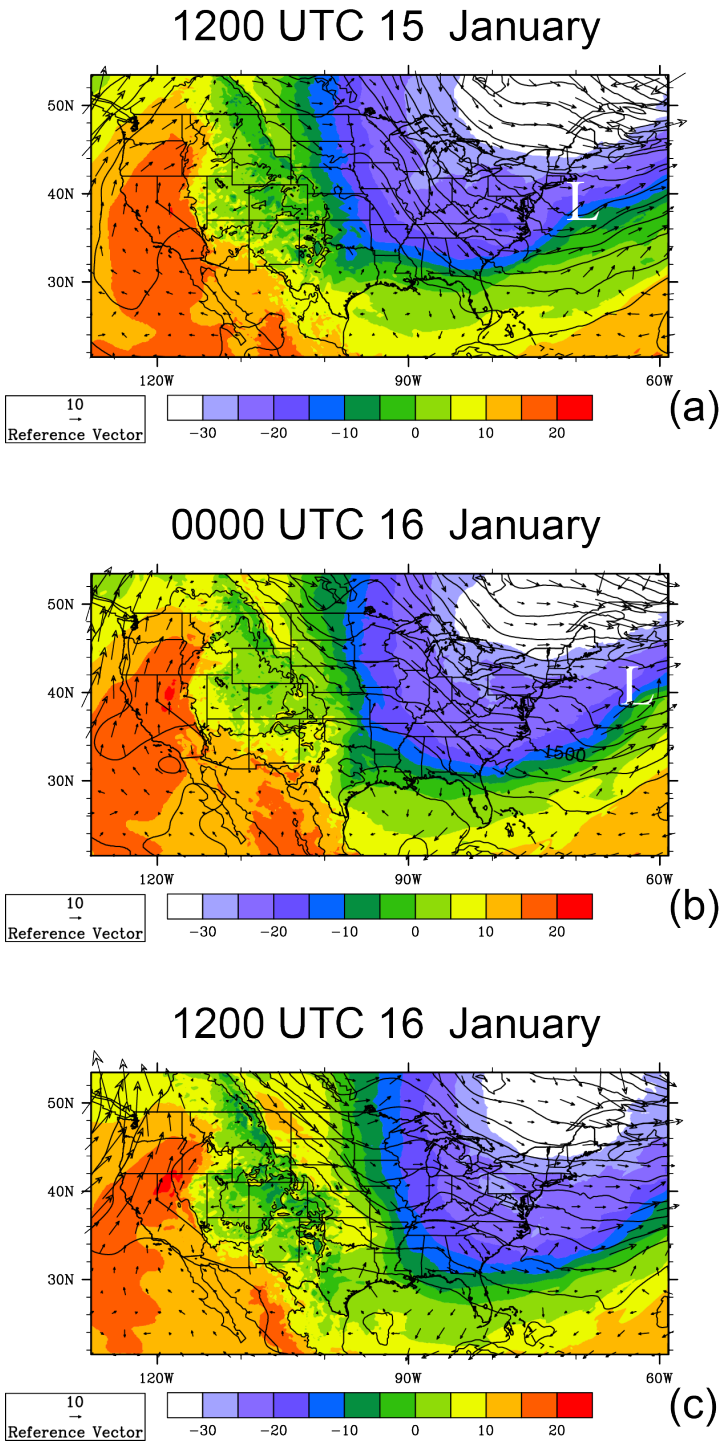

Figure 2.2. 850 hPa geopoential height (m), temperature (deg. C), and wind (m/s) from the North American Regional Reanalysis dataset at (a) 1200 UTC 15 January, (b) 0000 UTC 16 January, and (c) 1200 UTC 16 January. The position of the surface cyclone is indicated in the white L in (a) and (b).

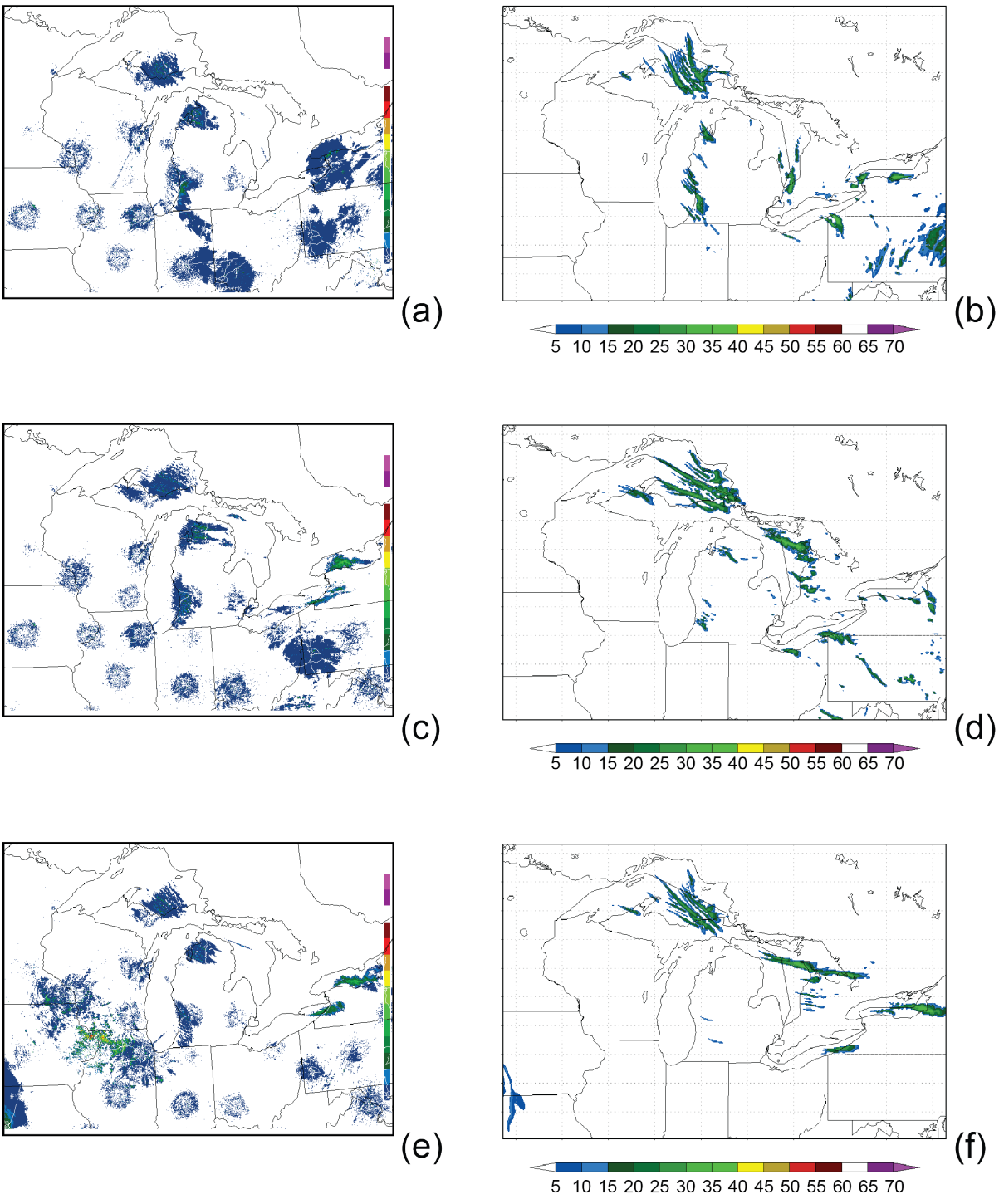

Figure 2.3. Observed (left column) and WRF-simulated (right column) composite radar reflectivity (dBZ) from 1200 UTC 15 January 2009 (a and b), 0000 UTC 16 January 2009 (c and d), and 1200 UTC 16 January 2009 (e and f). [Radar observations made available by the University Center for Atmospheric Research (UCAR) online at http://www2.mmm.ucar.edu/imagearchive]

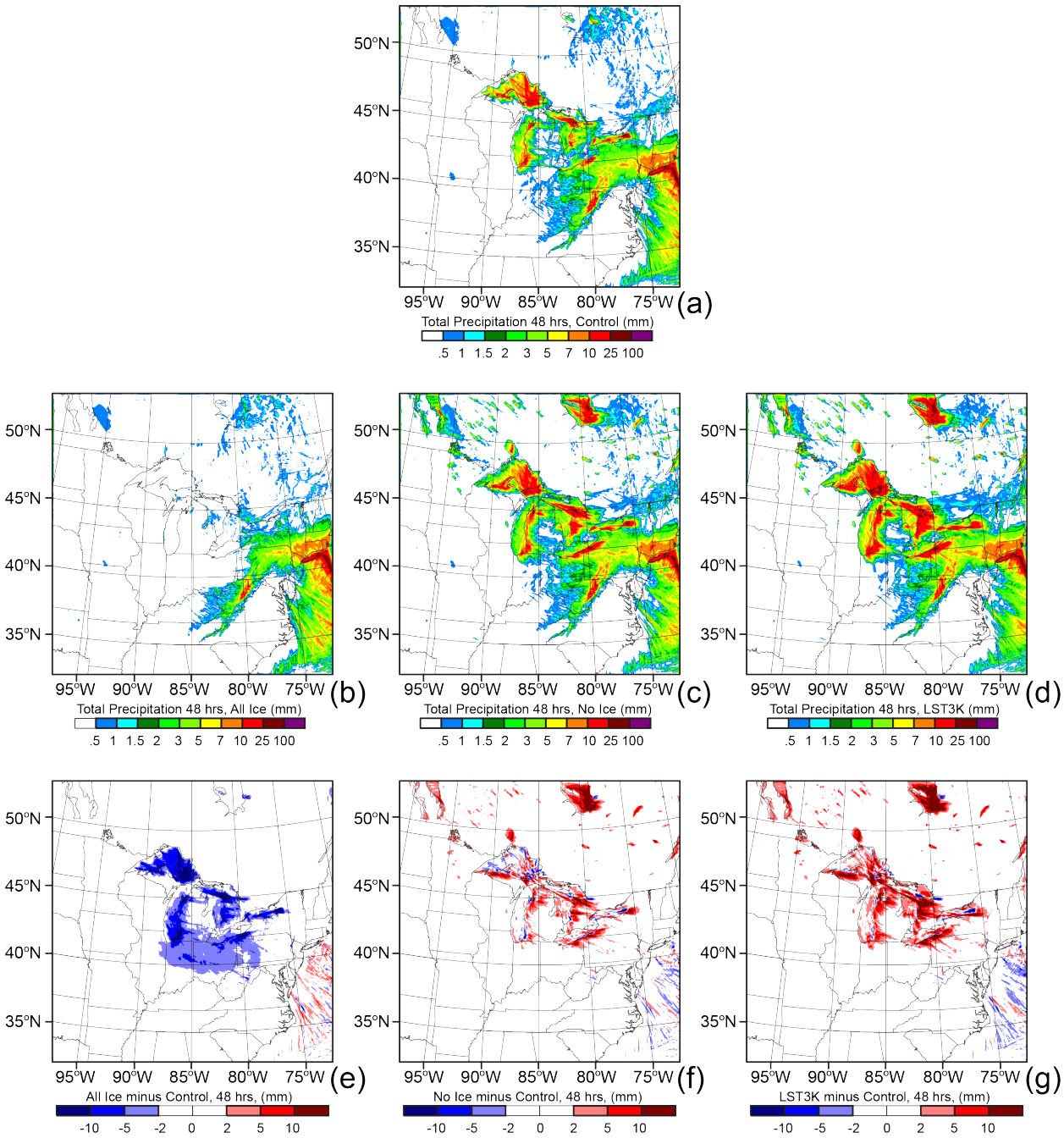

Figure 2.4. 48-hour (0000 UTC 15 Jan – 0000 UTC 17 Jan) accumulated precipitation (in millimeters) from (a) CTRL, (b) ALLICE, (c), NOICE, and (d) LST3K. Difference plots (taken with respect to CTRL) are depicted in the third row for (e) ALLICE – CTRL, (f) NOICE – CTRL, and (g) LST3K – CTRL.

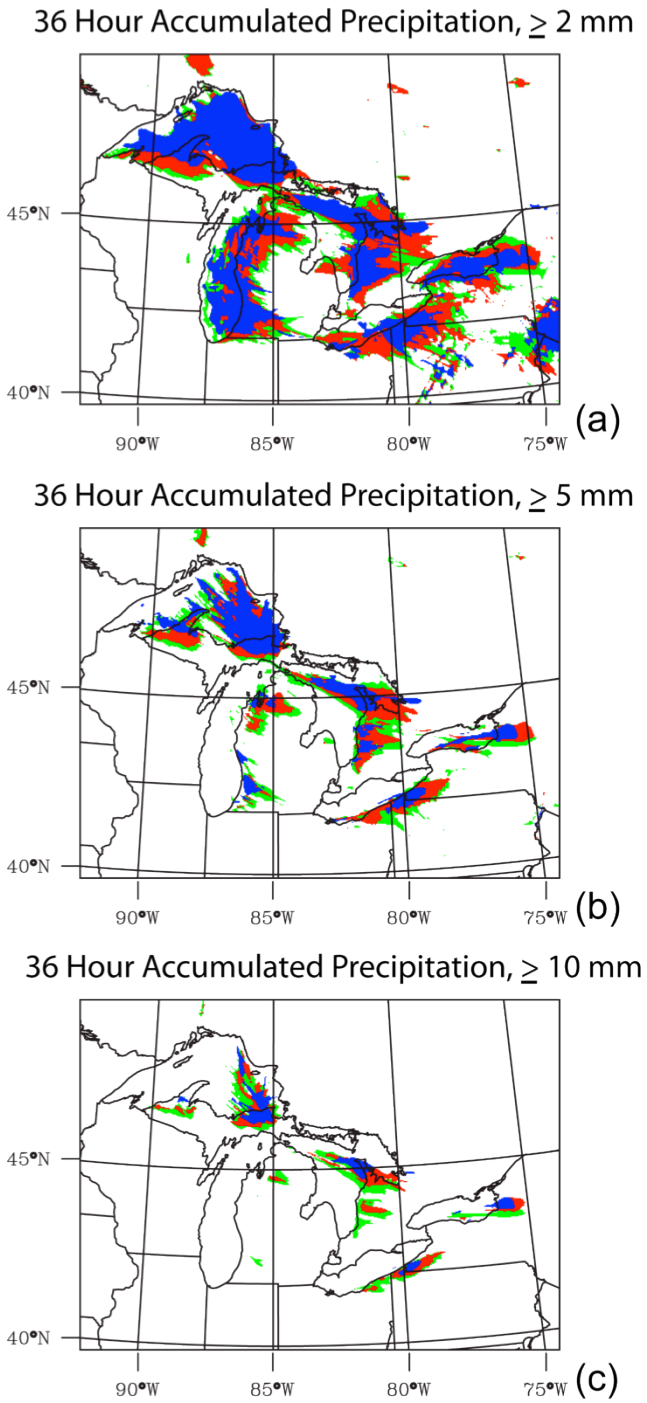

Figure 2.5. Mask enclosing regions of 36 hour accumulated precipitation greater than or equal to (a) 2 mm, (b) 5 mm, and (c) 10 mm. In each plot, the blue area encloses precipitation from CTRL, red from NOICE, and green from LST3K.

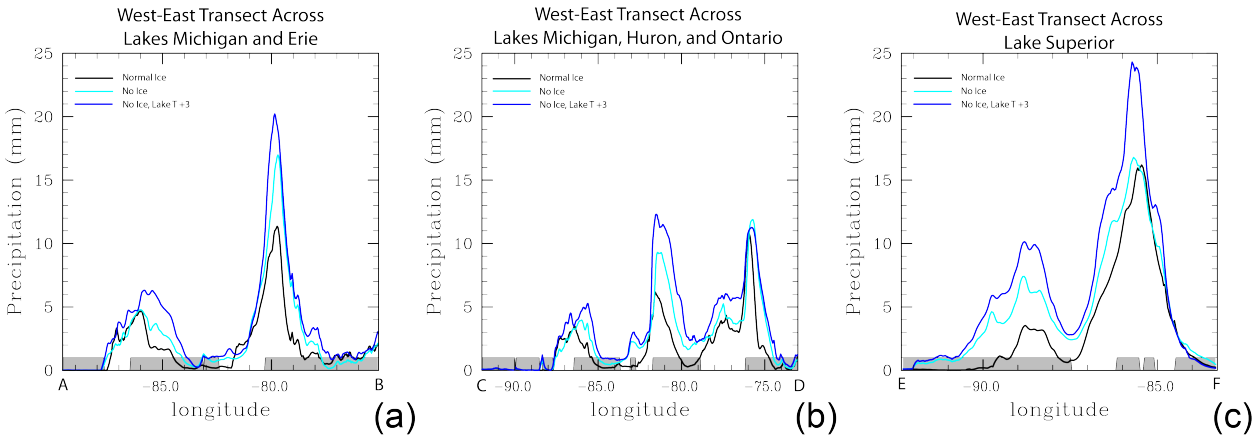

Figure 2.6. Precipitation averaged along the transects shown in Figure 2.1. Mean liquid equivalent precipitation (mm) is depicted for the control (black line), no-ice (cyan), and +3 K LST (blue) cases. The gray shading at the bottom shows the land area with white areas depicting the locations of (a) Lake Michigan (left) and Lake Erie (right) in transect A-B, (b) Lakes Michigan, Huron, and Ontario from left to right in transect C-D, and (c) Lake Superior in transect E-F.

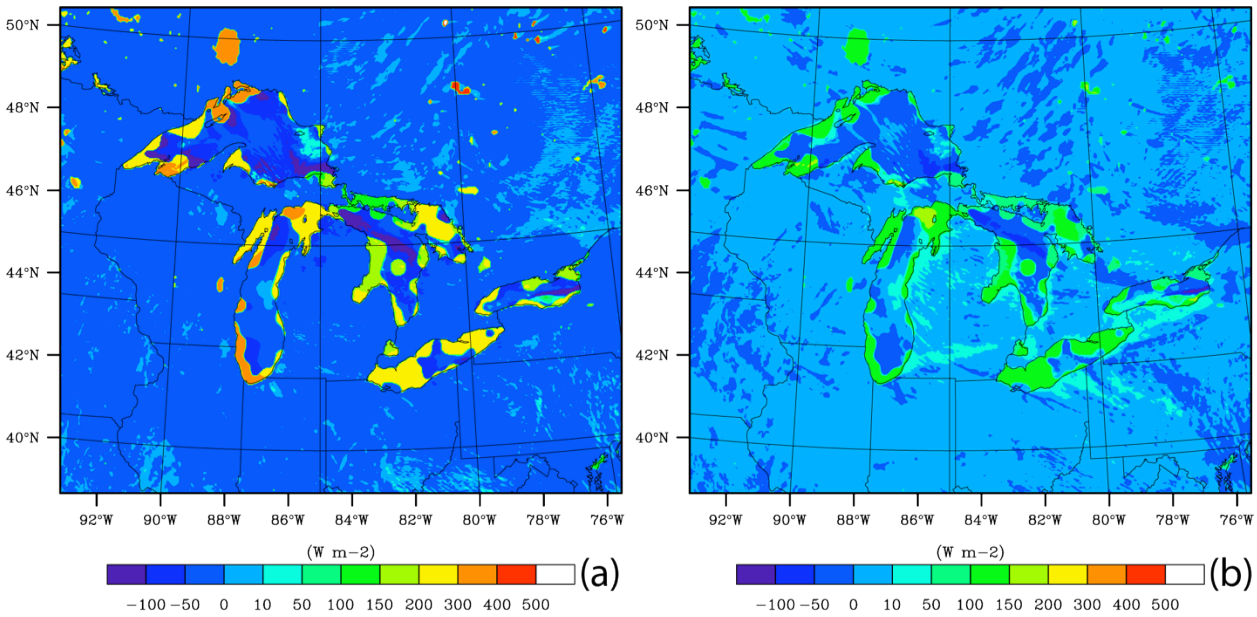

Figure 2.7. NOICE – CTRL change in the daytime mean (1600-1900 local time) surface (a) sensible and (b) latent heat flux.

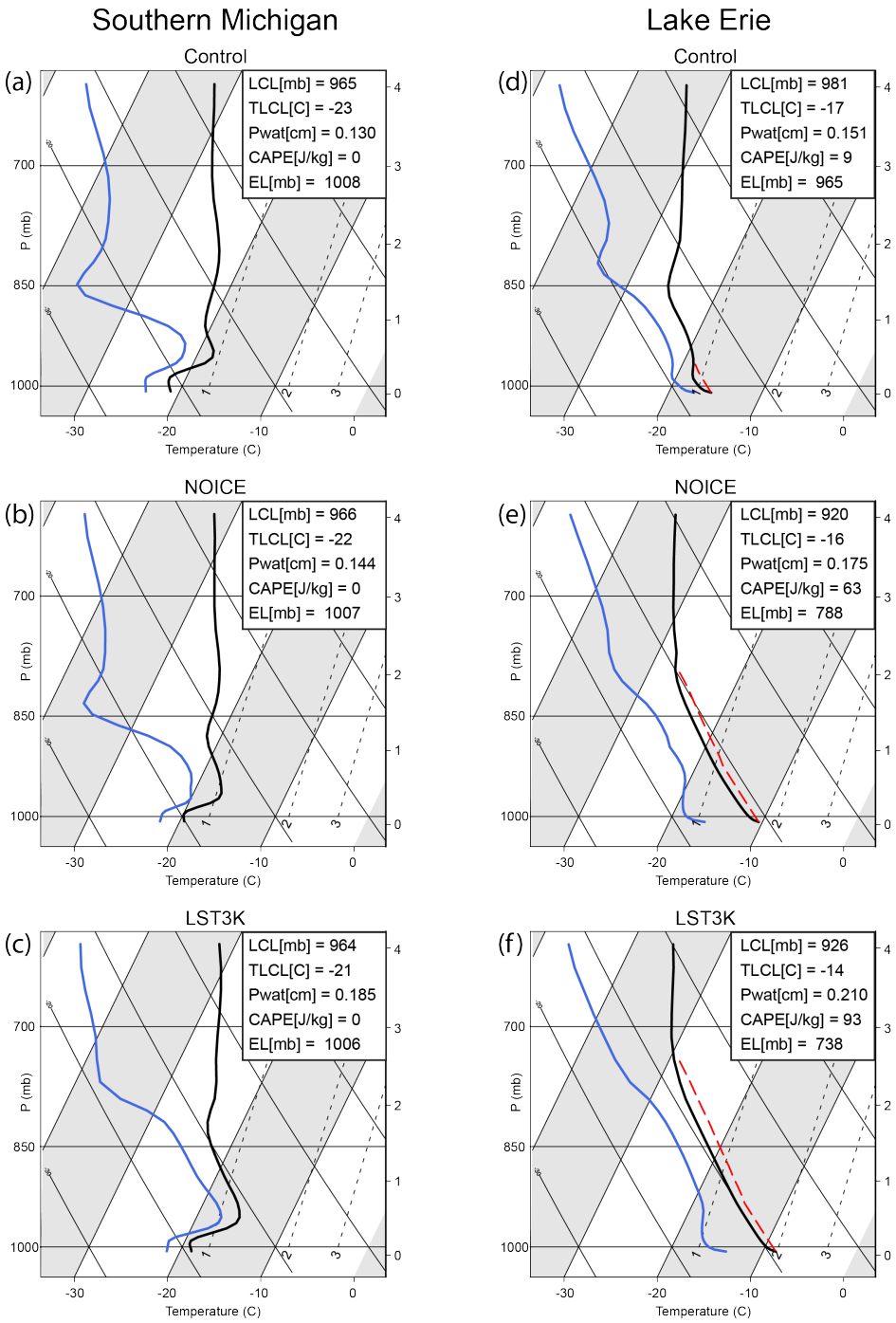

Figure 2.8. Skew-T, log-p plots of atmospheric soundings for (a and d) CTRL case, (b and e) NOICE case, and (c and f) LST3K case at 1200 UTC 16 January, and averaged over a 6x6km grid located over (a, b, and c) southern Michigan and (d, e, and f) Lake Erie. The location of each 6x6 grid is shown in the "X"s in Figure 2.1. In each figure, the black line represents the temperature, the blue line represents the dew point temperature, and the red dashed line represents the temperature of a parcel lifted from the surface.

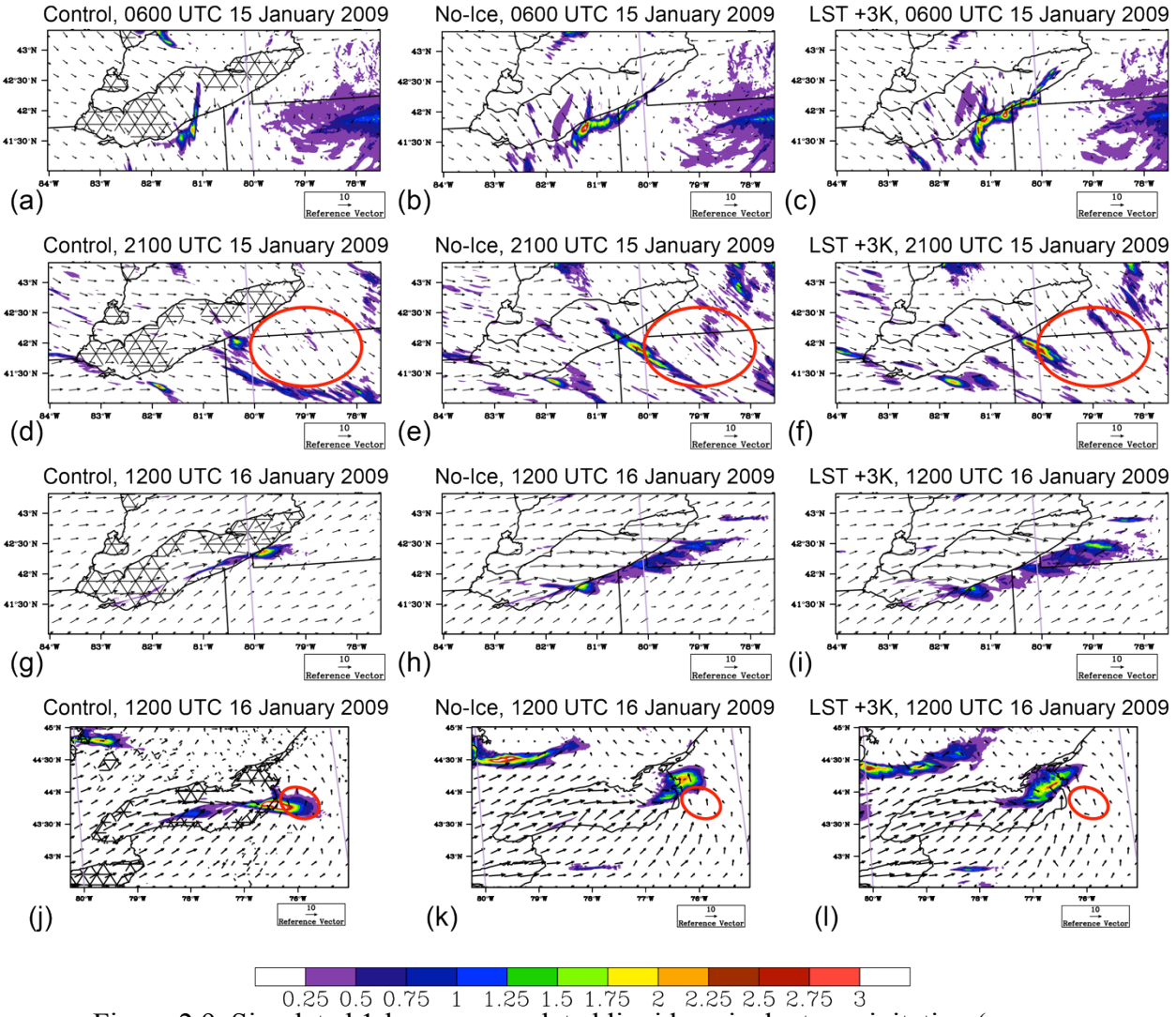

Figure 2.9. Simulated 1-hour accumulated liquid equivalent precipitation (mm, color filled contours) and 10-meter wind vectors (m/s) for the control (a,d,g,j), no-ice (b,e,h,k), and +3 LST (c,f,i,l) simulations at three different times (0600 UTC 15 January (a,b,c), 2100 UTC 15 January (d,e,f), and 1200 UTC 16 January (g,h,i,j,k,l)). The cross-hatched shading in the first column depicts the extent of ice cover in the control case. Note the first three rows depict Lake Erie, while the last row corresponds to Lake Ontario. Red circles in (d) – (f) and (j) – (l) depict the location of the Allegheny and Tug Hill Plateaus, respectively.

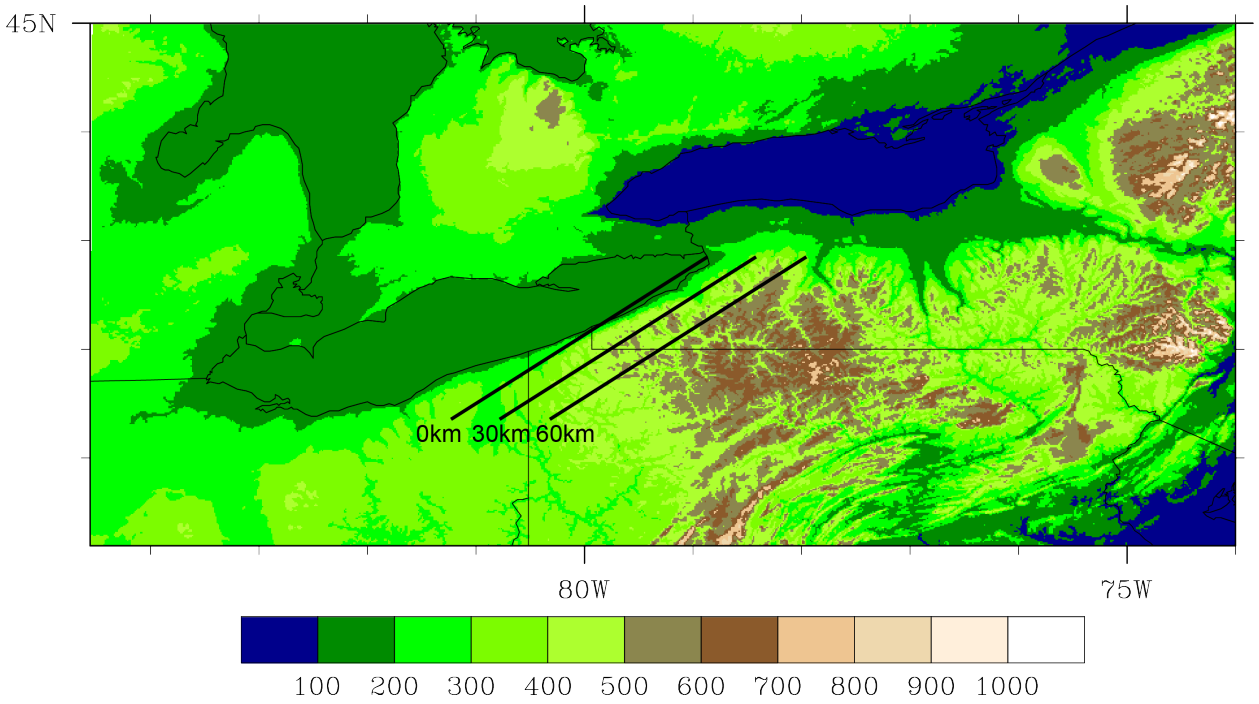

Figure 2.10. Terrain height above sea level in meters (color filled contours). The position of each transect in Figures. 2.11-2.13 are indicated in the solid black lines.

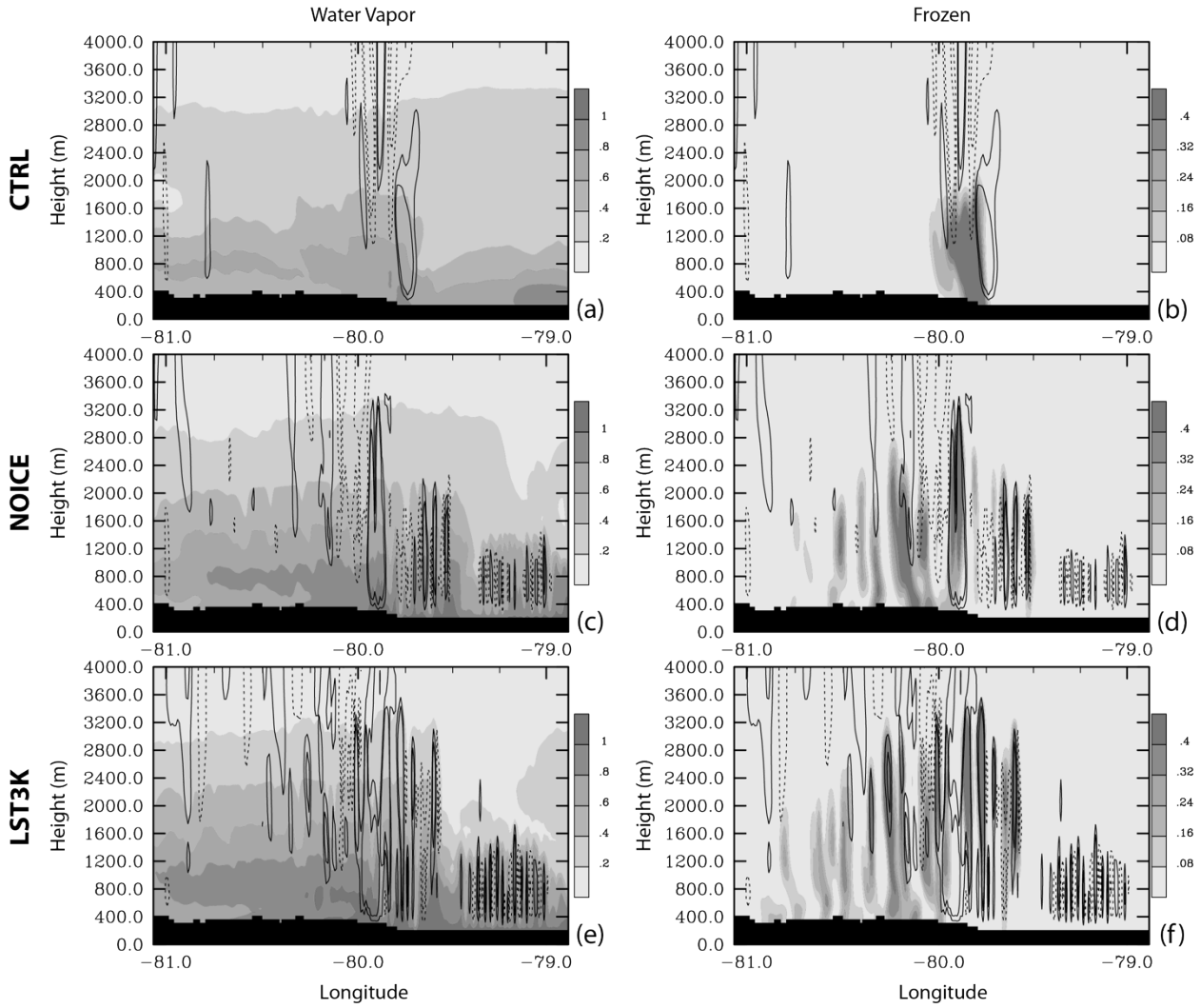

Figure 2.11. Vertical cross sections of water vapor and frozen (sum of snow, ice, and graupel) mass mixing ratios (in g kg^{-1}, grayscale filled contours) overlaid with contours of vertical velocity (in m s^{-1} every 0.5 m s^{-1} between -1.0 and 1.0 m s^{-1}, unfilled black contours; negative values are dashed) for 1200 UTC 16 January 2009 at the 0 km transect plotted in Figure 2.10. Note that the total liquid mass (cloud and rain) was negligible at this time.

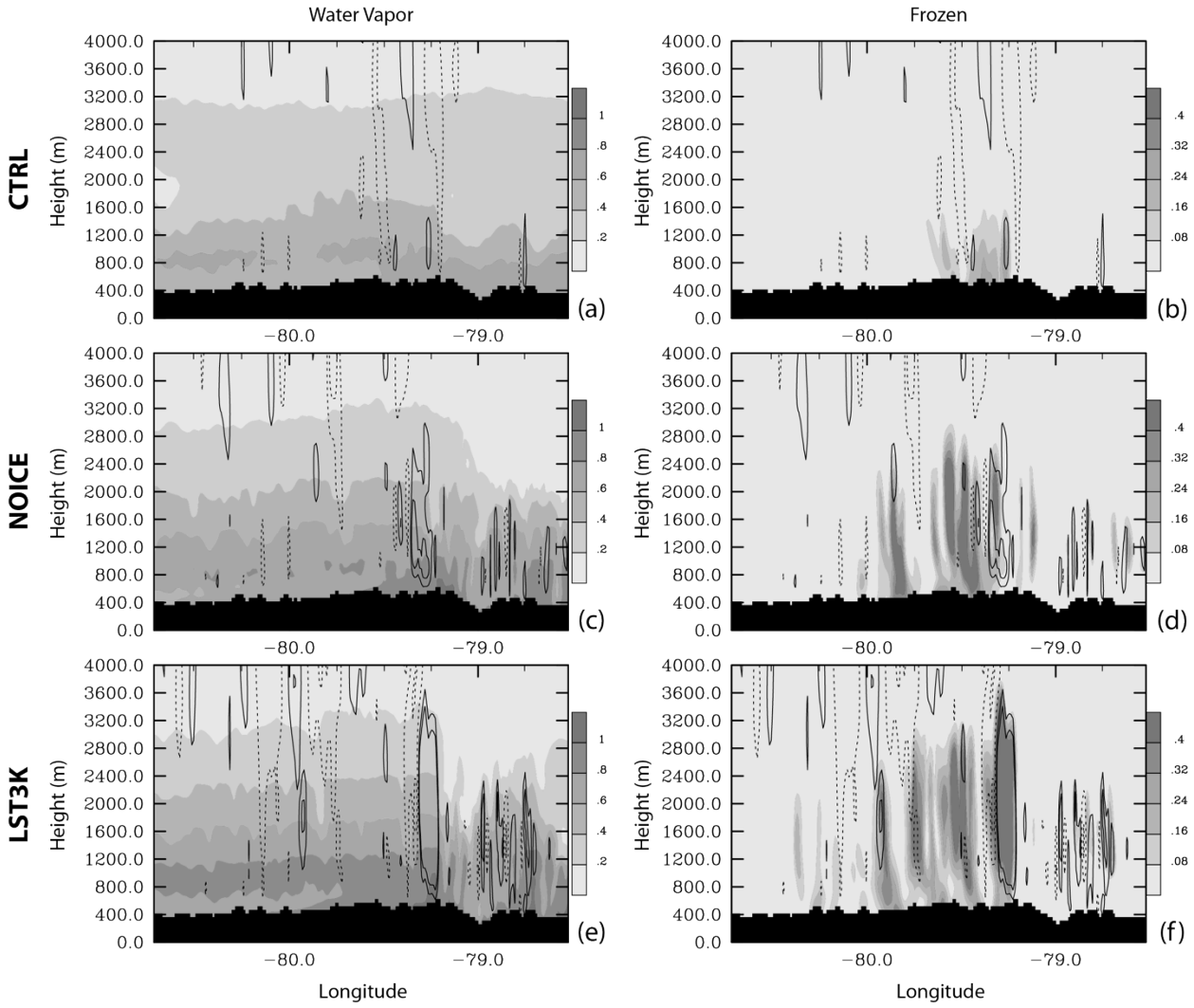

Figure 2.12. Same as Figure 2.11, except at a location 30km downwind of the southern Lake Erie shoreline.

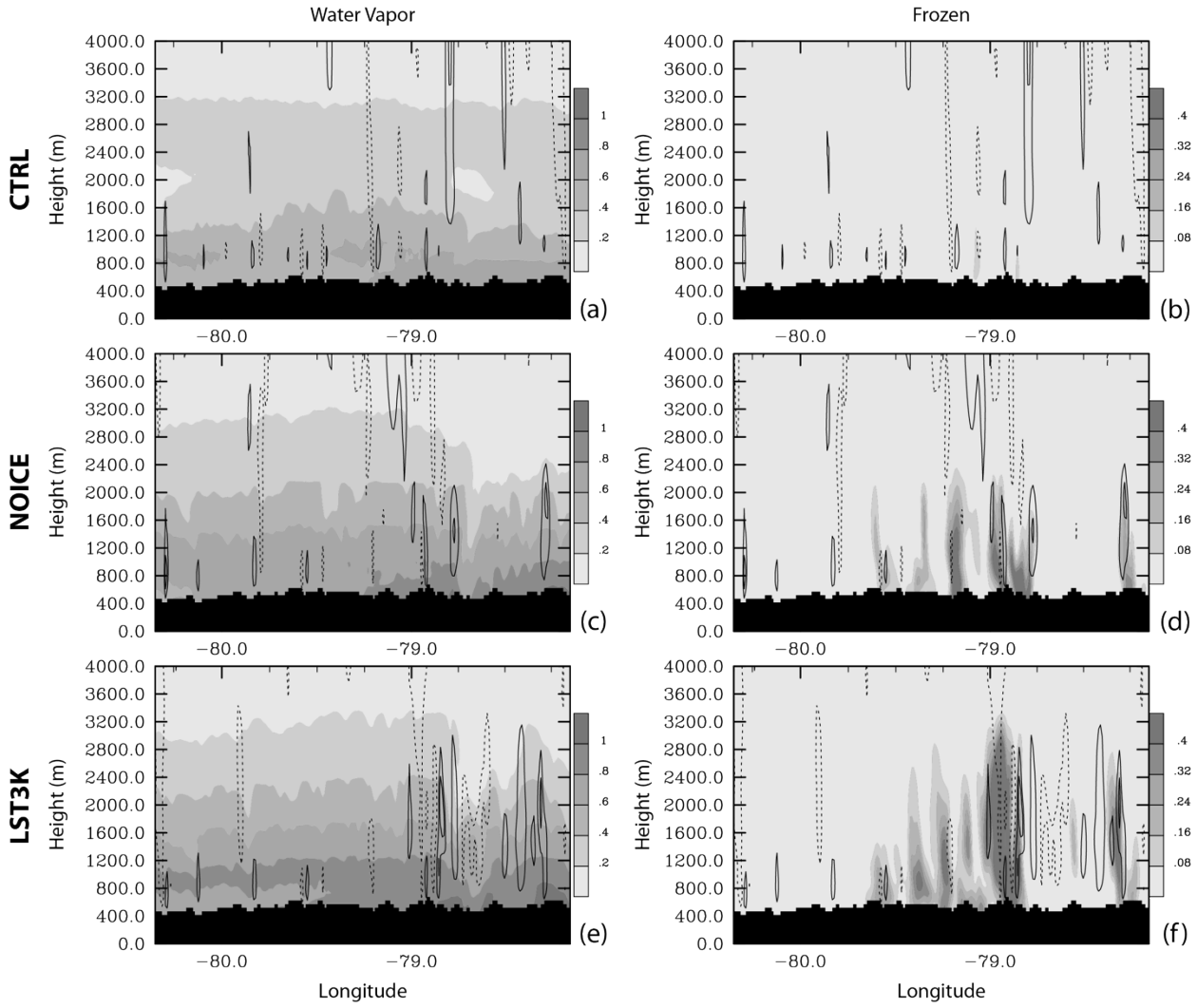

Figure 2.13. Same as Figure 2.11, except at a location 60km downwind of the southern Lake Erie shoreline.

CHAPTER 3. INTERACTION BETWEEN POTENTIAL VORTICITY AND THE SOUTHEASTERN LAKE MICHIGAN SHORELINE

3.1 Introduction

During the summer months, the lake surface temperatures of the Great Lakes are normally colder than the overlying air and surrounding landmass, producing a strong and often very shallow atmospheric stable layer near the surface of the lake. This temperature difference between the landmass and lake surface can also lead to the development of lake breezes. The faster warming of the land compared to water during the daytime allows for the formation of the lake breeze through localized pressure gradients initializing the onshore flow of cooler air.

Lake breezes in the Great Lakes region develop and have similar characteristics to sea breezes due to the large size of the lakes. Crosman and Horel (2012) used an idealized, large-eddy simulation, and showed that large lakes (100 km diameter) had very similar characteristics in terms of depth of inflow layer, total inland extent, and inflow wind speed as compared to sea breezes and observations of lake breezes made by Keen and Lyons (1978) on the western shore of Lake Michigan. Lake Michigan is approximately 185km wide. Onshore wind velocities have been measured to be on the order of 10 knots during lake-breeze events (Smith 2001). The depth of the onshore component of the lake breeze has been shown to be between 100m and 1000m, with a typical value around 500m (Moroz and Hewson 1966, Lyons 1972, Keen and Lyons 1978). This is shallower than sea breeze heights, which have onshore flows ranging between 300 and 2500m in depth (Miller et al. 2003).

Ryznar and Touma (1981) explored the lake breeze along the southwestern shore of Lake Michigan, using a series of ground-based weather stations within 20km of the lakeshore. Using records from 1973 to 1978, they observed that July and August had the most frequent lake breezes, followed by May. Most of these propagated inland between 5 km and 19 km, with almost half of the identified events moving more than 19km inland. Of these cases, most formed under clear skies and with weak offshore flow (less than 7 m/s). Lyons and Olsson (1972) found that the leading edge of a lake-breeze front could have updrafts that are 2km wide with 1m/s vertical velocities.

Smith (2001) examined the characteristics of lake breezes downwind of Lakes Michigan and Huron over the northern portion of the lower peninsula of Michigan. In his study, 4 stations were used along the lake (2 near Lake Michigan, 2 near Lake Huron), along with one in central Michigan to record the land temperature away from the lakes' direct influence. Lake breezes were observed to occur with differences in land and lake temperatures ranging from 2 to 25 degrees Celsius. It was found that 950mb wind speed and direction had a much stronger influence on lake breeze occurrence, with 950mb wind speeds greater than 12 to 18 knots (depending on the lake) nearly eliminating the onset of lake-breezes.

Biggs and Graves (1962) developed an index to predict the formation of lake breezes on Lake Erie's western shore based on the ratio of the inertial force to the buoyancy force. A strong positive buoyancy force was found to lead to more lake breezes due to a significant influence from the temperature difference between land and lake, creating local pressure differences across the shore. Lyons (1972) modified and applied the index to the southwest shore of Lake Michigan to create a climatology of lake breeze days and

test the forecast capabilities of this index near Chicago, IL. In his study, it was found that of 307 summer days during 1966-1968, the western shore of Lake Michigan exhibited a lake breeze on 36% of the days, while the eastern shore experienced a lake breeze on 25% of the days. This drop in frequency between the western and eastern shores was attributed to the westerly flow over the region making the identification of a convergence zone, typical of a lake breeze, difficult on the eastern shore. Most of the forecasting errors that occurred with the index were found when excessive cloud cover was present or the large-scale flow was not taken into account.

Laird et al. (2001) continued this work by creating a record of lake breezes for the eastern and western shores of Lake Michigan from 1982-1996. The authors used the change in wind direction from offshore in the morning to onshore in the afternoon, the temperature difference between land and lake, the average air temperature in the morning being lower than during the afternoon, and the average wind speed less than 5.5 m/s inland from the coast to define the occurrence of lake breezes that propagate more than 4km inland on the eastern and western shore of Lake Michigan. The frequency of lake breezes on the eastern shore was found to be 35% compared to western shore lake breezes having an occurrence rate of 41%, slightly higher than the frequencies reported by Lyons (1972). When applying the Lyons (1972) index, Laird et al. (2001) found that eastern shore lake breezes occurred on 24% of the days, closer to the original frequency. In hind casts, this method was able to accurately identify non-lake breeze days on the eastern shore 89% of the time. They also found that by self selecting lake breeze and non-lake breeze days by their guidelines and applying the lake breeze index from Biggs and Graves (1962), the index would under identify days with a lake breeze by 20% while

producing false detections on 60% of days without a lake breeze. The synoptic scale composite conditions for lake-breeze days on the eastern shore of Lake Michigan showed high pressure over western Ohio/Michigan with weak surface winds out of the southeast. High pressure centered over the lake led to a lake breeze on both eastern and western shores.

While these indices do aid in the forecasting of lake breezes, they are not able to represent the potential for convection and rainfall that can be associated with lake breezes due to the convergence and displacement of air vertically along the leading edge (e.g. Chandick and Lyons 1971). Convective storms interact with the lakes and lake breezes several times per year in the Great Lakes region and pose a challenge to forecasters due to lack of a complete understanding of how these storms interact with near surface features created by the lakes. Lyons (1966) observed several storms interacting with the east and west shores of Lake Michigan. In some of these cases, Lyons attributes an observed reduction in convective activity as a storm passes over Lake Michigan to colder, more stable air being ingested by a storm, causing it to reduce in intensity. The delay in the onset of convection to the east of Lake Michigan is attributed to convective plumes generated over land being suppressed by stable lake air moving over land, leaving the skies near the shore clear while cumulus clouds developed away from the shore. Wilson (2008) looked at the creation and suppression of convection by lake and sea breezes over the northeastern United States (including Lakes Erie and Ontario), through both observations and the North American Regional Reanalysis (NARR). From 2000 to 2006, a total of eleven cases where lake or sea breezes were believed to play a role in initiation or suppression of convection were studied. Of these cases, four were determined to be

purely lake/sea breeze induced convection, six were identified as having both local and synoptic forcing (mixed) leading to the convection, and one was determined as the existence of the water surface leading to the suppression of existing convection. In the mixed cases, the convection was attributed to the lake breeze providing the necessary lift to elevate near surface air to the level of free convection (LFC) with aid from weaker, background synoptic scale lift. In all six of these cases, an area of positive vorticity advection was present over the region. Subsidence over the water from the return flow of the lake breeze was attributed to inhibiting convection initiation over the lake for a single case.

King et al. (2003) observed that cumulus clouds tend to be more intense when synoptic scale forcing interacts with lake-breeze fronts off of Lake Huron than clouds that developed along similar lake-breeze fronts near Lake Huron. The authors also observed a rapid decrease in IR brightness temperature as a cold front moved from over Lake Huron to over land, signifying intensification of the convection. They attributed this rapid intensification to the interaction of the cold front with the lake breeze.

Kristovich et al. (2003b) investigated thunderstorms that formed along lake-breeze fronts off of the southern coast of Lake Erie. They examined 6 different cases of thunderstorms forming along the front, and discovered that the low-level shear of the environment played an important role in determining if the storms would intensify. The low-level shear caused storms to propagate either along or perpendicular to the front. Storms traveling along the front stayed in an area of enhanced low-level convergence, allowing the storm to strengthen. They did note that due to the small sample size, it was yet to be seen if this interaction was consistent across a larger set of similar storms.

Chandik and Lyons (1971) observed storms moving parallel to the convergence zone associated with a lake-breeze front and came to a similar conclusion. Kristovich et al. (2003b) also found that when the environmental shear was opposite the lake breeze induced low-level shear, the storms were stronger than if the environmental and lake breeze shear was oriented in the same direction.

Workoff et al. (2012) found that storms passing over Lake Erie had a tendency to decrease in intensity 60 minutes after passing the upwind shore. Storms were classified into four categories based on morphology of the system on the upwind side of the lake (linear, cluster, isolated, and complex), with isolated and cluster systems showing a decrease in radar reflectivity as storms moved from over land to the colder air over water. Lower intensity changes were observed for linear and complex systems with this transition, but changes were sensitive to wind speeds 3 km above the surface. They attributed the time over which storm intensity was reduced to the time needed to ingest cold air near the lake surface into the storm. These conclusions were highly dependent on storm structure, with linear storms showing the least influence from the lake. This is partially due to the dependency of isolated and cluster storm systems to local, low-level instability for their initiation and lifetime. Linear and complex systems maintained their intensity longer over a stable surface layer than the isolated and cluster systems.

Workoff et al. (2012) concluded that it may be possible for unstable air, originating over land, to move over the top of the over the lake-generated stable layer, providing the necessary instability at higher altitudes over the water to maintain existing convective storms, but further investigation was still needed.

While there has been extensive work on studying lake breezes, storms interacting with the stable layer over the lakes, and the forecasting of these features, there are still outstanding questions regarding the direct role the lakes have on the formation and interaction with existing summertime convection. There are still questions as to how much the lake surface and associated lake breezes assist in the initiation of convection downwind of the lake, and the relative frequency of occurrence. As pointed out in Workoff et al. (2012) and studied by Metz (2011), there is still a significant amount unknown as to the role the stable boundary layer over the lake has on existing convection. There are also questions regarding how this stable layer will change in a warmer climate and how those changes influence the local atmospheric circulations over the region. With lake temperatures predicted to increase by at least 3 Kelvin in a future climate (Trumpickas 2009), it is important to understand what role this increase would have on the stable boundary layer over the lake and convection associated with this layer. Arritt (1987) did study the sensitivity of lake breezes to lake surface temperatures using an idealized 2D model and found that a lake breeze would form until the lake and land temperatures were approximately equal, removing the stable layer over the lake.

In this paper, we introduce a case that occurred on May 5, 2003 in which a line of thunderstorms initiated along the eastern shore of Lake Michigan. We examine the characteristics typically associated with a lake breeze for the case study and show that, while the index predicts a lake breeze, the lake surface or a lake breeze does not initiate this case study. We also explore upper air features and sensitivity of the convection to the lake surface to show that convective initiation is related to the upper air forcing with little direct influence of the lake. This chapter is organized as follows: Section 3.2 describes

the case study and reviews the model setup; Section 3.3 provides the results; Section 3.4 contains a discussion of results, and Section 3.5 summarizes the conclusions.

3.2 Case Study and Model Configuration

3.2.1 May 5, 2003

On May 5, 2003 at 12 UTC, a mature low-pressure system was located over eastern Iowa (Figure 3.1). The surface low was nearly collocated with centers of low geopotential height at all levels of the troposphere, with only a slight tilt to the northwest with height. Over southwest Michigan, winds were out of the ESE with widespread rainfall. Winds began to shift to out of the southwest at 17 UTC as the skies cleared from south to north (Figure 3.2). Temperatures ranged in the afternoon from around 20 degrees Celsius over southwest Michigan to around 10 degrees Celsius over central Michigan. The stationary buoy (number 45007; NOAA/NDBC (1981)), located in south-central Lake Michigan, measured an air temperature of 6 degrees Celsius 4m above the lake surface and a lake temperature at .6 m below the surface of 3.2 degrees Celsius in the afternoon.

Just before 18 UTC, a group of cumulus clouds moving over Lake Michigan made landfall on the eastern shore (Figure 3.2b). When this happened, a narrow line of clouds developed along the shore and moved several kilometers inland from the lake. At 1915 UTC, a second cluster of clouds moved over Lake Michigan, eventually interacting with the initial line of clouds over land (Figure 3.2c). This line at 2030 UTC intensified to a line of convective clouds with clear skies to the west towards the lakeshore. This line continued to move away from the lakeshore, holding a similar structure to the southeastern portion of Lake Michigan (Figure 3.2d).

NARR calculated convective available potential energy (CAPE) values were between 1300 and 1500 J/kg ahead of this line of storms during the afternoon**.** This area of enhanced CAPE stretched from central Michigan to the south, parallel to the Indiana/Illinois state line. CAPE values in Illinois and Wisconsin were between 300 and 500 J/kg. A vorticity maximum at 500mb was located near the center of the surface low over southwestern Minnesota with a second area of vorticity over northern Illinois (Figure 3.3).

By 00 UTC on May 6th, the surface low moved to the east over central Wisconsin. During this time, the line of convection initiating off of Lake Michigan had developed severe thunderstorms. From 12 UTC on May 5th to 12 UTC on May 6th, the line of thunderstorms produced high winds, hail, and one tornado across southeast Michigan (NOAA/SPC 1999). These severe reports highlight the high-impact nature of this event, but extensive analysis on the formation of these phenomena is outside the scope of this project. This study will focus on the initial formation of the convective line and the placement off the eastern boundary of Lake Michigan.

3.2.2 Model Configuration

The Weather Research and Forecasting Model (WRF; Skamarock et al. 2008) version 3.4.1 was used to create a 10km horizontal grid (D01, 280x250 grid points) with a one-way nested 2km horizontal grid (D02, 851x631 grid points) centered over the Great Lakes to simulate the conditions surrounding Lake Michigan and the convective initiation (CI) on May 5, 2003 (Figure 3.4). 51 custom ETA vertical levels were used for both domains, with 20 levels within 1.5km of the surface (APPENDIX C). These domains simulated the 48 hours from May 4, 2003 at 12 UTC to May 6, 2003 at 12 UTC, with

initial and boundary conditions derived from the North American Regional Reanalysis (NARR; Mesinger et al. 2006, Rutledge et al. 2006). Table 3.1 shows the physics parameterization options for each domain (see APPENDIX D for discussion on physics options tested).

	Domain 1 (10km)	Domain 2 (2km)
Longwave Radiation	RRTM	RRTM
Shortwave Radiation	Dudhia	Dudhia
Planetary Boundary Layer	MYJ	YSU
Land Surface	Noah	Noah
Cumulus	Grell-Devenyi Ensemble	None
Microphysics	Morrison 2-moment	Morrison 2-moment

Table 3.1. Physics parameterization schemes used in the WRF simulations.

Lake surface temperatures were initialized from the NARR skin temperature and remained static throughout the simulation. In addition to the control simulation (Control) with NARR derived lake surface temperatures, two sensitivity simulations were performed to explore the role Lake Michigan played in the line of precipitation observed. The first sensitivity simulation raised the lake surface temperatures uniformly by 3 Kelvin (LST +3) across all lakes in D02 only. Lake temperatures remained unchanged for D01 as an attempt to look directly at the local scale changes while reducing the potential for synoptic-scale changes. This change in lake temperature (APPENDIX A), serves two purposes. The first is to explore the role of the lake surface temperature in this type of CI. Arritt (1987) explored the influence of the lake surface temperature on lake breezes using an idealized 2D model, finding that the development of the modeled lake breeze was not significantly altered by changes in lake temperature, as long as the lake was able to still create a stable boundary layer over the lake. When warming the lake to approximately 4 degrees Celsius greater than the inland surface temperature, the lake breeze was suppressed. When cooling the lake temperature to a uniform 0 degrees Celsius (a

reduction of approximately 12.5 degrees Celsius near the lakeshore), the winds of the lake breeze were unaltered. The greatest change was the distance the thermal internal boundary layer propagated inland. While the lake breeze itself may not be altered by lake temperature changes, if it is present, this case study will investigate the sensitivity of this CI to alterations to the stable boundary layer. Second, this simulation is used to explore the role of a potentially warmer lake temperature in a future climate on the placement and intensity of CI (Trumpickas 2009).

The second sensitivity study removes Lake Michigan (No Lake), similar to earlier studies by Sousounis and Fritsch (1994) and Metz (2011) to find the direct influence of the lake on atmospheric circulations. In this simulation, a lat/lon box is selected to encompass Lake Michigan and water grid points in this box are changed to a cropland/grassland mosaic (as defined by the USGS 24 land-use categories), a common type near the lake (Figure 3.5). Soil temperature, moisture and other land surface characteristics are also adjusted to reflect values within the region (APPENDIX B). The greatest soil temperature differences are on the order of 6 degrees Celsius located near the city of Holland, MI, with the former lake surface being warmer than the landmass at the initialization. Typical soil temperature differences are less than 4 Kelvin across the former lakeshore. The soil moisture fractional differences were on the order of .01, with the greatest being on the order of .08 near the Traverse City, MI area.

3.3 Results

For the following sections, only results from D02 will be presented, as the outer domain (D01) was primarily used to ensure the larger scale (synoptic) flow features and environment was contained within the model domain. Figure 3.6a and d shows the

simulated composite radar reflectivity at the time of convective initiation and observed composite radar reflectivity (NOAA/National Center for Environmental Information (1995)), respectively. CI first appeared on radar along a line parallel to the lakeshore at approximately 2010 UTC. The simulation does reproduce a line of convection, but three hours earlier at 1720 UTC and approximately 40km to the west. In the Control simulation, the storms first initiated and moved to the northeast, parallel to the shore. In reality, the line progressed to the east-northeast as a distinct line. By 1920 UTC, the Control simulation began to move the line of precipitation to the east, further inland, as a linear storm system.

The difference between the synoptic scale flow in the simulation and RUC analysis at 1200 UTC is minor, but the Control simulation does shifts the center of the low pressure system over Iowa to the southeast. With this shift in placement, the WRF simulations move the system to the east faster than reality. There is agreement at all levels of the atmosphere as to the wind speed.

300mb potential vorticity (PV) shows that two areas of enhanced PV moved over southwest Michigan during CI and several hours after (Figure 3.7a and Figure 3.8a**)**. The first area, with greater than 4 potential vorticity units (PVU), moved across Lake Michigan and over land between 1700 and 1720 UTC, coinciding with the time of CI seen in radar reflectivity. The second area, with greater than 7 PVU, moved onto land at 2000 UTC just after the change in storm motion. In vertical cross-sections of PV (Figure 3.9a), a tongue of upper level PV lowered and moved over land at CI. While PV does not directly measure convective initiation, it does measure the combined influence of both changes in upper level stability and vorticity over an area.

As described by Martin (2006), vertical motion occurs ahead of positive PV advection. Increases in positive PV occur via an increase in the absolute vorticity, increase in the stratification of potential temperature, or both. In this case, both are occurring, through increases in absolute vorticity (not shown) and the tilting of potential temperature contours to the east of the anomaly, increasing the stratification of potential temperature just below the PV max. To generate this tilting and stratification of potential temperature surfaces, in the absence of diabatic heating, there must be large-scale vertical motion.

This upper-level vertical ascent eventually provided the necessary lift of the moist and unstable air at the surface over land to create the convective storms. Over water, the high surface heat capacity limits low-level heating and the dome of stable air created by the colder water surface, air in the boundary layer is not able to reach the level of free convection (LFC). The two PV maxima closely reflect the two waves of cumulus clouds that are initially seen in the visible satellite images (Figure 3.2b and c) moving over the lake before the line of clouds develop along the lakeshore.

While convection in the Control simulation occurs earlier than it did in reality, it is clear that this is due to the shift in the model's placement of the low-pressure system, and thus the placement of the PV associated with it. Simulation of the low-pressure center southeast of its true position allows for the PV to interact with the land surface east of the lake earlier in the simulation than in reality. Since our goal is to obtain a realistic simulation of the lake induced stable layer and the convection over southern Michigan, exact placement and timing of the convective line is not critical. We deem the Control

simulation to be a sufficiently accurate representation of the CI and the interaction between scales.

3.3.1 Was there a lake breeze?

As was shown in the previous section, the large-scale flow played an important role in the initiation of convection. Visual inspection of satellite imagery does at first glance seem to indicate convection initiated along a lake breeze, as the cloud line parallels the lakeshore (Figure 3.2). In this section, the characteristics typically needed to form a lake breeze are examined to determine if one was present for this case study. Figure 3.10a depicts the 950 hPa wind speed and direction during the simulation. At 1500 UTC the winds were out of the SSW, nearly parallel with the southeastern coast of Lake Michigan with little onshore component. Wind speeds are also greater than 18 knots, exceeding the critical value typically used for lake-breeze initiation found by Smith (2001). Wind speeds, as discussed in the previous section, are out of the ESE (offshore) over southwest Michigan during the morning hours at 12 UTC. These winds changed to southwesterly over the next five hours, becoming parallel to the shoreline approximately one hour before the first line of clouds formed. Wind speeds are on average between 5 to 7 m/s.

The temperature contrast between lake and land is approximately10 degrees Celsius, with lower temperatures over the water, as seen in the 2m temperatures (Figure 3.11a). This temperature contrast is not as strong at 50 and 100m above ground level (on the order of 4 degrees Celsius), but there are visible signs of the lake over the central and western portions (not shown). There is also a temperature gradient from north to south, with warmer air temperatures to the south along the lakeshore and colder temperatures further to the north over central Michigan (not shown). Just before CI, the temperature

gradient between land and lake remained nearly stationary, particularly over the southeastern portion of the lake. If a lake breeze existed, one would expect the low level potential temperature to exhibit a gradient moving to the east away from the lake, signifying the movement of air from over water to over land.

Figure 3.12a depicts the simulated 2m above ground level water vapor mixing ratio. The influence from the lake is evident here as the air moving in from the south has higher values of water vapor than the air residing over the lake. Near the surface, as this moist air moves in from the south, it does not replace the air located over the lake. Before the initiation, there is little evidence of on-shore movement of low-level air over the lake, as would be expected in a lake breeze. The lack of a lake breeze can also be seen in the 10m-wind convergence (Figure 3.13a); there is no evidence of a down-stream lake parallel convergence zone. The patterns shown in Figure 3.13a are consistent at 50 and 100m above ground level (not shown).

Just before initiation, at 1700 UTC, there is an area of divergence of the low level winds along the eastern edge of Lake Michigan, but located north of where the convection initiates. There is a turning of the winds from parallel to the coast to onshore, but the predominant direction is still oriented parallel to the coast. Only minor convergence of air is occurring in this location and along the southern and southeastern edges of Lake Michigan where convection first initiates in the model. If a lake breeze was present, then it should show areas of both divergence offshore and convergence at a lake-breeze front. The component of the wind direction onto the shore is also minimal compared to the background wind speed.

The criteria defined by Laird et al. (2001) to identify lake breeze cases would characterize May 5, 2003 as a lake breeze. Winds during the morning hours (0500 – 0700 LST) were offshore, while during the afternoon (1600 – 1800 LST) they were onshore with an average wind speed of less than 5.5 m/s at the Kalamzoo/Battle Creek station. The average morning hour temperatures were approximately 8 degrees Celsius lower than the afternoon temperature, with the maximum temperature difference on the order of 18 degrees Celsius as compared to buoy observations. The Biggs and Graves (1962) lake breeze index, using surface observations over central Michigan and Lake Michigan buoy, positively identifies this day as having a lake breeze. The synoptic scale conditions, on the other hand, do not resemble those found by Laird et al. (2001), where high pressure is expected near or over Lake Michigan. The closest surface high-pressure system on this day is located off the east coast of North America (Figure 3.1d).

Both the simulations and synoptic scale analysis conclude that there was not a lake breeze present on this day. While the criteria for a lake breeze created by Laird et al. (2001) and Biggs and Graves (1962) do identify this day as having a lake breeze, these criteria have been shown to exhibit false positives and do not take into account the synoptic scale conditions. The following sections will further show that the lake was not necessary in the development of the convection over the region.

3.3.2 Role of the lake surface temperature in convective initiation

As described in Section 2, the lake surface temperature was raised by 3 Kelvin uniformly across all the Great Lakes to test the direct role the lake surface temperatures have on the overall CI, strength, and placement. Figure 3.6a and c depicts the radar reflectivity after initiation of both the Control and LST +3 case study, respectively. These

two simulations show similar results in the timing, placement, and intensity of the convection. Even with a warmer lake surface temperature, there is still a considerable stable layer located in approximately the same location (not shown).

2m water vapor mixing ratios (Figure 3.12c) depict a similar horizontal gradient from over water to over land, but weaker than in the Control simulation (Figure 3.12a). This weakening is due to a reduced moisture flux from the atmosphere to the surface in the LST +3 case.

The 10m wind convergence (Figure 3.13c) reveals minor differences in the convergence and divergence patterns along the lakeshore as compared to the Control simulation (Figure 3.13a). All of these metrics point to very little influence directly from the lake temperature on this initiation. These results are consistent with Arritt (1987) who looked at the lake temperature influence on lake breeze formation (further discussed in Section 3.4).

3.3.3 Influence of the lake surface

As described in Section 2, Lake Michigan was removed from the simulation and replaced with land to directly measure the influence of the lake on the CI. Figure 3.11a and b shows the comparison of the 2m temperatures between the Control and No Lake simulations, respectively. The 2m temperatures over the former lake surface are approximately the same as the temperatures over land, greatly reducing the horizontal temperature gradient. 2m water vapor mixing ratio (Figure 3.12b) also displays a reduced west to east gradient in the No Lake simulation, with values near uniform across the former lakeshore. Vertical cross-sections (Figure 3.9b) also depict a warmer boundary layer over the new land surface, as seen in the increase in potential temperature at 850mb.

The location and strength of the positive potential vorticity feature has also not changed, demonstrating that the removal of the lake has changed the overlying air to be similar to that over the and surface near the lake, without changing the large scale circulation.

Figure 3.6b shows that, despite removal of the lake, convection still occurs at the same time and approximate location as it did in the Control. The No Lake simulation does change the orientation of the line of storms from N - S along the lakeshore to NE - SW. The radar reflectivity values do change slightly between the two simulations, with the No Lake simulation depicting larger cells while the Control produces stronger but smaller cells.

3.4 Discussion

Through the previous results, specifically the removal of Lake Michigan, it is shown that during this case study the predominant forcing for convective initiation (CI) was the passage of an upper level potential vorticity anomaly over a convectively unstable region. After removing the lake, CI still occurred at the same time as in the Control case, but slightly to the west and at an angle that matched the leading edge of the upper-level PV feature. Wilson (2008) attributed events in which a positive PV anomaly passed over the lake as being partially contributed to by the lake breeze. While this could be possible, in particular in helping to change the intensity along the edge of the stable lake boundary layer, this single case study shows little influence on the CI directly from a lake breeze.

The lake did play a role in determining the placement of the convection in the following ways. First, the cold lake water produced a stable layer that inhibited convection over the lake. Workoff et al. (2012) examined how this stable layer may play a role in lifting unstable air from over land to a position above the stable boundary layer

of the lake such that parcels either become positively buoyant (initiating convection) or help to maintain existing convection crossing the lake. While this process may operate in other cases, it is not observed it in this case in either observations or simulations. Convection initiated over land east of the lake, not above the lake induced stable layer. It is possible that the type of initiation described by Workoff et al. (2012) could have happened in this case had the unstable air south of Lake Michigan been transported due north to interact with the upper level PV feature as it passed over the lake surface.

Lyons (1966) observed a similar case study to the one presented in this paper along the western shore of Lake Michigan, in which a mesoscale convective system interacted with a lake breeze north of Chicago, IL, producing stronger rainfall near the interaction between the mesoscale cold front and the lake-breeze front. The meso cold front moved from northwest to southeast, and radar returns diminished as the front moved over the lake. Later, the line of convection reinitialized on the southeastern shore of Lake Michigan, removed from the lake and lake breeze. The case examined by Lyons (1966) bears some similarity to the case study presented here, except the convection did not initiate on the western shore of the lake due to limited convective instability over Wisconsin. Convection was delayed from starting over the lake and eventually initialized downwind of Lake Michigan in a more favorable convective environment on May 5, 2003. Lyons proposed that the entrainment of lake-cooled air into the convective system eroded the storm over the lake surface, while the convectively favorable air over the southern lake surface allowed for the convection to reinitialize. In the case study presented here there is little evidence of air cooled directly by the lake being lifted from near the surface in either vertical velocities (not shown) or the 10m-wind convergence.

In another case study, Lyons (1966) showed the formation of cumulus clouds forming 25 miles inland from the eastern shore of Lake Michigan, with clear skies near the shore. Lyons also mentions the passing of altocumulus over Lake Michigan, while other clouds were limited to areas over land away from the lake. This displacement of clouds east of the lakeshore is attributed to the heating caused by the surface eventually creating convective plumes strong enough to break through the strong lake-induced stable inversion to create cumulus clouds. This interaction of altocumulus remaining over the lake and cumulus clouds forming over land is analogous to the case study presented here. The clouds seen in satellite images moving across lower Lake Michigan (Figure 3.2) can be attributed to the PV anomalies generating clouds cover over land on the western shore and being maintained over water, before finally interacting with the unstable air mass over land to produce convection. To summarize, the convection typically associated with cold fronts in this case was delayed due to the lack of surface heating and convectively unstable air over the water.

The lake may not have had a direct role in the initiation of convection, but did have a secondary role in making modifications to the storms. Simulated radar reflectivity displayed smaller storms at initialization when the lake was present compared to when the lake was removed. This also depicted a failure for storms to form over central Michigan when the lake was removed (Figure 3.6c). Lyons and Olsson (1972) observed updrafts ahead of a lake breeze front of 1 m/s and on the order of 2km wide. While these simulations may not explicitly represent this updraft due to the limited resolved horizontal resolution, this updraft width could be possible along weak convergence of surface air with the stable lake boundary layer air. This area of weak convergence of air

and moisture at the surface could help to play a role in changing the structure of CI. Later in the simulation, differences in intensity and storm structure were negligible. The largest factor the lake had in the initiation was the placement of the CI due to discrepancy in surface heating and instability placement.

Raising the water temperature by 3 Kelvin, the lower bound Trumpickas (2009) predicted lake temperatures could increase in a warming climate, tested the sensitivity of this type of CI to lake temperature changes. In this study, these changes produced little change in intensity and location of the CI. This is consistent with the results of Arritt's (1987) study, in which lake breezes continued to initiate in a 2D idealized model as lake surface temperatures were increased, until the lake was approximately the same temperature as the air over land (removing the stable boundary layer over the lake). While it was shown that a lake breeze was not present in our simulations, a stable boundary layer did form over the lake. The convection in this case study shows little sensitivity to changes in the strength of the stable layer; the simple presence of the stable layer was the controlling factor in the placement of initialization. It maybe possible for larger changes in lake temperature to change the over-lake stable layer and the placement of CI, but those would be outside the realm of realistic lake surface temperatures in May. While the presence of the lake did not play a significant role in modifying the convection that occurred in this case, it could certainly play a significant role in other summertime convective systems, as well as in the climate of the region by providing an enhanced local source of sensible and latent heat. Further investigation of this direct role of the lake and surface temperature are still needed to fully understand the coupled lake-land-atmospheric system over the region.

3.5 Conclusions

On May 5, 2003 a line of thunderstorms initiated parallel to the east coast of Lake Michigan and eventually produced severe thunderstorms and a tornado several hundred kilometers to the east. While the convective initiation (CI) resembled what may be expected from CI along a lake breeze front, the simulations presented in this study do not depict a lake breeze. In exploring the mechanisms that led to CI near the lakeshore, we found the following:

1. CI, while appearing to occur in close association with a lake breeze, in fact was initiated through the advection of positive PV across Lake Michigan. CI occurred once the positive PV feature intersected a region of relatively large heating and moisture that provided a more favorable environment for deep convection over land east of the lake.
2. Removal of the lake in our simulations shifted the CI to the west, signifying the role of the lake in modifying the placement of the storms and delaying their onset. It also highlighted the limited direct role of the lake in initiating convection in this case. The lake may still play a role in developing stronger convection and placement from convergence between the lake boundary layer and terrestrial air masses.
3. This type of CI, in which a PV anomaly interacts with an unstable boundary layer in the presence of a lake-induced stable layer, showed very little sensitivity to changes in lake surface temperature consistent with a future climate.

The results found in this study highlight the combined influence of lake-induced thermodynamic anomalies and the synoptic scale conditions in the Great Lakes region.

Attempting to conduct climatological studies of convection initiated by lake breezes without accounting for the synoptic scale environment may lead to a large number of false positives, or incorrect attribution of the triggers of convection. Forecasting for convection near the Great Lakes should not simply rely on lake induced mesoscale processes (e.g., lake breezes) to determine the location and incidence of convection near the shore, but should also consider the upper air processes that played a significant role in the timing and placement of convection in this case

It should be noted in closing that we examined a single event, and further investigation is needed to understand the strength, frequency, and placement of this style of convective initiation near Lake Michigan and the rest of the Great Lakes. Further examination of the differences between lake-breeze and delayed synoptic scale initiation is needed to better understand near-lake convective frequency and intensity.

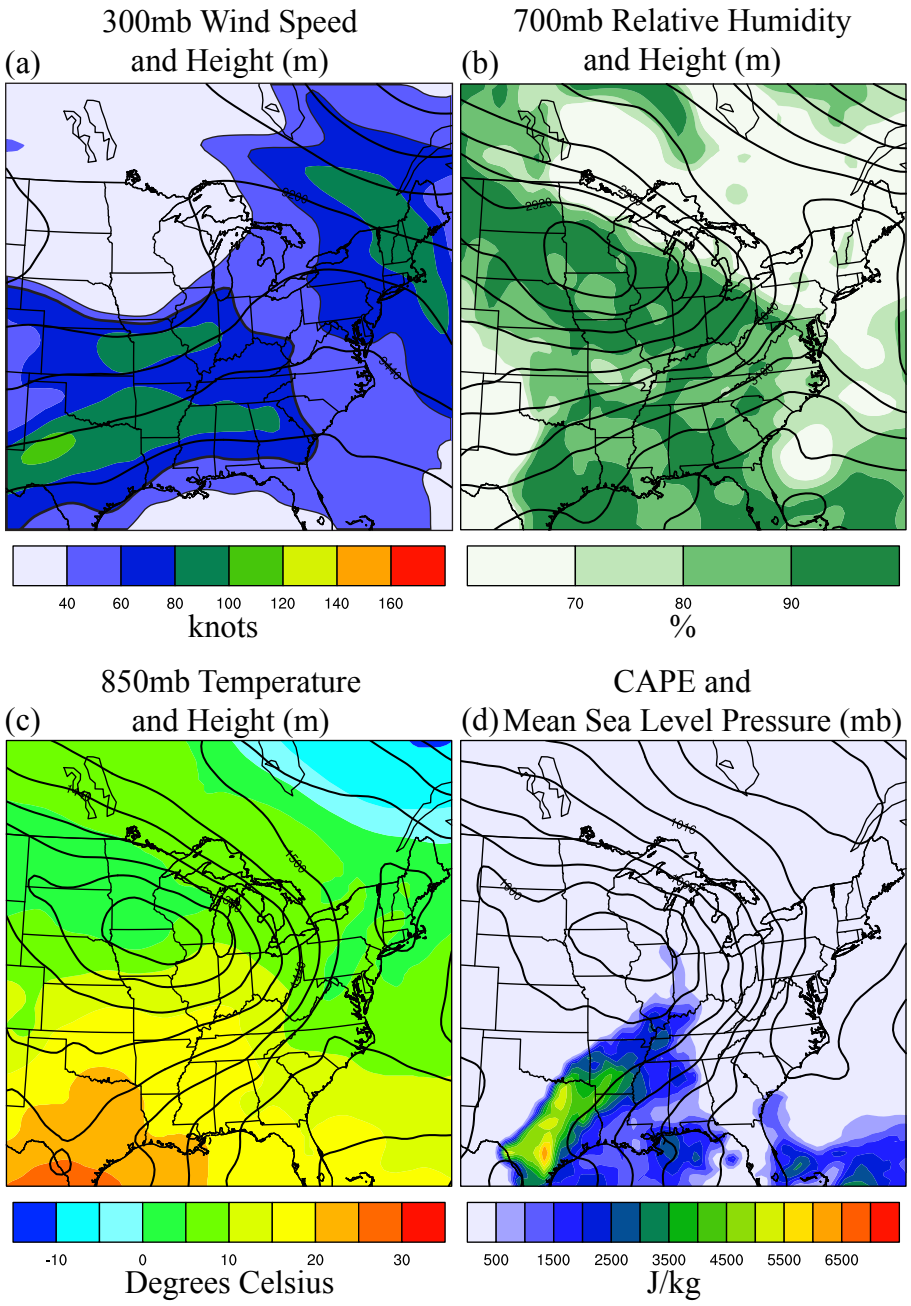

Figure 3.1. RUC model analysis on May 5, 2003 at 12UTC for (a) 300mb height (m) and wind speed (knots), (b) 700mb height (m) and relative humidity (%), (c) 850mb height (m) and temperature (degrees Celsius), and (d) mean sea level pressure (mb) and convective available potential energy (CAPE; j/kg).

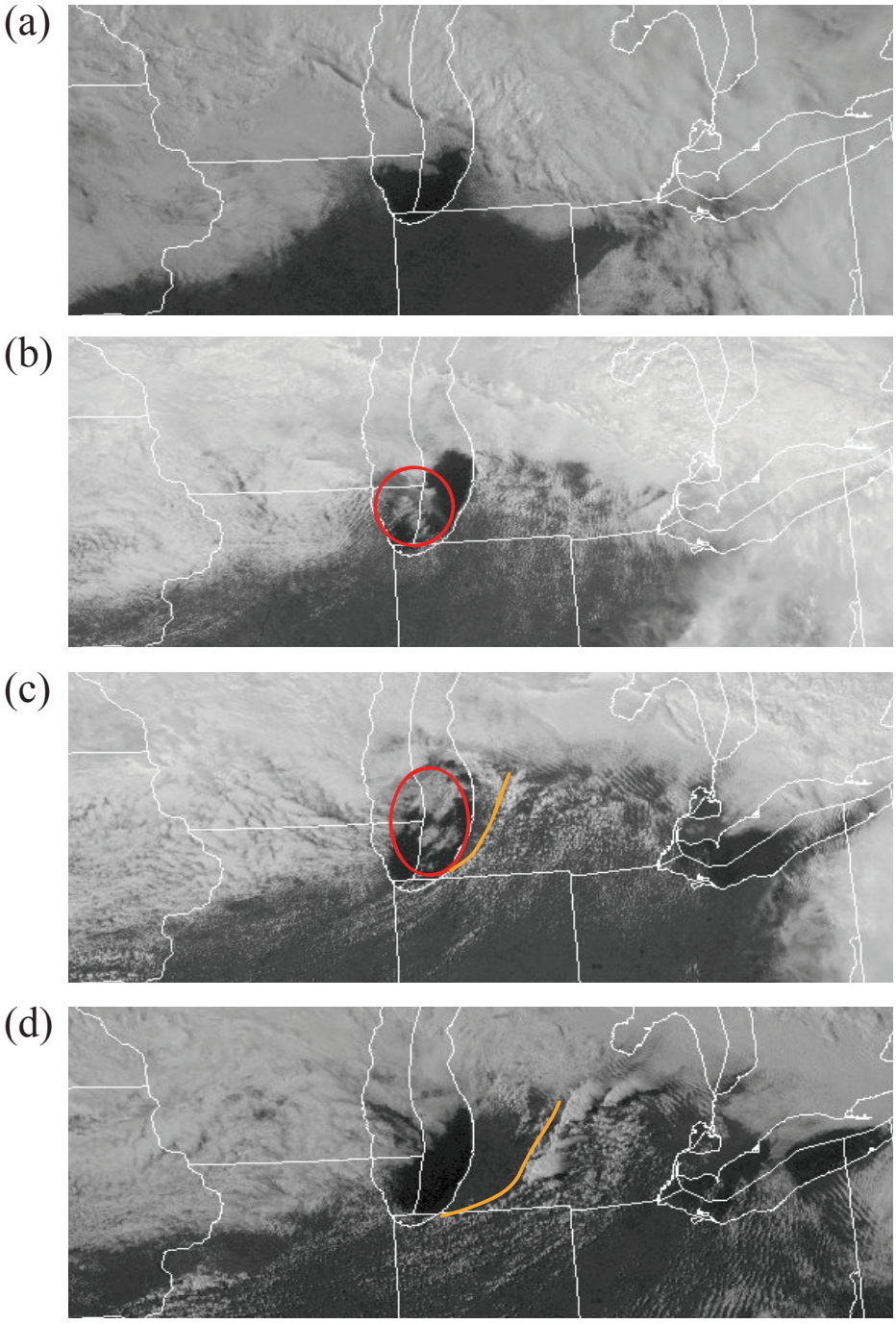

Figure 3.2. Visible satellite images of cloud cover over the southwestern Great Lakes at (a) 1400 UTC, (b) 1700 UTC, (c) 1915 UTC, and (d) 2115 UTC on May 5, 2003. Red circles represent two different groups of clouds passing over Lake Michigan before convective initiation. Orange line represents the approximate location of the line of convection. [Images available online at http://www2.mmm.ucar.edu/imagearchive]

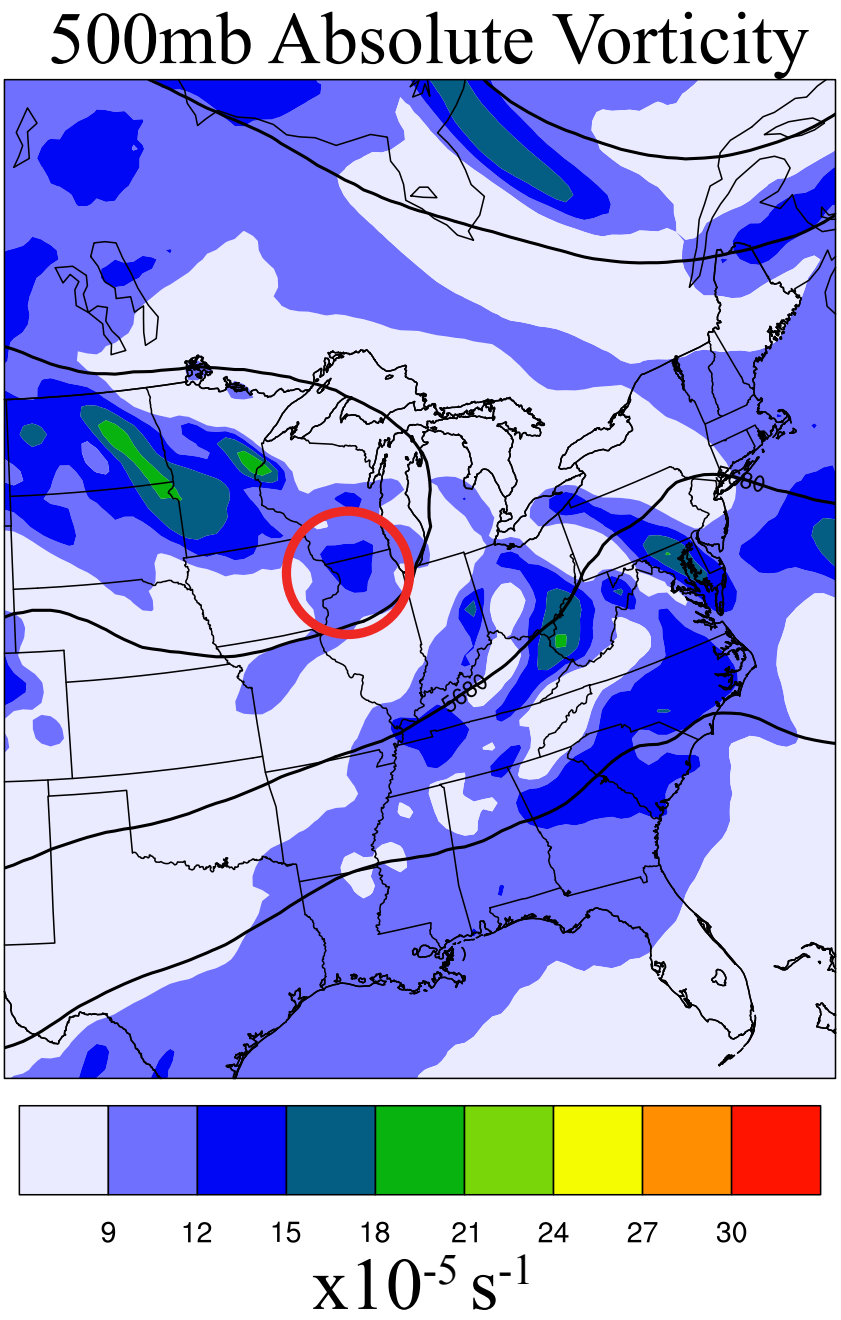

Figure 3.3. 500mb geopotential height (m) and absolute vorticity (x10^-5 1/s) on May 5, 2003 at 12 UTC calculated from NARR output fields. The red circle highlights the area of positive absolute vorticity over northern Illinois.

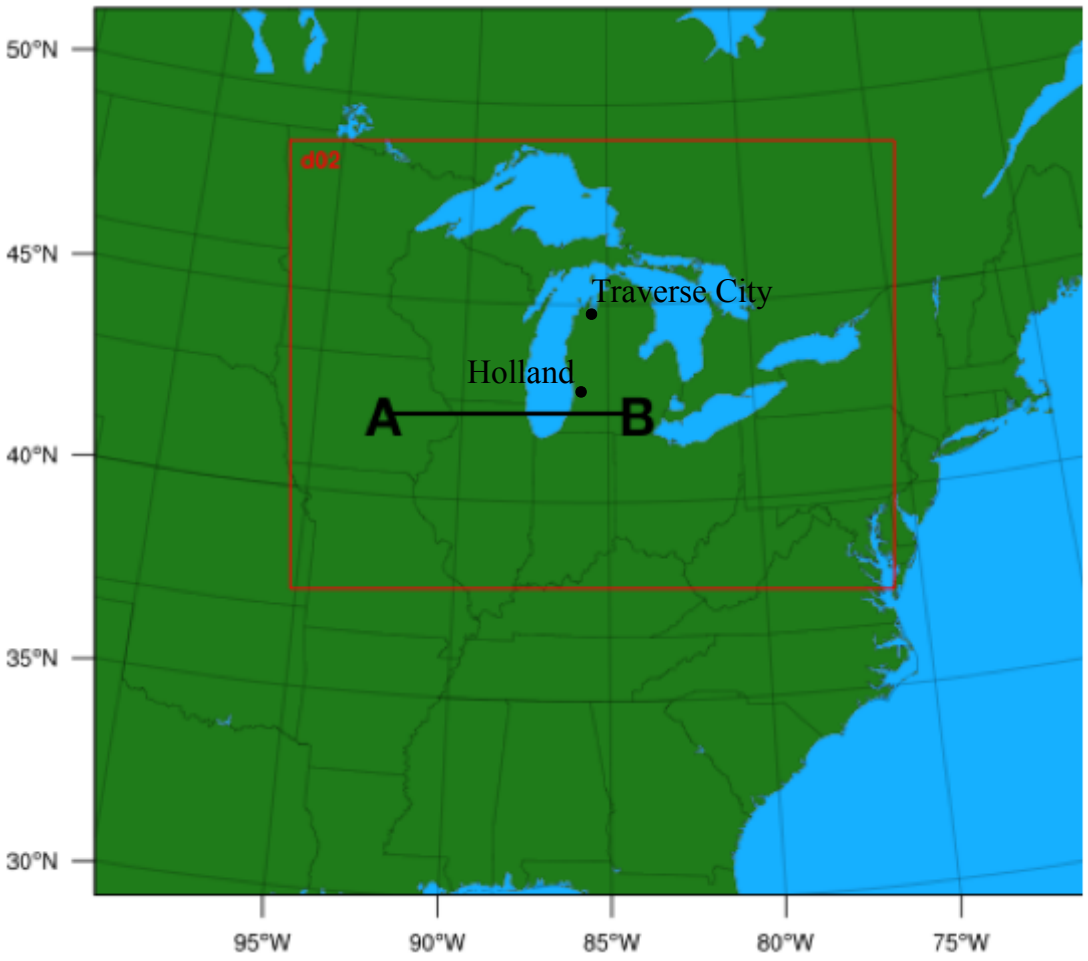

Figure 3.4. 10km outer domain (d01) and 2km inner nest (d02) used in the WRF simulations. Cross-section taken from point A to B is represented in Figure 3.9.

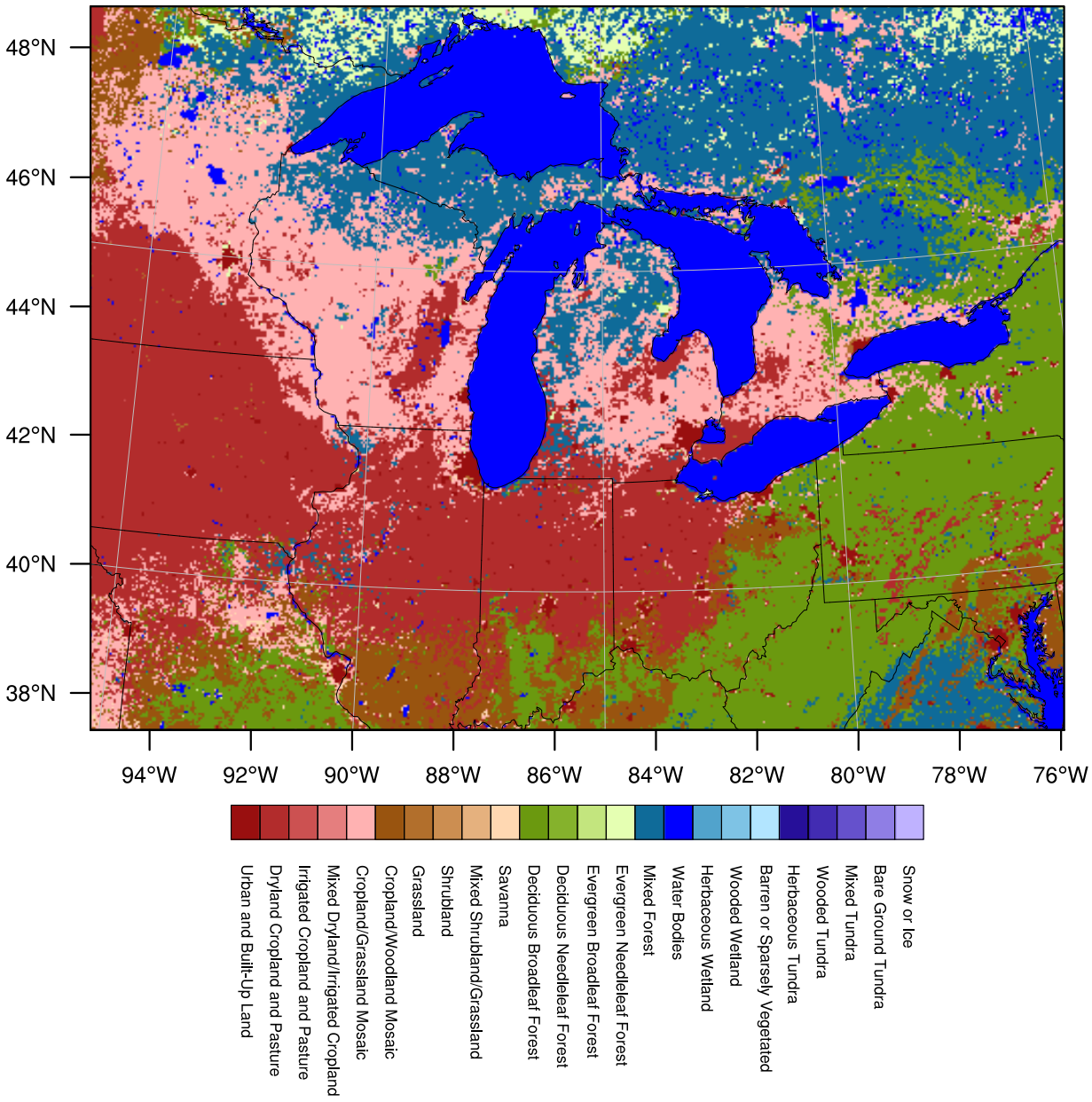

Figure 3.5. USGS 24 Land-use category for d02.

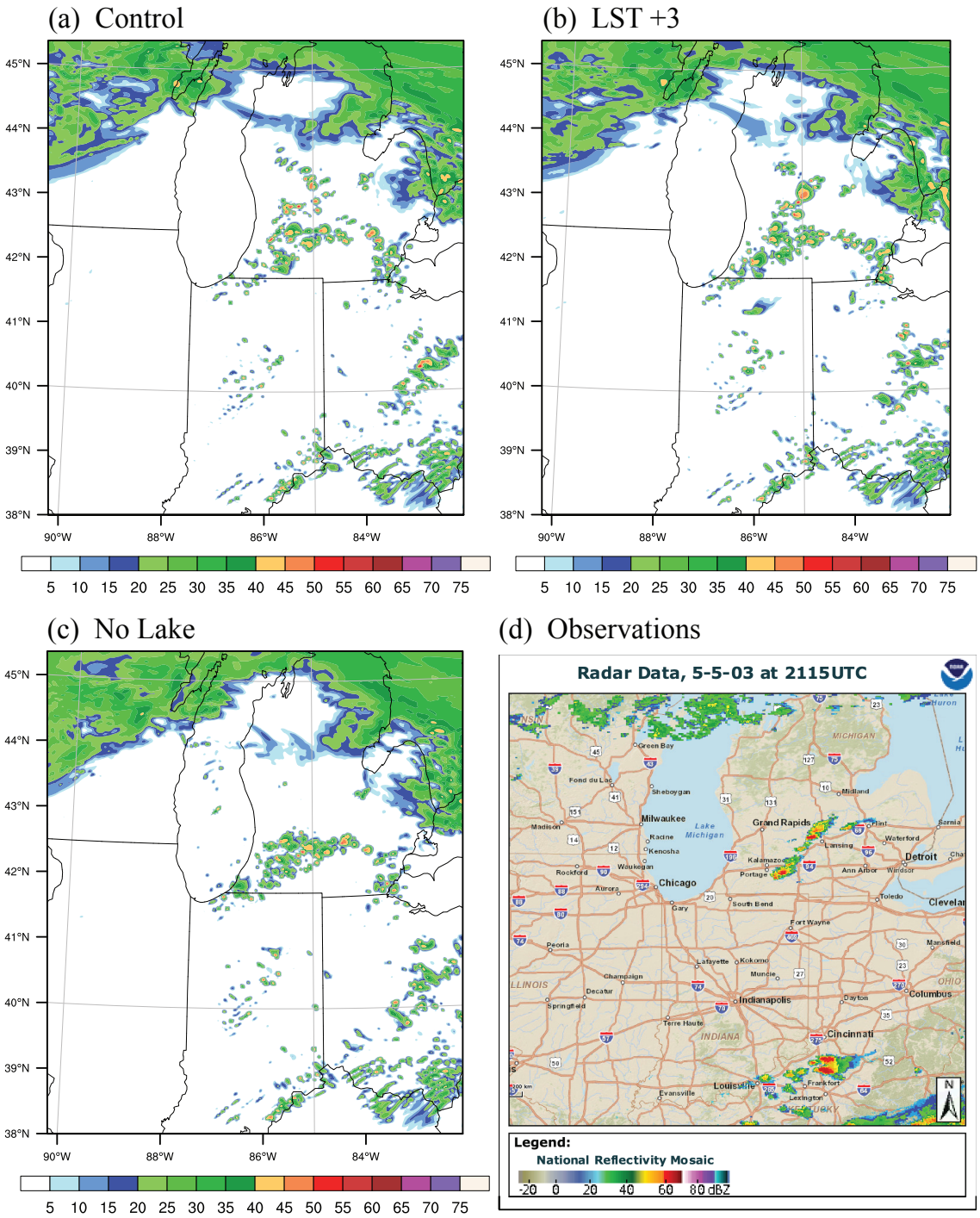

Figure 3.6. Observed radar reflectivity vs. modeled radar reflectivity (dBZ) at convective initiation (1740 UTC for simulated, 2115 UTC for observed) for (a) Control, (b) LST +3, (c) No Lake, and (d) observed reflectivity. [Observed radar reflectivity available online at http://www.ncdc.noaa.gov/nexradinv/]

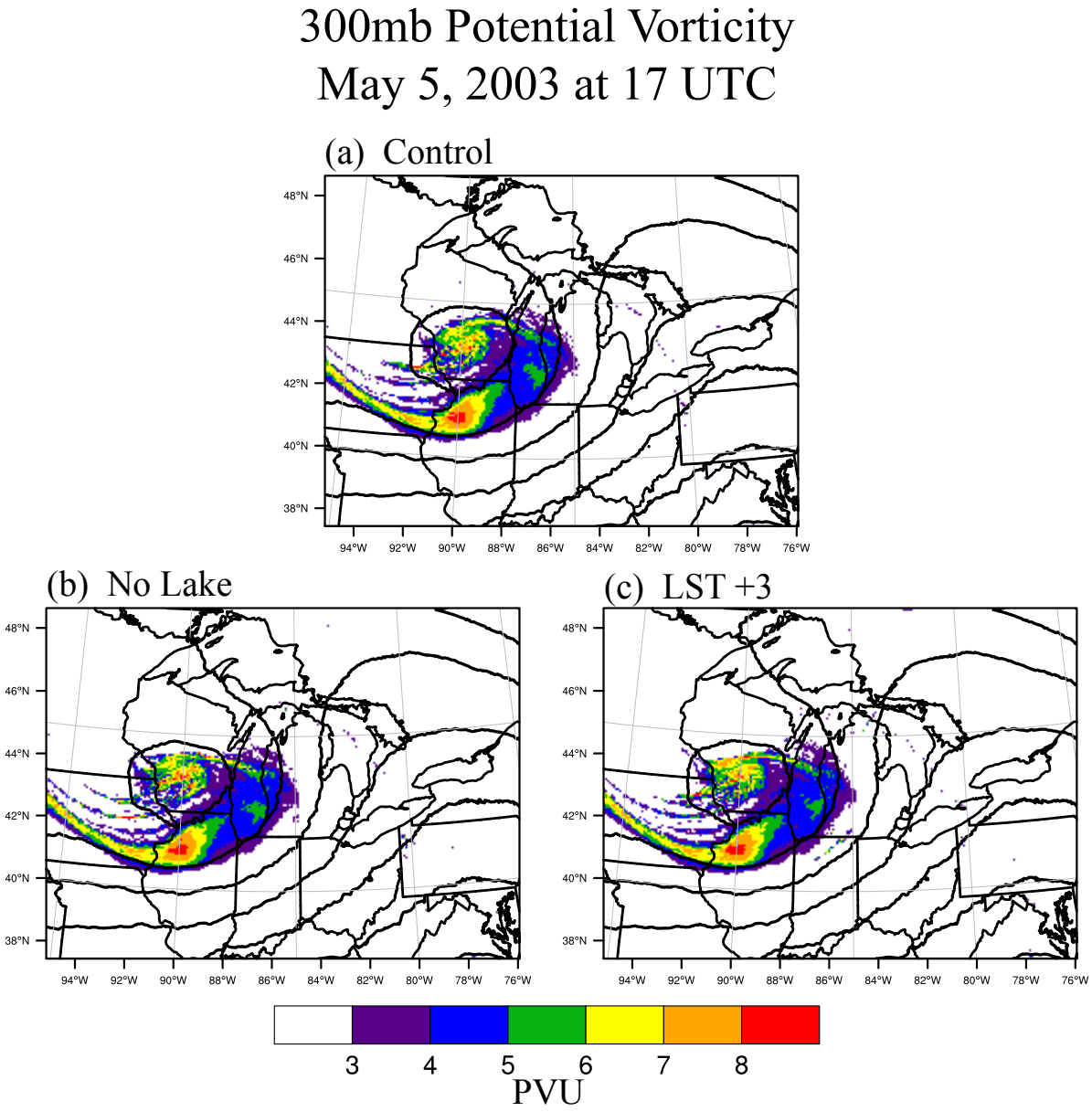

Figure 3.7. 300mb geopotential height (contour) and potential vorticity (filled contour) at 1700 UTC of May 5, 2003 for (a) Control, (b) No Lake, and (c) LST +3 simulations.

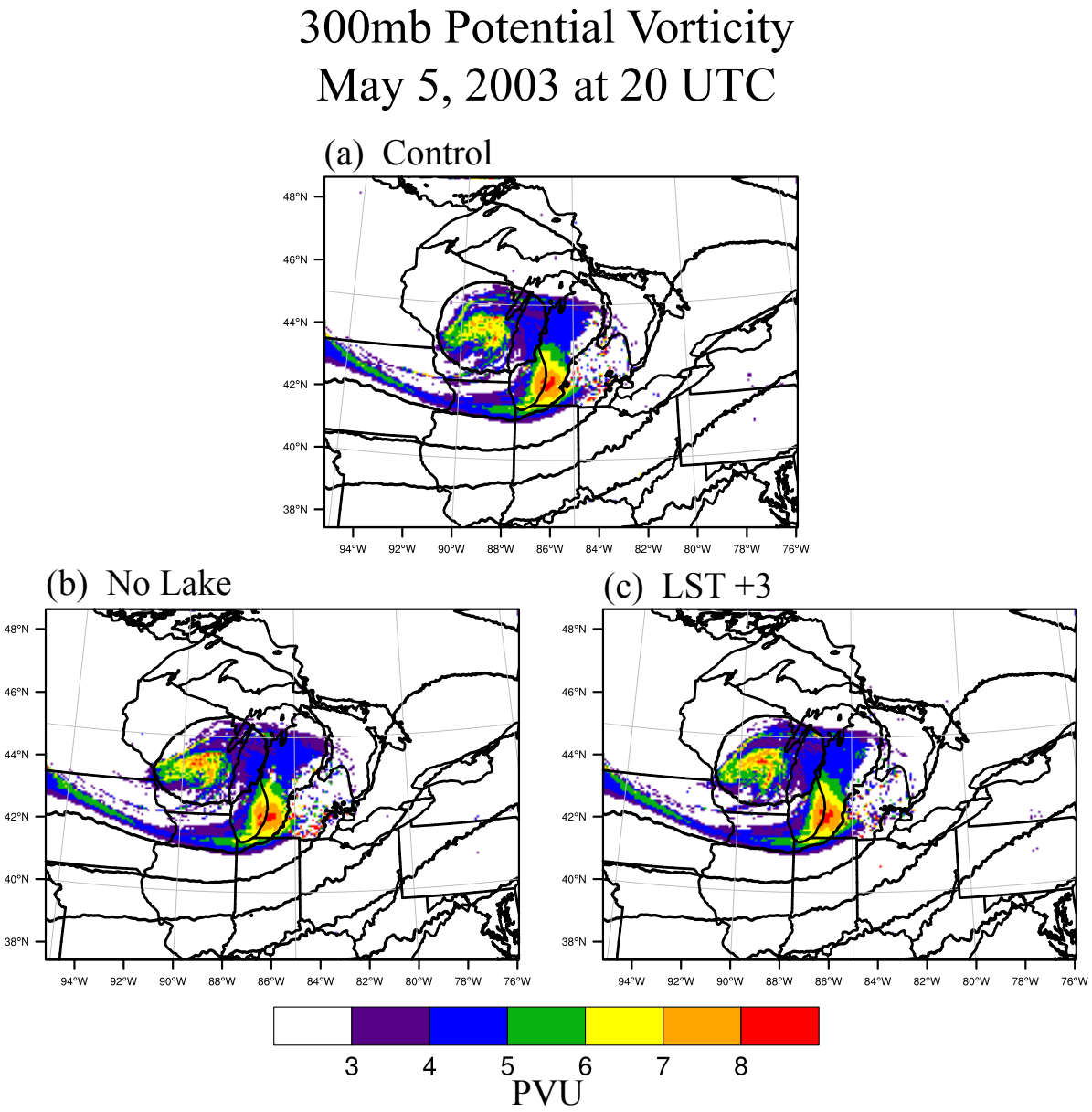

Figure 3.8. Same as at 2000 UTC on May 5, 2003.

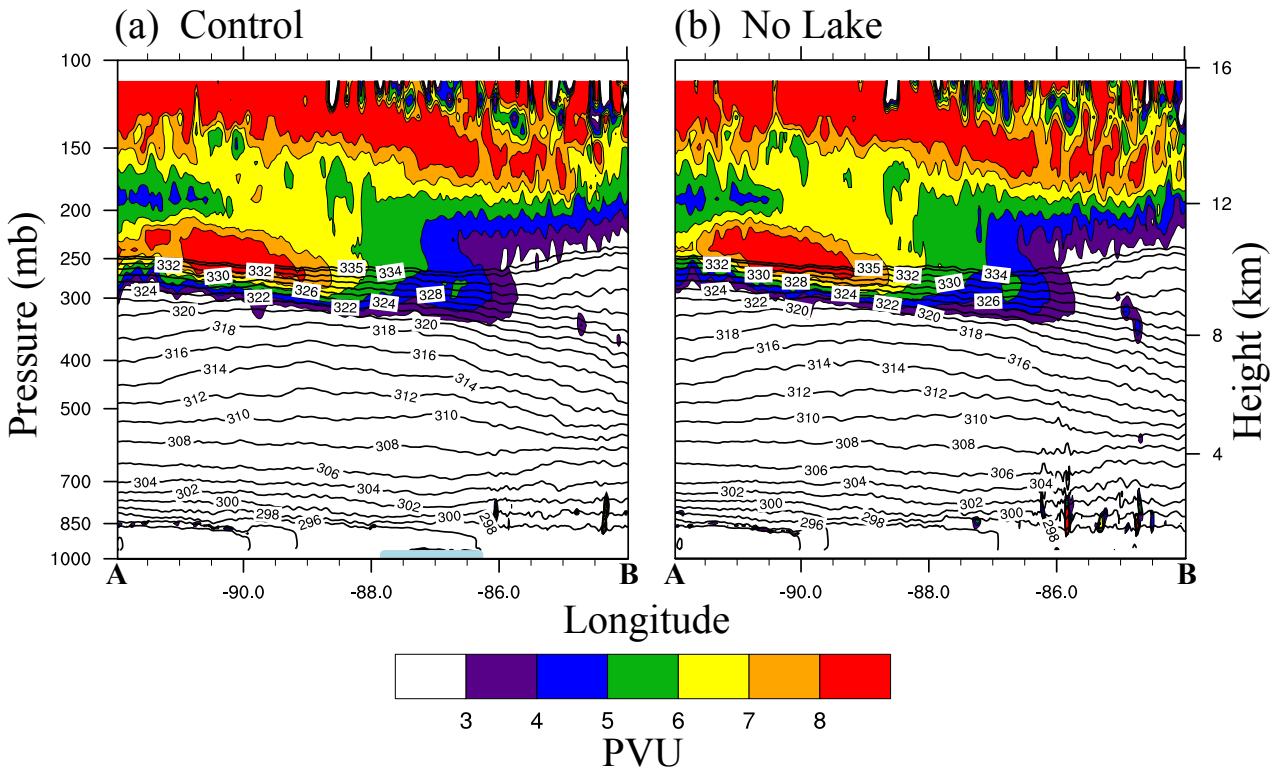

Figure 3.9. Vertical cross-section from point A to point B (see Figure 3.4 for location) of potential vorticity (filled contour) and potential temperature (contour) for (a) Control and (b) No Lake at 17 UTC on May 5, 2003. Light blue shading at the bottom of (a) represents Lake Michigan.

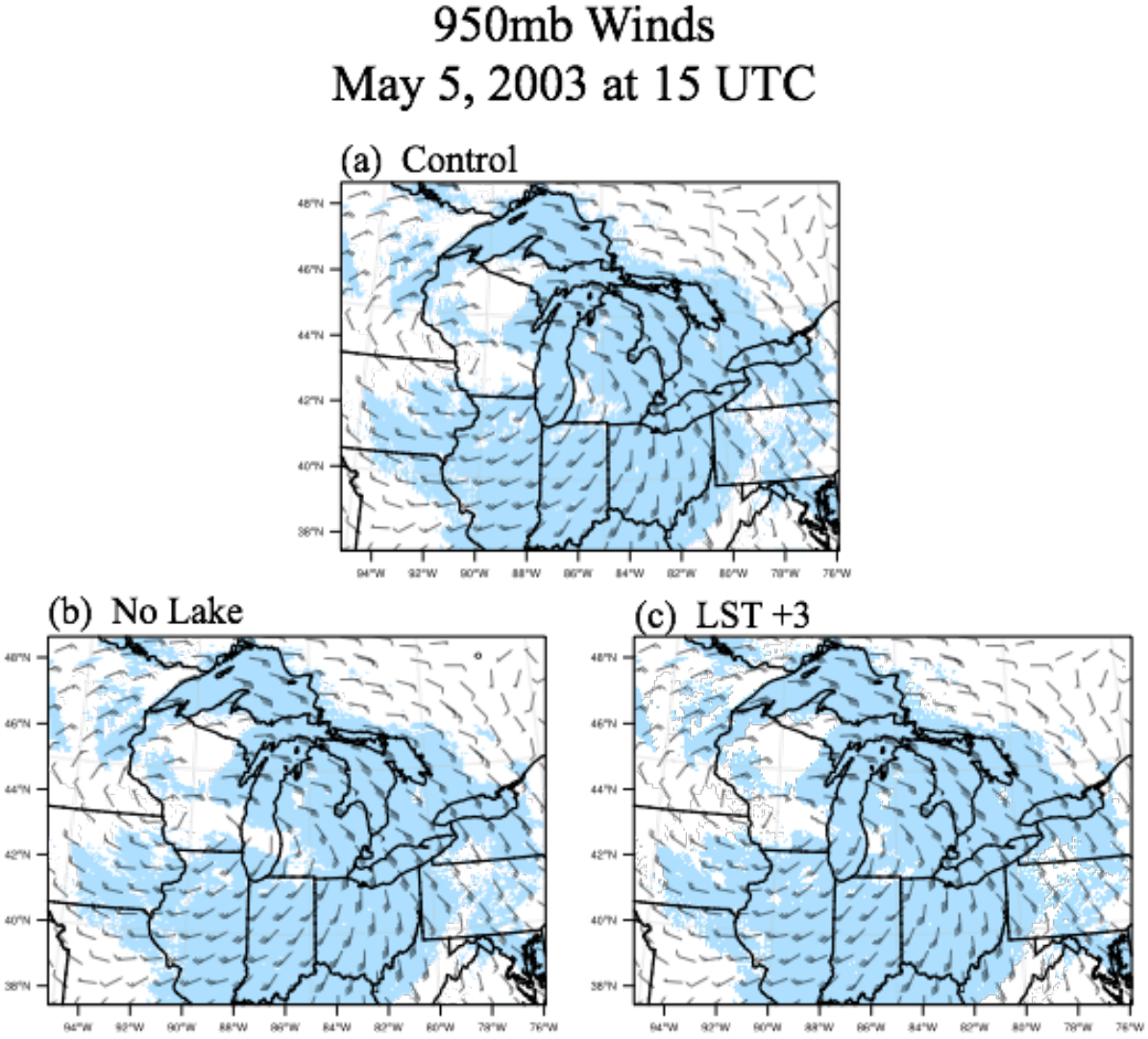

Figure 3.10. 950mb winds (knots) for (a) Control, (b) No Lake, and (c) LST +3. Contour shows wind speeds greater than 18 knots at 15 UTC on May 5, 2003.

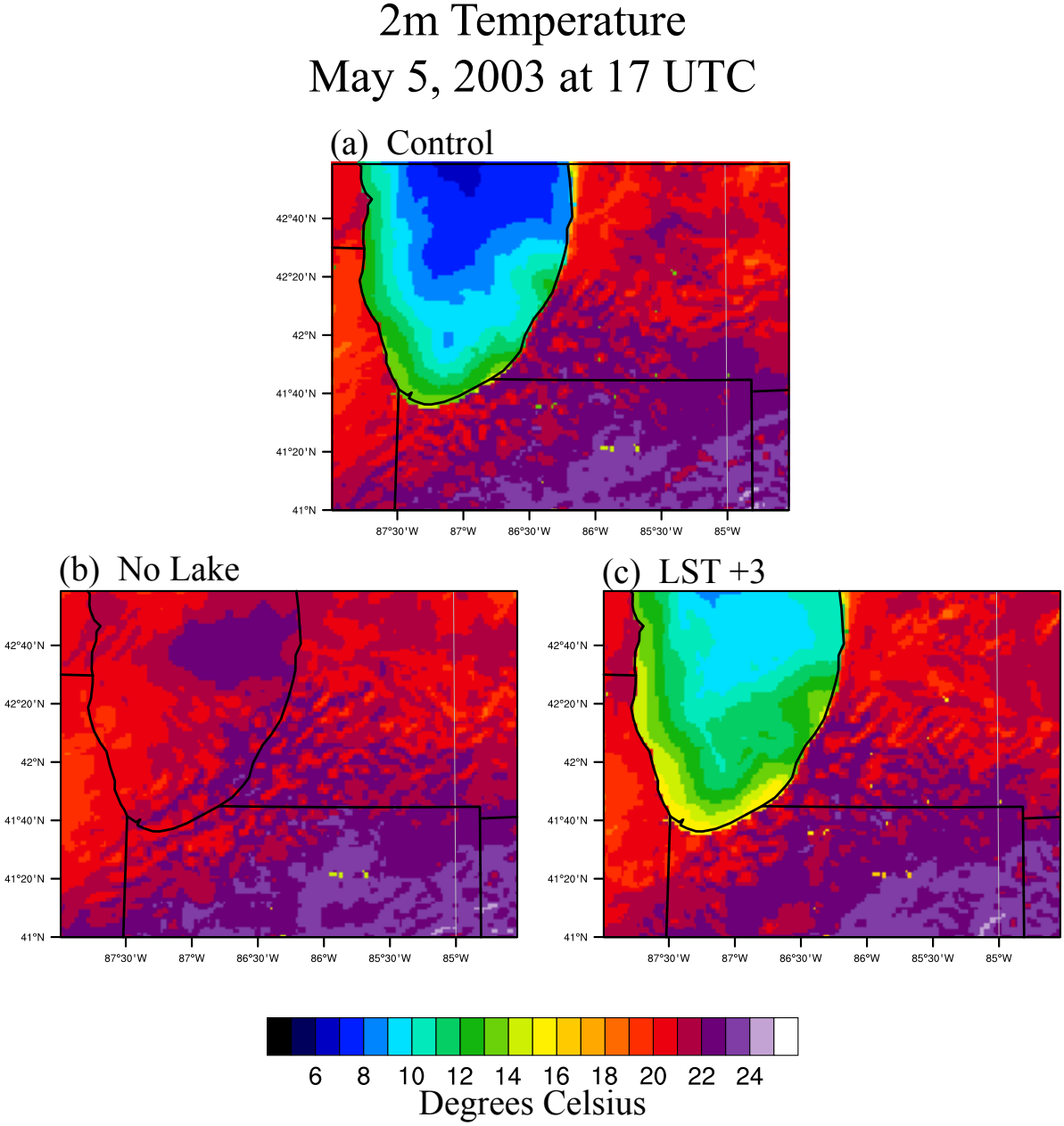

Figure 3.11. 2m Temperature for (a) Control, (b) No Lake, and (c) LST +3 simulations at 17 UTC on May 5, 2003.

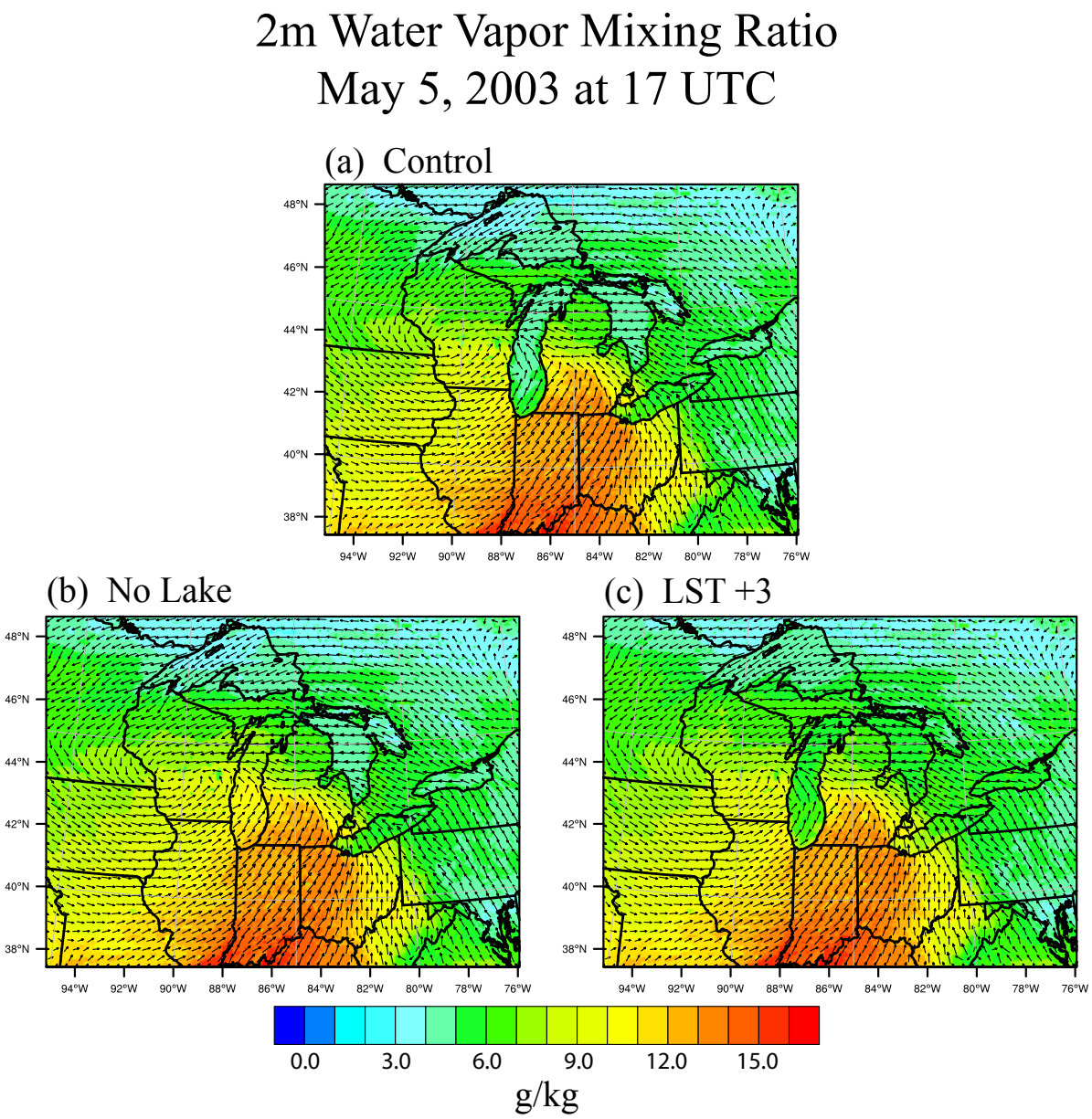

Figure 3.12. 2m water vapor mixing ratio (g/kg) for (a) Control, (b) No Lake, and (c) LST +3 simulations at 1700 UTC on May 5, 2003.

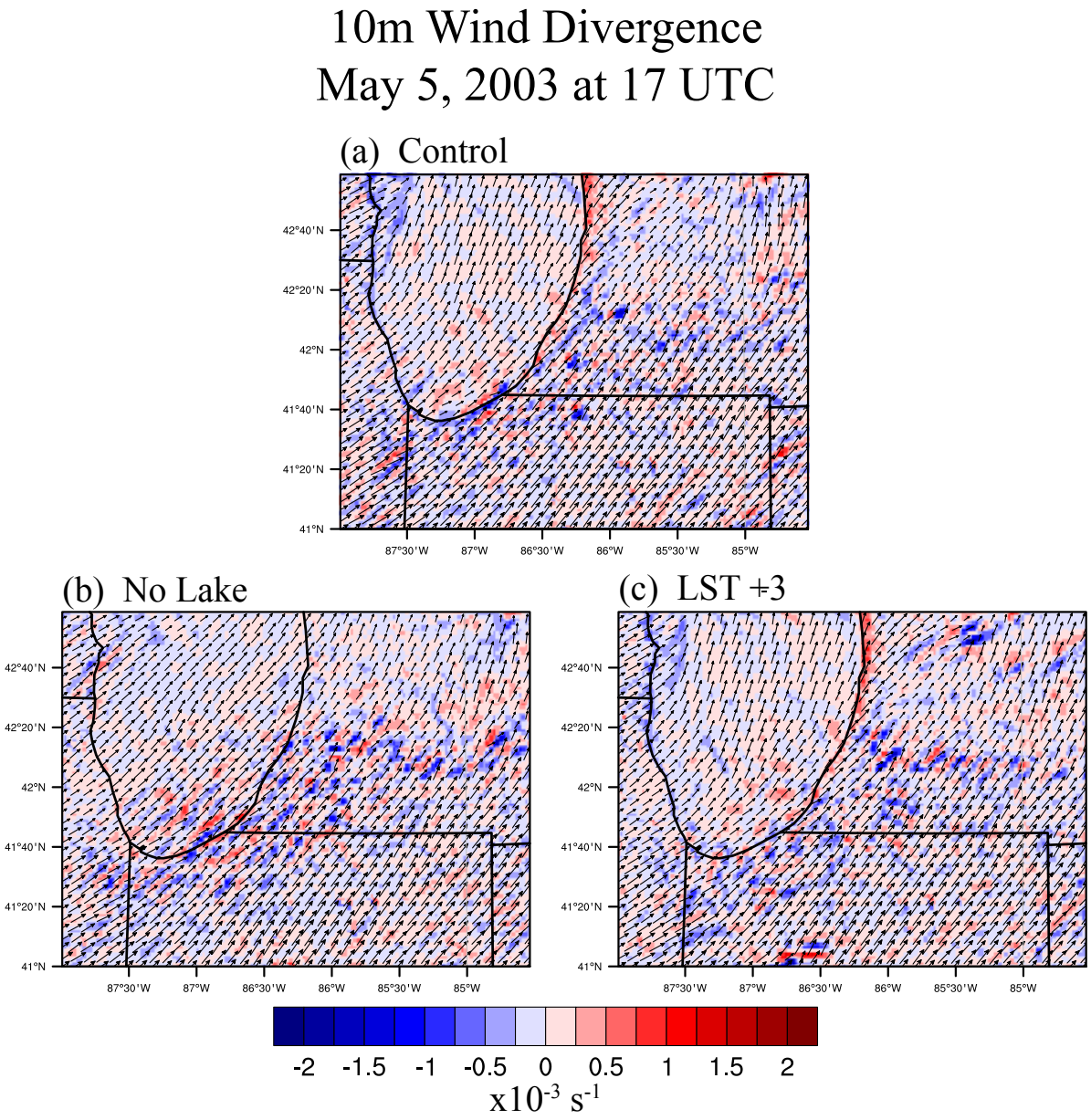

Figure 3.13. 10m wind convergence (blue) and divergence (red) at 1700 UTC on May 5, 2003 for (a) Control, (b) No Lake, and (c) LST +3 simulations.

CHAPTER 4. THE INFLUENCE OF LAKE SURFACE TEMPERATURE ON A MESOSCALE CONVECTIVE SYSTEM PASSING OVER LAKE SUPERIOR

4.1 Introduction

Mesoscale convective systems (MCSs) are deep convective storms that are on the order of 100km or more in a single horizontal direction (Houze 2004). Visually, through radar reflectivity returns, these storms have a linear pattern or a bow like structure caused by an accelerating cold pool behind a leading front. Often, these storms will produce high winds and heavy rainfall (e.g. Sepic and Rabinovich 2014).

These systems have been observed to cross the Great Lakes during the spring and summer months, in particular the southern half of the region (Johns and Hirt 1987). Sixty-one MCSs were found to cross Lake Michigan from 1996 to 2001 (Graham et al. 2004; hereinafter referred to as G2004). The authors divided these MCSs into 7 unique synoptic flow regimes that led to the creation and propagation of MCSs over Lake Michigan. From 2002 to 2007, Metz (2011; hereinafter referred to as M2011) found 110 cases of MCSs crossing Lake Michigan. Both of these studies were exploring the role Lake Michigan had in the propagation, dissipation, or weakening of the storms while over the lake. G2004 found that 68% of the cases propagated across the lake, while M2011 found 43% crossed the lake, but there were inconsistences between the studies in terms of the minimum strength used to define a MCS. Both studies found that storms with an air temperature of 2.5 degrees Celsius greater than the water temperature taken at buoys over central Lake Michigan were able to maintain over the lake. A weaker temperature difference, approximately 1 degree Celsius, between air and water

temperatures was speculated to result in near-surface air being ingested into the storm causing it to weaken or dissipate. M2011 also concluded that the near surface temperature inversion might not be as significant of a factor as the climatology concluded. M2011 removed Lake Michigan in simulations for both a passing and a dissipating MCS, and in both cases found that the storms crossed the former lake surface. This continued propagation of the storm once the lake was removed was attributed to the increased instability introduced over the new land surface.

Observations have shown the Great Lakes to influence the dynamics of other existing systems during their passage over the lakes. For example, Gallus and Segal (1999) observed that cold fronts accelerated while over Lake Michigan due to changes in temperature gradient across the front and differences in friction from over land to over water.

Zhao et al. (2015) explored a MCS propagating over the Great Salt Lake, another large body of water found in northern Utah. Their simulations showed minimal influence on the system from when the lake was present to when it was removed, with changes in total rainfall of less than 5%. Over Lake Erie, Workoff et al. (2012) showed through a series of observations that convective storms that passed over Lake Erie substantially decreased in intensity after spending 60 minutes over the water, with linear storms lasting the longest before decreasing in intensity. They also found that cooler over lake air temperatures compared to upwind air temperatures were a key component in determining if storms would weaken over the lake. The authors did note that linear systems were not as sensitive to this temperature difference as they were to the 3km wind speeds. Parker (2008), through a series of idealized simulations of an organized convective system,

showed that these systems could continue to maintain in an environment where the surface was cooled by over 10 Kelvin before inflow into the storm was cutoff. It was also found that a decrease in temperature ahead of the cold pool could increase the amount of boundary layer tracers in the middle atmosphere late in the simulation, signifying an increase in updraft strength during the stalling phase.

Lake Superior has many unique features that are either not observed or not as strongly pronounced over the other lakes in the region. The lake has seen a faster increase in summer lake temperature than the other lakes, with an increase of about 2.5 degrees Celsius from 1979 to 2006 believed to be caused by a combination of less winter ice coverage leading to earlier water stratification and warmer air temperature (Austin and Colman 2007). The water and over lake air temperature were also shown to be warming faster than the terrestrial air temperatures. This warming of the lake water has caused an increase in wind speeds over the lake surface (Desai et al. 2009).

Lake Superior can form a barrier jet along the northwest coast from a combination of the cold, stable over lake air and southerly flow moving this air towards the north to interact with the Duluth Complex, a rock complex along the northwest shore of Lake Superior with an elevation of approximately 500m (NOAA/GLERL 1980). This stable air, unable to flow over the higher terrain, is deflected to the southwest through a balance of a synoptically generated pressure gradient force, the Coriolis force, and a mesoscale pressure gradient force generated by the damming of cold air along the elevation (Stull 2015). The balance of these forces produces a jet parallel to the shore at the surface. This feature has been observed over other parts of the world with higher elevation near colder marine water (e.g. Reynolds and Dennis 1986, Loescher et al. 2006, Barrett et al. 2009).

In this chapter, a case study from July 3, 2012 where a MCS propagated over Lake Superior will be presented. From a series of modeling results with varying lake surface temperature, the importance of the near-surface stable layer will be examined directly on a passing MCS to determine the influence of lake temperature on the distribution of precipitation and intensity. Parcel trajectories will be used to begin to explore the movement of near surface air out of the stable boundary layer. Cotton et al. (1995) found that MCS are efficient at moving air out of the boundary layer and into the free troposphere. Since pollutants can collect within the lake boundary layer (Brook et al. 2013), it is important to understand the redistribution of this air from both a dynamical and air quality standpoint. The results from this case study of a MCS passing over Lake Superior will be compared to G2004 and M2011 to see if conclusions made for MCSs interacting with Lake Michigan can be applied to other lakes.

An overview of the case study and description of the model setup are presented in Section 4.2. The results of the simulations are described in Section 4.3. Sections 4.4 and 4.5 discuss the results and present conclusions, respectively.

4.2 Case Study and Methods

4.2.1 July 1-3, 2012

On July 2, 2012 at 12 UTC, a ridge was present over the northern Great Plains and southern Canada from 700 to 300mb, with the ridge axis oriented from north to south along the border of Minnesota and North Dakota **(**Figure 4.1a-c**)**. A shortwave feature was located over Saskatchewan, Canada at 300mb. Throughout the day, the shortwave moved to the east behind the upper level ridge. Flow at 850mb was out of the SSW ahead of the feature (Figure 4.1d). By 20 UTC, a cluster of convective storms that was moving

parallel to a stationary front stretching from northern Minnesota to the southwest through North and South Dakota began to organize over northern Minnesota and southern Manitoba, Canada into a linear structure. NAM analysis at 18 UTC showed a large area of enhanced surface based CAPE (4500 J/kg; not shown) over Minnesota and North Dakota, with some areas in Minnesota over 5500 J/kg of CAPE at this time. This linear system began to transition into two systems as it moved into this region of enhanced CAPE at 00 UTC, one over northern Minnesota and another over Ontario, Canada (Figure 4.5). The system over Minnesota quickly moved to the southeast, producing a distinct bow echo in radar reflectivity, glancing the western portion of Lake Superior starting between 02 and 03 UTC on July 3rd. The Manitoba system also moved to the southeast, but over Lake Superior starting between 02 and 03 UTC with a less defined bow structure. At 05 UTC, the systems were to the east of the Keweenaw Peninsula with minimal changes in their radar reflectivity between 02 and 05 UTC (Figure 4.5).

The bow structure that moved to the west and south of Lake Superior produced numerous reports of wind damage and hail (NOAA/SPC 1999). The storm initiation followed closely with the "ridge rider" scenario for MCS creation described by G2004, but shifted further to the north**.** This was not the only MCS created by this system, as several days beforehand another MCS was generated and propagated along the southern Great Lakes and onto the east coast of the United States, producing a meteotsunami on Lake Michigan (Sepic and Rabinovich 2014).

In this case study, temperature differences between buoy measured air temperature (at 5m above the water surface) and water temperature were 3.8 degrees Celsius over the eastern portion of the lake, 2.5 degrees Celsius over the northern portion, and 4.8 degrees

Celsius over the western portion at 0250 UTC on July 3rd (NOAA/NDBC 1981). This storm did propagate over Lake Superior, as is predicted by G2004 using the relationship between air and water temperature of buoys being greater than 2.5 degrees Celsius. G2004 does mention that this relationship begins to break down late in the summer season, when water temperatures begin to reach their peak. It should be noted that this relationship has only been studied for Lake Michigan.

4.2.2 Model Setup

The Weather Research and Forecasting Model (WRF, Skamarock 2008) is used to model the atmospheric environment of the MCS passing over Lake Superior. A 10km horizontal resolution parent domain (D01, 460x360 grid points) with a one-way nested, 2km horizontal resolution grid over the western Great Lakes, (D02, 921x791 grid points) is run from July 1, 2012 at 12 UTC to July 3, 2012 at 18 UTC for a total of 54 simulated hours (Figure 4.2; see APPENDIX D for details on the start time sensitivity testing conducted). This allows for approximately 39 hours of spin up before the MCS reaches the shore of Lake Superior and about 24 hours before the MCS initiates within the D02. D01 boundary and initial conditions are created using the North American Model Analysis (NAM-ANL; Rutledge et al. 2006) with boundary conditions updated every six hours. 51 custom vertical eta levels are used for both domains (APPENDIX C). The physics parameterizations for each domain can be found in Table 4.1.

	D01	D02
Microphysics Scheme	Morrison 2-Moment scheme	Morrison 2-Moment scheme
Longwave Radiation	RRTMG	RRTMG
Shortwave Radiation	RRTMG	RRTMG
Land Surface Model	Noah	Noah
Planetary Boundary Layer	Mellor-Yamada-Janjic	Yonsei University
Cumulus Scheme	Kain-Fritsch	None

Table 4.1. Physics parameterizations used for each domain in the WRF simulations.

4.2.3 Sensitivity Studies

Three sensitivity studies are performed to explore the direct role the lake surface temperature has on the passage of the MCS over Lake Superior. These studies use uniform increases or decreases in lake temperature to explore both the role the lake temperature has on the propagation of and distribution of precipitation associated with the MCS along with exploring how a warmer lake could alter similar storm systems in a future climate over Lake Superior. The first two studies uniformly raise the lake surface temperature at the start of the simulation by 3 (Plus 3) and 6 (Plus 6) Kelvin. A next two sensitivity studies reduce the lake temperatures by 3 Kelvin (Minus 3) and 6 Kelvin (Minus 6). This change in lake temperature is accomplished by selecting water points within two latitude/longitude boxes, one around Lake Superior and the second around Lakes Michigan, Huron, and western Erie, within D02. This selection method isolates the Great Lakes themselves, minimizing the changes to smaller, inland bodies of water that are resolved at the 2km horizontal resolution (APPENDIX A).

A fifth sensitivity study attempts to reduce the strong stable layer that is present over the lakes in the summer months due to the cold lake surface temperature (PBLH Temp). To adjust the lake surface temperature, the planetary boundary layer (PBL) height's

potential temperature is calculated in the Control simulation at 22 UTC on July 1, 2012. This results in a non-uniform change of the in lake temperature, with temperature changes ranging between an increase of 8 Kelvin over Lake Superior to less than 1 Kelvin over western Lake Erie (Figure 4.3). The PBL height temperature at 22 UTC on July 1 allows for the PBL to reach near its maximum daily height before cloud cover forms over the lakes and alter the height. This sensitivity study, along with the Plus 3 and Plus 6 studies, are referred to as the Positive case studies, due to their general increase in lake temperatures. The Minus 3 and Minus 6 are referred to as the Negative case studies. All changes to the lake temperature are static in time, creating a constant forcing in time.

4.3 Results

4.3.1 Simulated Radar

Unorganized convection begins to enter D02 in southern Manitoba at 12 UTC on July 2nd, approximately 15 hours before contact with the lake. At 20 UTC, the convection strengthens as it moves to the east along the United States and Canadian border. The cluster of storms organizes at 23 UTC to form a linear MCS moving to the southeast (Figure 4.4a). At 03 UTC (Figure 4.6a), the MCS in the Control case reaches the northwestern shore of Lake Superior, consistent with Canadian radar observations (Figure 4.5). Over the next 8 hours, until 11 UTC on July 3rd, the system moves over Lake Superior to the east. During this time, there is an initial increase in reflectivity as the storm interacts with the northwest shore of Lake Superior in the Control case. While the MCS is over the lake at 06 UTC, a split in maximum reflectivity forms (Figure 4.7a). The portion closer to the northern coast of Lake Superior travels to the east while the southern portion moves to the southeast, following the southern coast of Lake Superior. The

simulated reflectivity over central Lake Superior reduces by 5 to 10 DBZ between the two cells. By 09 UTC on July 3rd, the leading edge of the MCS makes landfall along the eastern shore, and by 16 UTC the system exits the eastern boundary of D02.

The Control radar reflectivity compared to the observations does depict a few differences. At 00 UTC on July 3, the simulated radar reflectivity depicts the system lagging the observations by approximately 50km (Figure 4.5**)**. The simulated and observed Canadian radar show an agreement with the orientation and strength of the convection. The single cell over Bemidji, MN is simulated approximately 100km too far to the north. At 05 UTC, the simulated system still lags the observations by approximately 50km and is shifted to the north by approximately 100km. This results in the bow echo that forms along the southern coast of Lake Superior to form over the lake. Reflectivity intensities are in agreement with both Canadian and United States observations. Even with these placement and timing errors, the intensity of the storm is captured and the system still interacts with Lake Superior, a key component in answering the questions set out by the study. The remainder of the chapter will be compared to the Control simulation to the sensitivity studies.

The sensitivity studies do not show large differences in the overall structure of the system in simulated radar reflectivity (Figure 4.4b-f, Figure 4.6b-f, and Figure 4.7b-f). Each sensitivity simulation reaches the shore within 30 minutes of the Control case. These do converge on placement by approximately 0730 UTC. The overall intensity of each system is approximately the same as the Control case, with minor differences in intensity placement and timing. The Negative case studies show a similar structure to the Control over the southern portion of the MCS while over land, while the over lake

portion has a broader area of weaker intensity (40 dBZ; Figure 4.7b-c). There is less evidence of the splitting in intensity that is seen in the Control case (Figure 4.7a) in each sensitivity study as they maintain greater intensity over the lake (Figure 4.7b-f). The Positive case studies (Figure 4.7d-f) have lower reflectivity develop along the southern portion of the storm over land, but a more continuous line of reflectivity over the lake.

4.3.2 Accumulated Precipitation

The Control case has the strongest rainfall occurring over central Lake Superior from northwest to southeast (Figure 4.8a). Several local maximum of rainfall occur along the south and east coasts of Lake Superior, with another local maximum over Lake Michigan and Lake Huron. All sensitivity studies show an increase in rainfall over land to the northwest of Lake Superior, predominantly due to changes in the environment created by changes in the lake temperature (discussed later).

Directly over the lake, all simulations show various degrees of reduction in rainfall, with Plus 6 having the greatest reduction (Figure 4.8e). The Minus 3 case has a delay in the reduction of rainfall amounts that does not occur until after the storm passes the Keweenaw Peninsula (Figure 4.8b). The Minus 6 case has a general reduction in rainfall amounts over and downwind of the lake (Figure 4.8c). All simulations shift precipitation to the north, away from the center of the lake, and to the south with varying degrees of enhancement.

	Control	Minus 6	Minus 3	Plus 3	Plus 6	PBLH
Lake Superior	1323348 mm	-1.165%	6.375%	6.284%	7.640%	8.869%
D02	2574697 mm	-4.740%	1.552%	4.281%	7.424%	4.587%

Table 4.2. Total accumulated rainfall percentage change from 02z to 16z on July 3rd over Lake Superior region and Domain 2.

As shown in Table 4.2, the Minus 6 case study has the lowest amount of overall rainfall, followed by the Control case study. All other case studies experience an increase in precipitation. It is also shown that the Lake Superior region (45.5 to 49.5 degrees North latitude and 94.0 to 82.0 degrees West latitude, area displayed in Figure 4.9) accounts for about half of the overall precipitation in D02.

4.3.3 Rainfall Rate

The depiction of hourly rainfall rate clarifies the structure seen in the accumulated precipitation (previous section). All simulations show a rapid intensification of rainfall rates from 03 UTC to 05 UTC as the MCS reaches the northwest shore of Lake Superior (Figure 4.9). The Minus 3 has smallest area of hourly rainfall rates greater than 20 mm/hour of all the simulations, but a larger area of greater than 15 mm/hour leading to a broader area of rainfall (Figure 4.9b). The Minus 6 study has an area of rainfall greater than 20 mm/hour comparable to the Control simulation, but shifted slightly to the southwest (Figure 4.9c). From 05 to 06 UTC, the pattern of rainfall intensity changes, with the Minus 3 case intensifying over the Control just west of the Keweenaw Peninsula (Figure 4.10b). The Minus 6 case has a similar structure to the Control during this time except more intensity along the northern coast of Lake Superior (Figure 4.10c). The Positive case studies intensify further to the north along the northern coast of Lake Superior (Figure 4.10d-f). By 08 UTC, the Plus 3 and Plus 6 case studies show a similar pattern to the Control, but shifted to the north (Figure 4.11). The Plus 3 and Plus 6 have the highest rainfall rates along the northern shore of Lake Superior compared to the other simulations. The Minus 3 and Minus 6 case study have a reduction in rainfall rate across most of the lake (Figure 4.11b-c), while the Minus 6 has an area of intense rainfall at

approximately the same location as the Control (Figure 4.11c). The reasons for these shifts are discussed in Section 4.4.

4.3.4 Local Circulation Changes

At 12 UTC on July 2nd, 10m winds over the southern part of Lake Superior are out of the south, originating from Michigan's Upper Peninsula (Figure 4.12**)**. Further to the north over the lake, the winds begin to the turn counterclockwise to out of the northeast along the northwest coast, parallel to the coast. At 03 UTC, just as the MCS reaches the lake, the winds are predominantly out of the south-southeast except for along the northwest coast, where the winds are still predominately out of the northeast (Figure 4.13). This northeast wind represents the barrier jet. After the MCS passes, winds become predominantly out of the southwest across the lake.

The sensitivity simulations do show significant changes in local wind speeds. At 12 UTC on July 2nd, the Negative simulations have higher wind speeds over the western half of the lake, with lower wind speeds along the shoreline on the western third of the lake on the order of .5 to 1 m/s (Figure 4.12b-c). This pattern is inverted for the Positive cases, where the central portion of the lake has increases in wind speed but decreases in speed along the southern, eastern, and northern coasts (Figure 4.12d-f). The magnitude of these changes vary based on the case study, with Plus 6 and PBL Temp studies showing reductions on the order of 3 to 4 m/s in locations.

At 03 UTC on July 3rd, a line of decreased wind speed stretches from Isle Royale to the northeast near Marathon, Ontario in the Minus 3 and Minus 6 cases (Figure 4.13b-c). This pattern is flipped in the Positive cases with wind speed increasing instead of decreasing (Figure 4.13d-f). The Plus 3 and PBL Temp have slight increases in wind

speed, while the Plus 6 has the most discernable increase. This feature is relatively stationary over the next three hours, with some variations in wind speed. This pattern remains until the MCS moves to the east across the entire lake.

The convergence of the 10m winds show a convergence zone over northern Wisconsin at 16 UTC, created by the barrier jet converging with the background flow out of the south over land (Figure 4.14**)**. The inland extent of this convergence does change based on the lake temperature, with lower lake temperatures causing the convergence to occur further inland. Warmer lake temperatures result in this feature occurring along the coast. Over the next seven hours, there are no significant convergence or divergent features over the lake. After 23 UTC, a convergence feature begins to form in the same area as the wind speed changes to the northeast of Isle Royale. All the simulations produce this feature, with varying degrees of convergence and placement. The Positive case studies create the feature closer to the northern shore and weaker than the Control case. The Negative cases keep the same relative intensity as the Control case but further south. This convergence line moves slightly to the north from 00 UTC until the passing of the MCS when the feature is removed.

While the MCS is over the lake, there are significant changes in the low level convergence. For the Minus 3 case study, at 06 UTC, the 10m-convergence zone remains closer to a straight line over the lake (north to south), while the Control case study begins to accelerate and generate a bow (Figure 4.15a-b**)**. A bow does form in the Minus 6 case study, but it is not as severe as the Control case (Figure 4.15c). The Positive case studies do create similar bows to the Control case study at this time, but shifted further to the north (Figure 4.15d-f**)**.

	Minus 6	Minus 3	Control	Plus 3	Plus 6	PBLH
≥ 0.5 m/s	28.59	29.98	29.31	29.61	31.58	30.66
≥ 1.0 m/s	10.16	11.06	10.65	10.89	11.31	11.23
≥ 2.0 m/s	3.69	3.94	3.82	3.96	4.13	4.03
≥ 5.0 m/s	1.07	1.16	1.12	1.17	1.20	1.18

Table 4.3. Percentage of Lake Superior region with vertical velocity greater than or equal to 0.5, 1.0, 2.0, and 5.0 m/s from 02 to 12 UTC on July 3rd.

Table 4.3 shows the percentage of the Lake Superior region that contained a maximum vertical velocity of a certain critical value from 02 to 12 UTC on July 3, 2012. The Minus 6 has the lowest percentage of grid boxes with maximum vertical velocities greater than the critical values, followed by the Control case. The Plus 6 case study has the greatest area covered by the strongest vertical velocities (≥ 5.0 m/s) than all other simulations.

4.3.5 Low-Level Stability Changes

Simulated atmospheric soundings of the lowest 2.5 km of the atmosphere are shown in Figure 4.16 at model initialization. This sounding represents the northern portion of the lake, just east of Isle Royale. The influences from the changes in the lake temperature can be seen in Figure 4.17b-f near the surface, where higher temperatures raise the lowest level temperature and lower lake temperatures reduce it. The temperature profiles above the near surface environment show minimal changes throughout the first 14 hours. By 02 UTC on July 2nd, there are minor changes within the first 1km of the surface, but this is less than 1 degree Celsius, with Positive cases warming this region and the Negative case studies cooling it. Throughout the simulation, the Negative cases have a significant deepening of condensed air near the surface, where dew point and atmospheric temperatures are equal. Before 02 UTC on July 3rd, the soundings have similar characteristics to the Control, with only minor differences in low-level temperature and

dew point temperature (Figure 4.17**)**. There is still a stable layer present near the surface, shown by increasing temperature with height for approximately the first 300m, meaning the PBLH case study did not achieve its intended purpose (more on this in Section 4.4).

The 4m temperatures over the lake, calculated from linear interpolating between the 2m temperature and lowest model level (~34m above the surface), are compared with the skin temperature, a proxy for the lake water temperature at a depth of 1m, to look at changes to the lowest stable layer that G2004 and M2011 used to determine if a MCS would propagate or dissipate over the lake. For the Control simulation, the temperature difference is greater than 2.5 degrees Celsius over most of the lake at 03 UTC. Along the northwest shore of Lake Superior there is a narrow band of values between 0 and 1.5 degrees Celsius. Changes to the lake temperature in the sensitivity studies results in only minor changes to this feature along the shore, and little to no change in the over lake environment for the central and eastern portions of the lake in terms of reducing the temperature difference to below the critical value. This then predicts that the storm should propagate over the lake surface in all simulations. To have the storm dissipate over the lake, the temperature difference would potentially need to be lowered to 1 degree Celsius through a simultaneous warming of the lakes and a cooling of the near surface air.

4.3.6 Skin Temperature Changes

The skin temperature is plotted to illustrate how the changes made to the skin temperature at initialization influence the region 24 hours after initialization (Figure 4.18). The clearest signal is visible around Lake Superior, with the Positive case studies having an increased temperature around the lake, particularly to the northwest. The

Negative case studies have a reduction in temperature in the same areas, but not as large of an absolute change as the Positive cases. On top of this relatively stationary change, there are gravity waves that originate off of convection over central Wisconsin.

These waves travel to the north over the next several hours. At 20 UTC, these waves begin to interact with the line of convection as it moves over northern Minnesota (areas circled in black in Figure 4.19). The wave is consistent in placement and intensity amongst all the sensitivity studies, producing an area of lower skin temperatures ahead of the MCS. It is at this point that the MCS begins to diverge in the sensitivity runs from the Control, slowing down the system by approximately 30 minutes by reducing the near-surface horizontal temperature gradient across the MCS. This interaction alters the environment around the MCS resulting in the change in precipitation amounts near the northern portion of the domain (Figure 4.8).

4.3.7 Parcel Trajectories

The Read/Interpolate/Plot program version 4.5 (RIP4; Stoelinga 2009) is used to calculate the trajectory of air parcels. Parcels are released at the lowest model level, approximately 34m above the lake surface, in a line offshore of the northwest coast of Lake Superior (Figure 4.20**)**. A total of 31 parcels are initialized at 03 UTC on July 3rd, within 30 minutes of the MCS reaching the lakeshore. Winds are linearly interpolated to every 5 minutes from the 10-minute output of WRF to calculate the Cartesian coordinates of each parcel until 12 UTC on July 3rd.

	Minus6	Minus3	Control	Plus3	Plus6	PBL Temp
Above 1.5km	12	10	14	11	17	15
Above 3.0km	9	9	10	10	12	14
Above 6.0km	4	4	5	6	7	8

Table 4.4. Number of parcels (31 total) that reach above a critical height during their trajectory.

Table 4.4 shows the number of parcels that are elevated to critical heights in their lifetime. For parcels reaching above 1.5km, there is a local maximum in the Control case study, with fewer parcels reaching this height in the Minus 3, Minus 6, and Plus 3 studies. The Plus 6 case study has the most parcels reaching above this height of the other sensitivity studies. For critical height values of 3km and 6km, in general, the number of parcels reaching these heights goes up as the lake surface temperature increases, although changes are minimal. This does not take into account where the parcels reached this height, as the parcel may have been transported over land where the heating of the land surface may aid in elevating the parcels.

Figure 4.21 depicts the parcel height over time from 03 UTC to 11 UTC. Of the 31 parcels released in the Negative case studies, there is a preference for parcels to reach above 1.5km at a higher number, meaning closer to the northern portion of the lake. This is echoed in Figure 4.22, which only displays the Cartesian location of parcels that reach over 1.5km in the vertical direction in their lifetime. When the lake temperature increases, more parcels reach above 1.5km along the southwest portion of the lake. In all the simulations, the parcels are typically elevated between 04 and 05 UTC.

The position of the parcel when it reaches the critical height is calculated to show the direct influence from the lake surface. For the Control case, 7 of the 14 parcels that

reached 1.5km did so while still over water. Both the Plus 3 and Minus 3 case studies had similar results, with 6 out of 10 and 6 out of 11, respectively, reaching 1.5km. The Plus 6 and PBLH Temp studies have significant increases in the number of parcels reaching the height while still over water. The Plus 6 has 13 out 17 parcels reach this height, while the PBL Temp study has 12 out of 15. The Minus 6 study has all 12 parcels reaching 1.5km while still over water.

4.4 Discussion of Results

While the storm structure does not visibly show large changes in the radar reflectivity, the hourly rainfall rate depicts a clear split in intensity of rainfall to the north and south. This is only a change in the distribution of rainfall, as the overall changes in precipitation totals are minimal, especially over D02. While local changes are greater over Lake Superior, the change in intensity for all sensitivity studies are less than 10% of the Control. These are slightly larger than Zhao et al. (2015) observed changes in rainfall for removing the Great Salt Lake in simulations of a MCS passing over the lake, which were deemed insignificant.

There are several factors that lead to the increases in precipitation for five out of the six sensitivity studies. First, the increases in the Minus 3 case study are mainly due to changes to the near surface convergence over the lake. The lack of a bow formation allows for greater convergence to occur along the front with winds ahead of the system out of the southeast. By creating the bow in the convergence front, the convergence focuses along the southern half of the bow where the wind components ahead and behind the front are opposite; while the northern half of the bow has wind components that are perpendicular to the winds ahead of the system. Along the northern shore of Lake

Superior, the wider barrier jet compared to the Control simulation increases the area of convergence along the front due to the northeasterly flow. This creates an increase in vertical motion and rainfall.

For the Positive case studies, the rainfall increases are a result of changes in mechanical forcing and thermodynamic changes. The increase in lake temperature reduces the overall strength of the surface stable layer by warming the near-surface air resulting in surface air being more conducive to convective motions. These simulations form a bow at the leading edge of the MCS, similar to the Control, but shifted further to the north. This shift in placement to the north changes the placement of maximum convergence along the southern half of the bow and the location of the greatest rainfall. The shift also alters the convergence line near the southern coast of Lake Superior, from northeast to southwest oriented in the Control case to a north-south oriented line in the sensitivity studies. This change in orientation results in a change in the strength of convergence and a reduction in rainfall along this region. There are also changes in the circulation along the coasts due to variations in the temperature gradient across the coast that could have important roles in near shore modifications to the front. To fully test the role of these circulations, the removal of the lake or increases in temperature to be the same as the land in simulations would be needed.

Barrett et al. (2009) observed a case study where a cold front interacted with a barrier jet over Chile. It was found that the barrier jet impeded the northward movement of a cold front, both slowing down the front and creating a convergence zone along the cold front leading to increased precipitation. Similar to the Barrett et al. (2009) case study, the MCS in the simulations interacts with the northeasterly winds of the barrier jet,

increasing the convergence in this region. The barrier jet placement, especially near the northern most extent of the lake, is found to be sensitive to lake surface temperature. Reducing the lake temperature widens the barrier jet and increases the area with winds directly opposing the MCS. With increases in the lake temperature the barrier jet narrows, shifting the region of greatest convergence with the MCS further to the north. This combination of greater instability in the lowest levels, increased low-level water vapor mixing ratios (not shown), and changes in low-level convergence patterns help to increase the overall rainfall amounts along the northern shore in the Positive cases.

In the Minus 6 case study, while the temperature reduction does increase the width of the barrier jet, other factors are at play to reduce the overall precipitation amounts. There is increased stability of near surface air parcels, reducing the amount of air that can be lifted and the height it can be lifted. The colder lake surface also reduces the amount of available water vapor in the lowest levels. These two factors overcome the mechanical forcing to reduce the amount of rainfall over Lake Superior.

Gallus and Segal (1999) observed the effects of a cold front over Lake Michigan and found the front would move faster over the lake than over land. They concluded that the lake altered the flow due to changes in the temperature gradient across the front and the lower stable layer reducing the influence of friction on elevated winds. This idea is potentially observed in the Minus 3 case study, where the front does not create a bow. The Minus 3 case alters the environmental temperature in front of the storm, reducing the gradient and in turn reducing the acceleration of the system since the speed of the system is proportional to the gradient of the potential temperature of the cold pool and the environment (Rotunno et al. 1988). The evolution of the cold pool and the MCS

associated with it are also dependent on other conditions like the low-level wind shear balancing the shear induced by the cold pool and strength of the cold pool (Rotunno et al. 1988, Szeto and Cho 1994, James et al. 1996). A combination of these effects is likely in this case, with the characteristics of the low level air being ingested by the storm have been changed and the low-level environmental shear being changed due to wind speed changes (see Figure 4.13). The change in the Positive cases bow placement may also be related to the previously described characteristics. The bow formation in the Minus 6 case study shows similar placement and characteristics to the Control case, going against the ideas presented in this paragraph. Further investigation is needed to determine the exact role of the environment and lake surface on the change in orientation of the MCS.

As the parcel trajectories show, the control case has a local maximum in the number of parcels reaching above 1.5 km above ground level compared to the Plus 3 and Minus 3 case studies. As the lake warms, though, a greater number of these parcels reach higher levels. This trend is again due to the thermodynamic and mechanical forcing. With both of these happening in unison, it is difficult to distinguish the dominating factor.

The parcel trajectories also highlight the potential for a MCS passing over the stable boundary layer of the lake to redistribute the near-surface air to the free troposphere. Cotton et al. (1995) created a review of the literature at the time, looking at different types of clouds and their roles in venting mass from the boundary layer. The authors concluded that MCS are only second to extratropical cyclones in the amount of mass elevated out of the boundary layer, meaning that MCSs are effective at moving pollutants released near the surface to the free troposphere. MCSs also provide an ideal environment for aqueous phased chemistry to occur from boundary layer chemical species. While

local pollution and air quality are not as important for Lake Superior due to the limited population and industrial processes surrounding the lake as compared to the other Great Lakes, enhanced boundary layer venting from passing MCSs over the region could play a larger role in chemical distribution and air quality. Brook et al. (2013) observed that pollutants could collect over the lakes during the evening due to local circulations induced by the lakes. Higher lake temperatures and passing MCSs have the potential to aid in the redistribution of pollutants to the free troposphere.

The PBLH Temp case study was not successful in achieving what it was initially set out to accomplish by fully removing the stable layer present over the lake while still keeping the water surface. The main reason for this is the use of the PBL height over the lake generated in the YSU boundary layer scheme (Hong et al. 2006). This scheme uses a critical bulk Richardson number of zero to define the height of the boundary layer, meaning the bulk Richardson number would need to be a vertical gradient in virtual potential temperature equal to zero. As shown in Figure 4.16, it appears that the lake has a deeper influence on the overlying air temperature than the calculated PBL height. A better representation of the PBL height would be to focus on the vertical gradient in potential temperature. This value would not be as influenced by the vertical distribution of moisture as the PBL height calculated by the bulk Richardson number. This technique, though, would result in temperature increases exceeding 10 Kelvin in most locations and potentially lead to new circulations being generated. These circulations could lead to precipitation, altering the direct signal of changes in the MCS from the lake surface.

The storm system did not show signs of significantly weakening or dissipating while traveling over the lake with varying lake temperatures. G2004 and M2011 looked at

observations of the differences between lake temperature and air temperature of buoys over the lake to correlate them with the dissipation and propagation of MCSs over Lake Michigan. Both these studies found that the strength of the near surface inversion was able to discriminate between MCSs that crossed over the lake and those that dissipated or weakened over the lake. G2004 did note that this relationship was not as strong late in the summer, when MCSs were able to maintain over a lake with a weak inversion that could result in more stable air being ingested by the storm leading to the weakening or dissipation of the storm. This weakening of the stable layer was mainly due to lake temperatures reaching their summer peak, which would mean near surface air was not as detrimental to the storm strength or formation. In the case study provided here, it is shown that even with a colder lake and stronger low-level stability, the storm still ingests air that is originally near the surface while maintaining over the lake and increase overall rainfall amounts. While there are different local circulations, like the barrier jet aiding in the movement of low-level air into the storm, over Lake Superior that do not exist over Lake Michigan, the large-scale flow may still be a significant factor in determining the lifetime and intensity of the storm.

M2011 does conclude that the larger scale environment is a much stronger, more robust factor in whether a MCS will dissipate while crossing Lake Michigan, with more instability downwind of Lake Michigan resulting in more storms maintaining over the lake. The author does mention that the strength of the stable layer over the lake can also be a determining factor. These two factors may not be independent of one another, as the over lake stable layer is controlled by both the lake surface temperature and the air temperature. While the lake may influence the air temperature at 5m, this could be a

smaller factor compared to the large-scale environment. With increased near surface air temperature over the region, this will increase the strength of the stable layer while leading to the chance of increasing the instability over land. Further investigation is needed in order to fully understand the role of the lake in spring and early summer versus late summer MCS propagation or dissipation over a lake is due to the lake itself or a combination of large scale and lake conditions. The results of this study highlight the local circulations that can change over Lake Superior which are not present over the other Great Lakes, which means extra caution is needed when applying conclusions drawn from other lakes to Lake Superior.

Finally, it should be noted that there are a number of large environmental changes that occur across the domain due to changes in the initial conditions. Most of these are related to convection interacting with the lakes and a lake breeze off of Lake Michigan in Wisconsin (not shown). Some of the overall changes described in this study may be a result of larger environmental changes induced by changes in the lake surface temperature (such as moisture and cloud cover distributions).

4.5 Conclusions

On July 3, 2012 a mesoscale convective system (MCS) formed over the northern Great Plains and eventually crossed Lake Superior showing little change in intensity while propagating over the lake surface. To test the direct role the lake surface temperature has on this storm system, the lake temperature was reduced by 3 Kelvin, increased by 3 and 6 Kelvin, and changed to the equivalent to the planetary boundary layer (PBL) height potential temperature in a series of Weather Research and Forecasting Model (WRF) simulations. The following conclusions were found:

1.) Lake temperature shows little influence on the overall amount of precipitation from this storm system. Increasing and reducing the lake temperature increases the percentage change in accumulated rainfall over the Lake Superior area. These increases are due to local changes in surface thermodynamics and local wind circulations**.**

2.) The change in structure and evolution of the storm is not distinctly observed in radar reflectivity, but rather in the rainfall rate. The storm creates a split in precipitation over the lake, with rainfall along the northern and southern coasts. This distribution is also influenced from the formation of a bow echo and the convergence associated with the MCS front and barrier jet, both of which are altered from varying lake temperature.

3.) Parcel trajectories show an increase in the amount of air escaping above 1.5km with increasing in lake temperature. Increases in parcel trajectories above 1.5km when lake temperature is reduced are due to changes in area to convergence over the lake.

4.) Changes in lake temperature do not alter the storms lifetime while passing over the lake at the distribution of temperatures tested here.

More questions are raised from this case study regarding the role of the lake on a passing MCS. Most importantly is still the direct role of the lake surface in generating a stable layer near the surface versus the background environment on controlling the lifetime of an MCS. While the lake does play a role in the passing of this feature, it is not significantly altered leading to the belief that the lake plays a minor role in the evolution of this specific MCS. Further case studies are needed, particularly earlier in the season, to

see if the influence of the lake temperature on the system is consistent with this study. Further investigation is also needed in order to determine the extent of findings from G2004 and M2011 over Lake Michigan are applicable to Lake Superior, which has significantly orographic features creating unique flow fields over the lake.

Finally, there is little mention of the barrier jet formation along Lake Superior currently in literature. Further investigation is needed to begin to quantify the overall influence of this feature on local weather and climate of the region and changes that could be experienced in a changing climate.

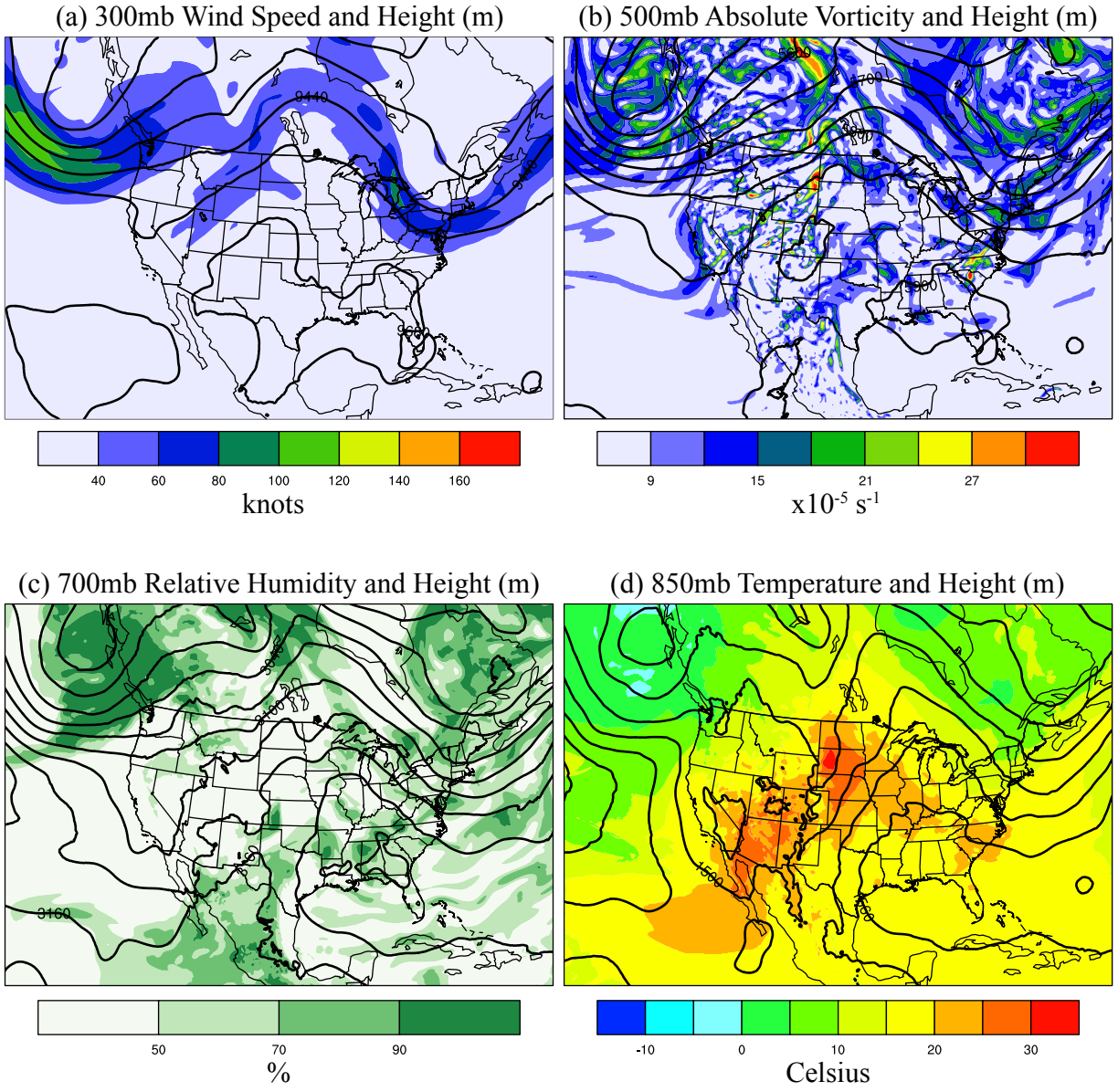

Figure 4.1. 4-panel plot on July 2, 2012 at 12 UTC. Panel (a) displays the 300mb geopotential height (m) and wind speed (m/s), (b) is the 500mb geopotential height (m) and absolute vorticity (1/s * 10^-5), (c) is the 700mb geopotential height (m) and relative humidity (%), and (d) is the 850mb geopotential height (m) and temperature (degrees C). Fields are plotted from the NAM-ANL.

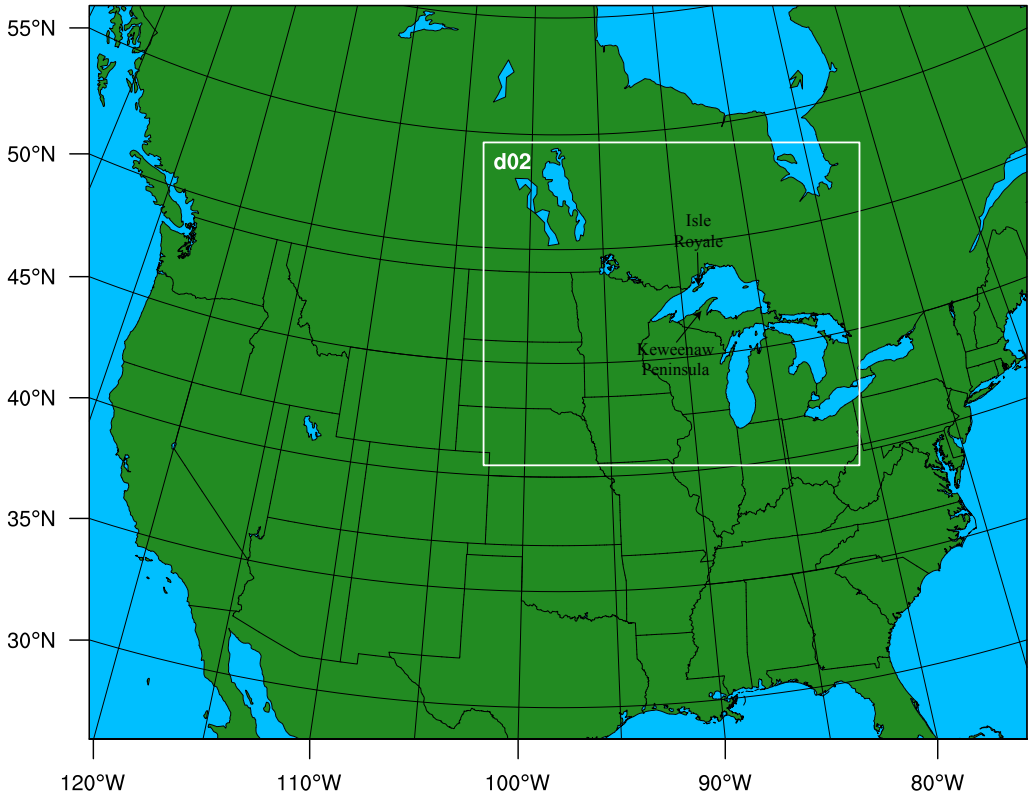

Figure 4.2. The WRF model domain setup. Domain 1 (D01) is a 10km horizontal resolution parent domain for Domain 2 (D02), a 2km horizontal resolution domain.

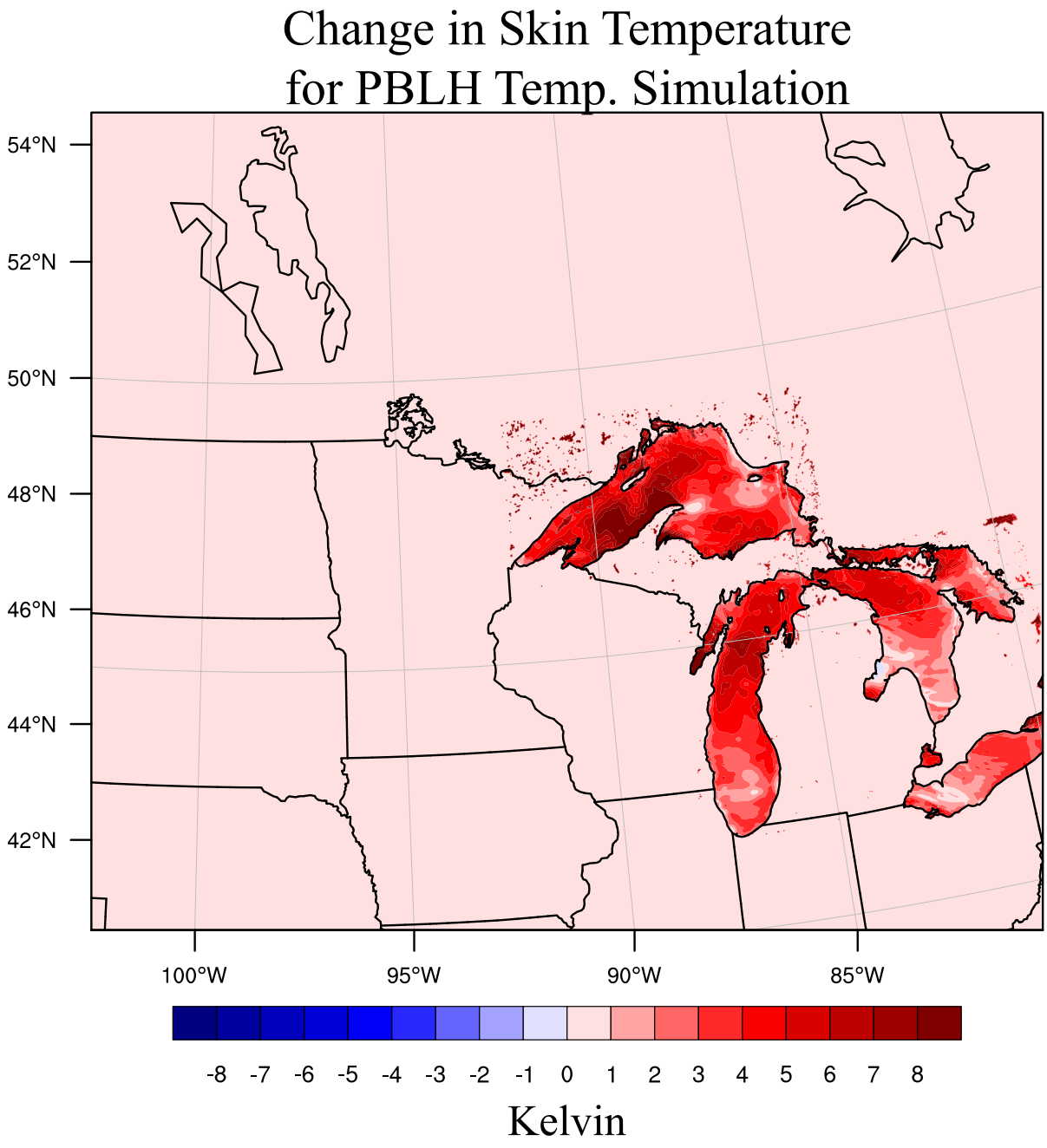

Figure 4.3. Change in skin temperature (Kelvin) for the PBL Temp case study from the Control on July 1, 2012 at 12 UTC.

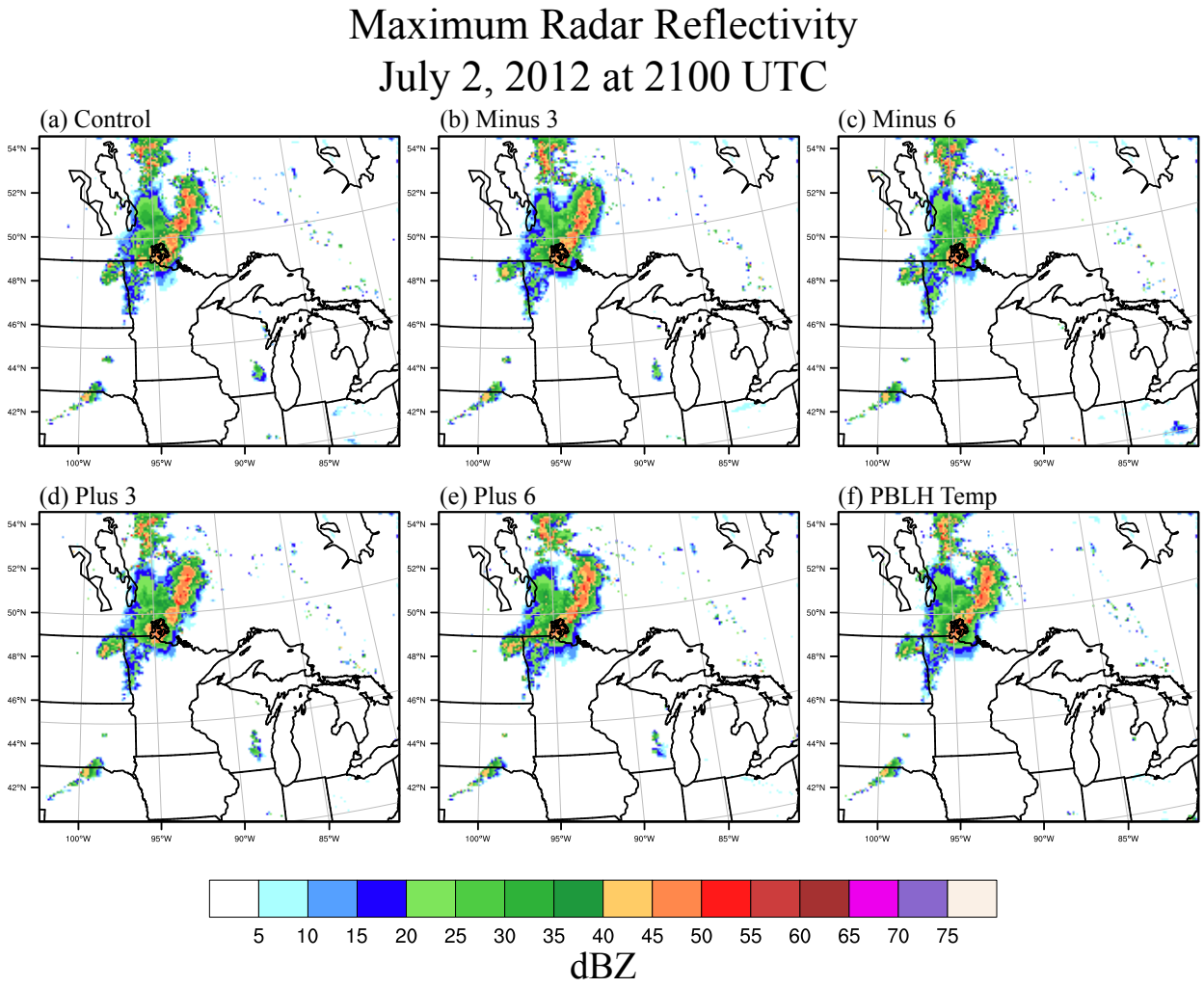

Figure 4.4. Simulated composite radar reflectivity at 23 UTC on July 2, 2012 for (a) Control, (b) Minus 3, (c) Minus 6, (d) Plus 3, (e) Plus 6, and (f) PBL Temp.

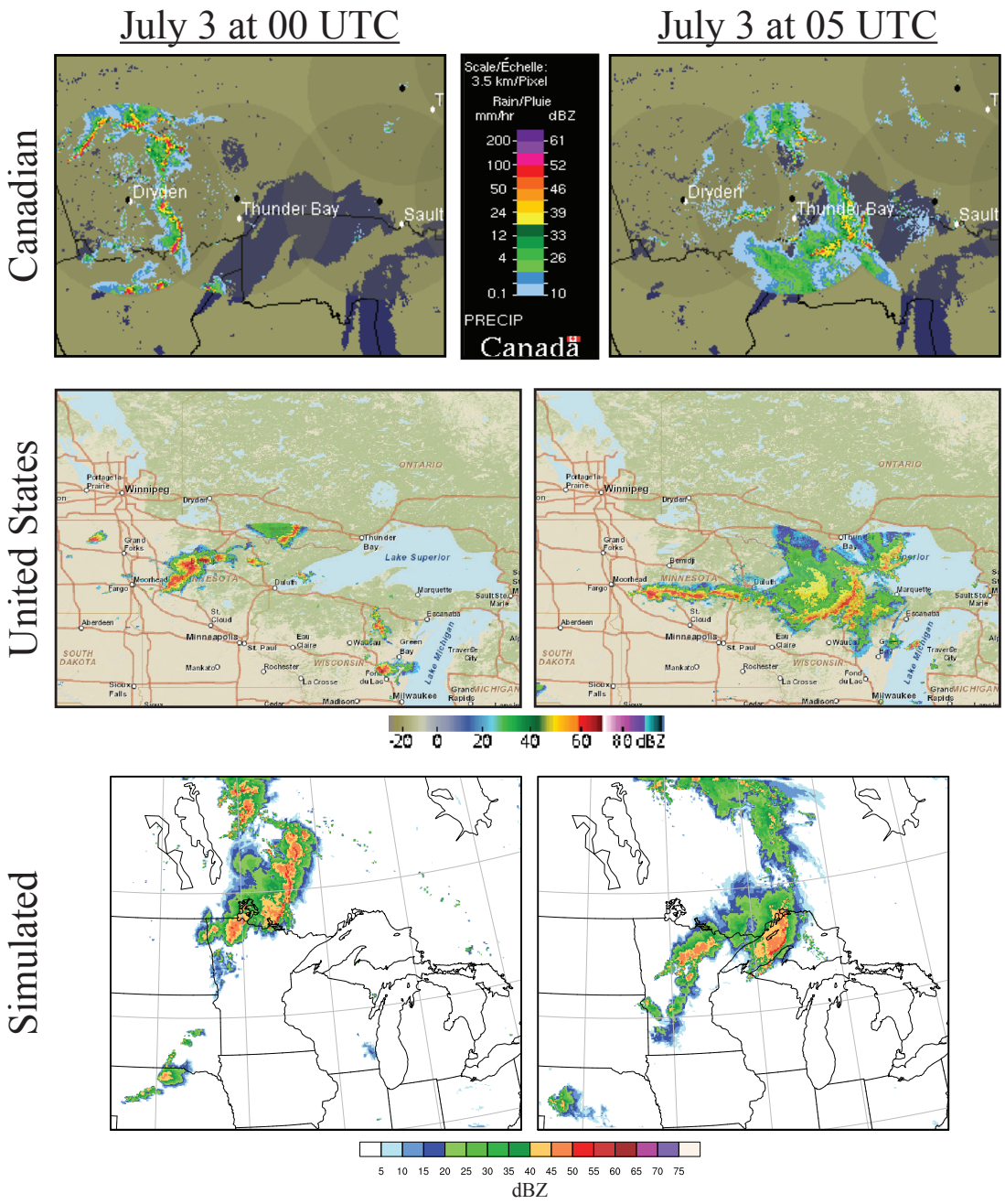

Figure 4.5. Observed composite radar reflectivity from Canadian based radars (top row) and United States based radars (middle row). Simulated maximum radar reflectivity from the Control Simulation in the bottom row. [United States radar reflectivity available online at http://www.ncdc.noaa.gov/nexradinv/. Canadian radar reflectivity available online at http://climate.weather.gc.ca/radar/index_e.html]

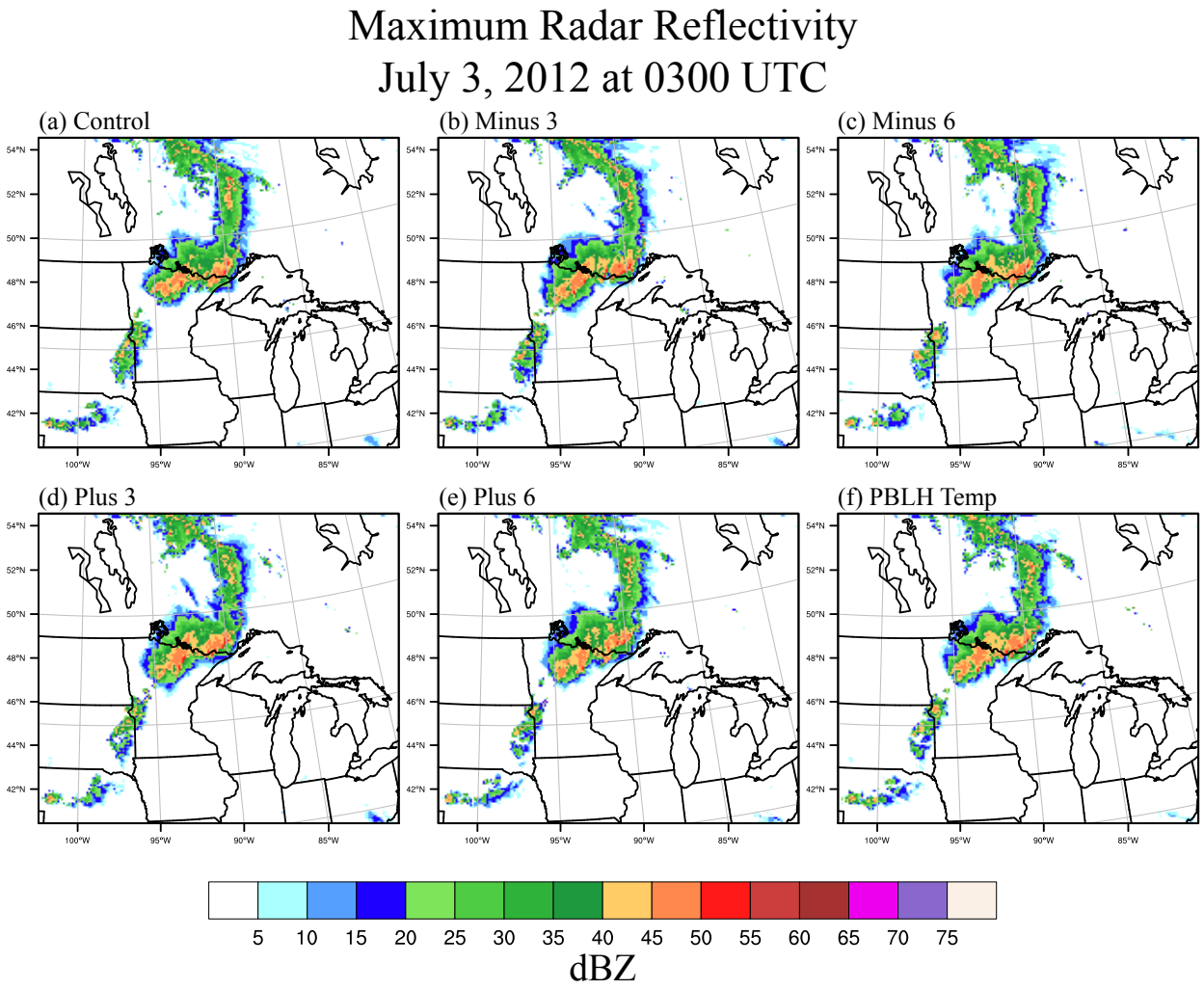

Figure 4.6. Same as Figure 4.4, but at 03 UTC on July 3, 2013.

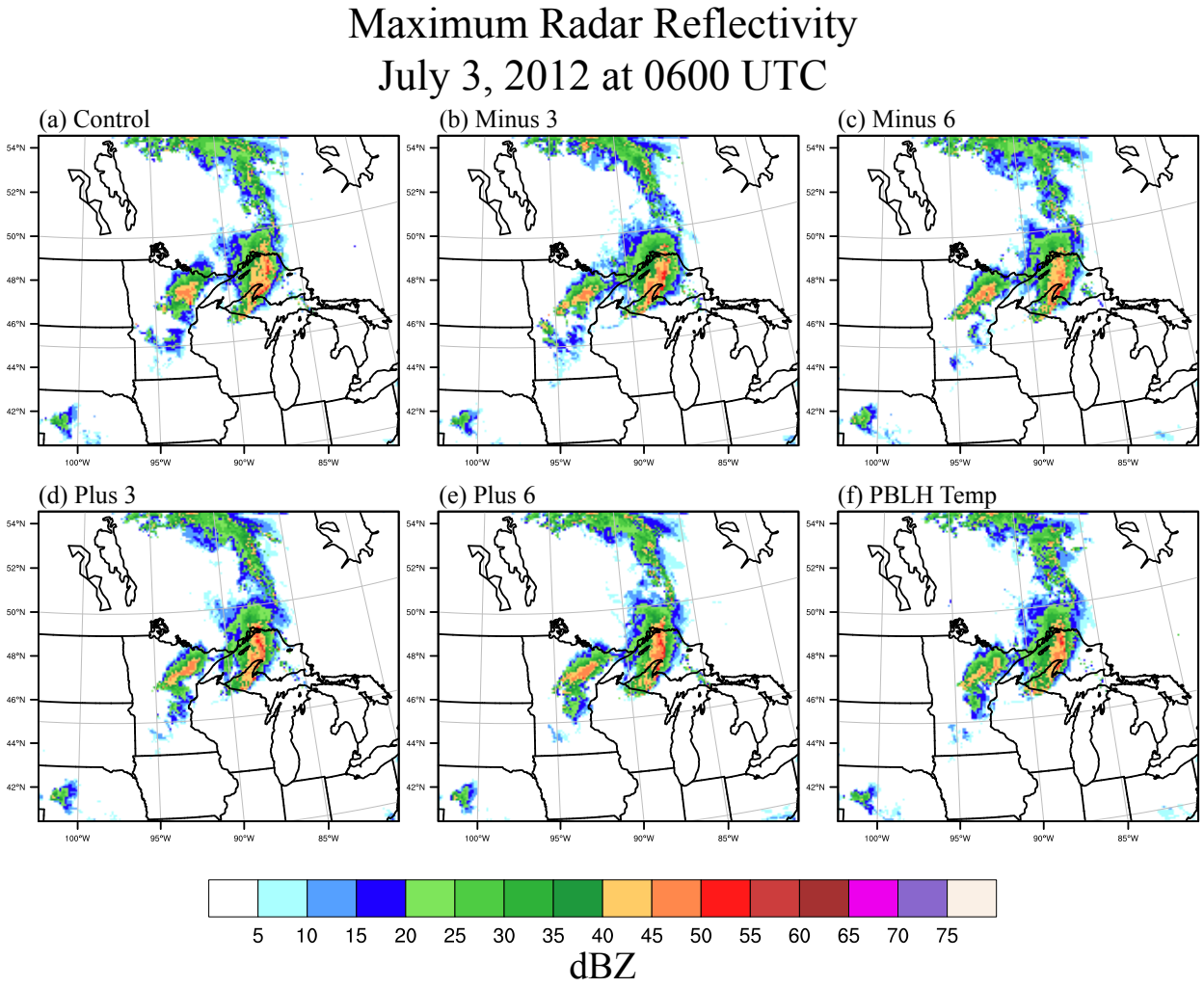

Figure 4.7. Same as Figure 4.4, but at 06 UTC on July 3, 2012.

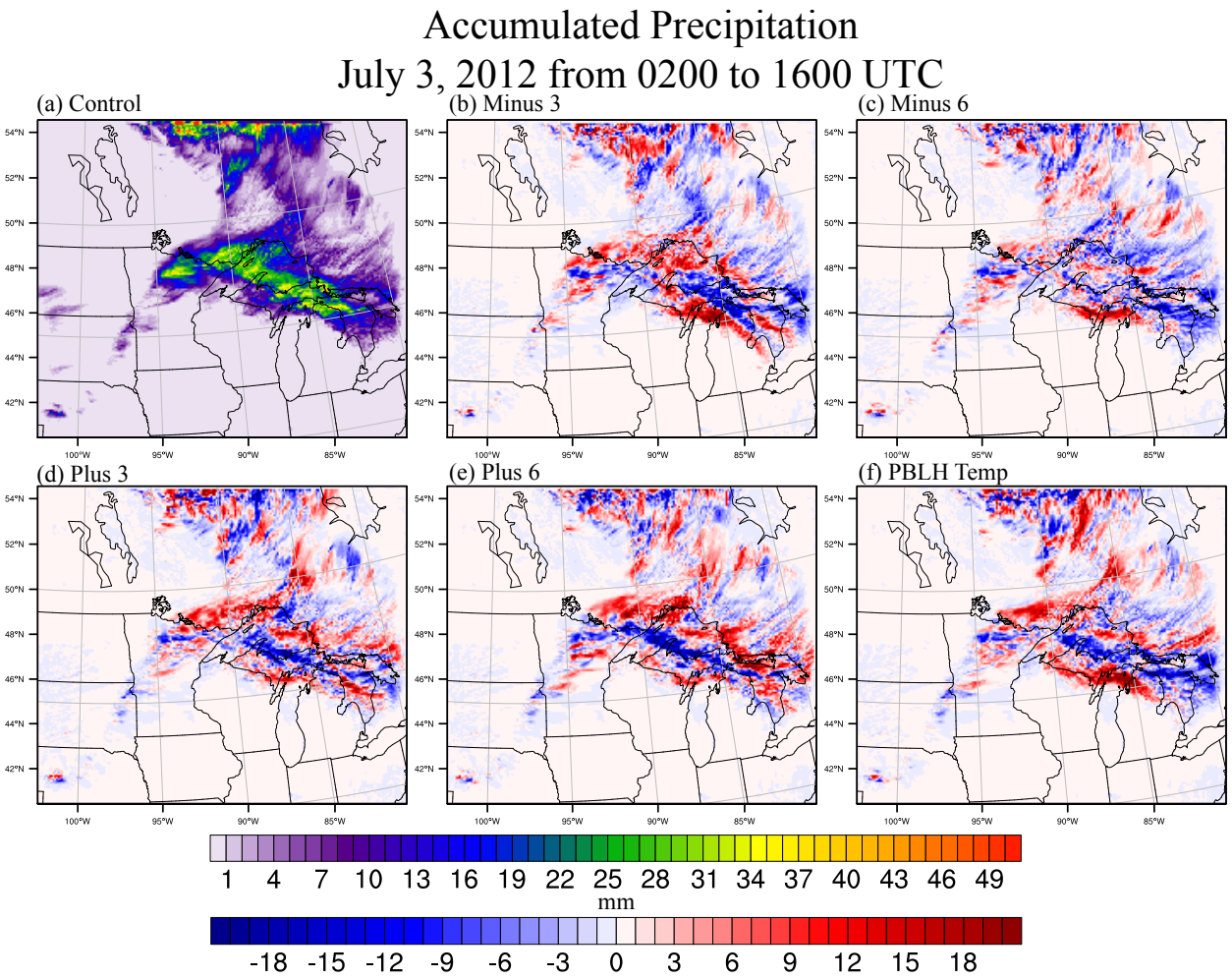

Figure 4.8. Accumulated rainfall (mm) from 02 to 16 UTC on July 3, 2012 for Control (a). Panel (b) displays the difference between the Minus 3 case study and the Control, (c) Minus 6 and Control, (d) Plus 3 and Control, (e) Plus 6 and Control, and (f) PBL Temp and Control.

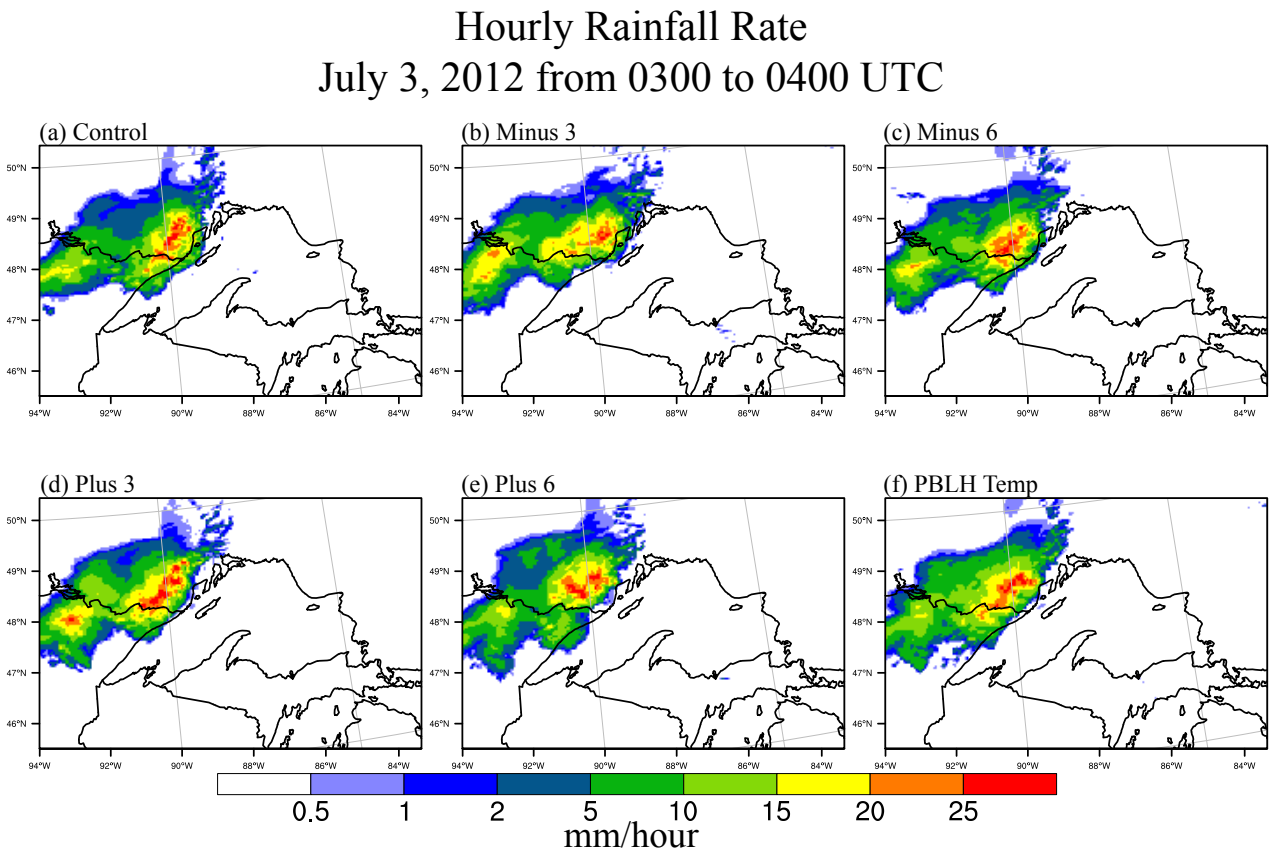

Figure 4.9. Hourly rainfall (mm/hour) from 03 to 04 UTC on July 3, 2012 for (a) Control, (b) Minus 3, (c) Minus 6, (d) Plus 3, (e) Plus 6, and (f) PBL Temp.

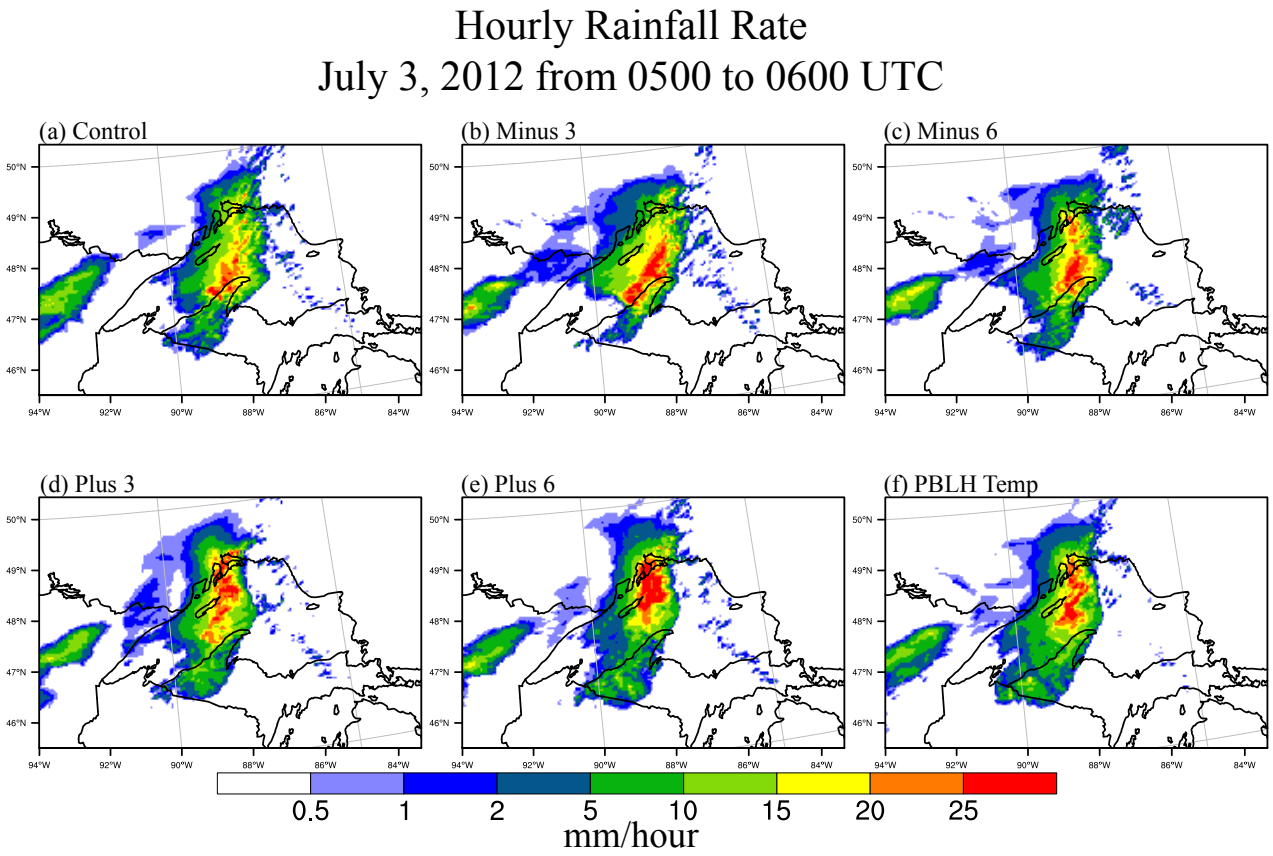

Figure 4.10. Same as Figure 4.9, except from 05 to 06 UTC for July 3, 2012.

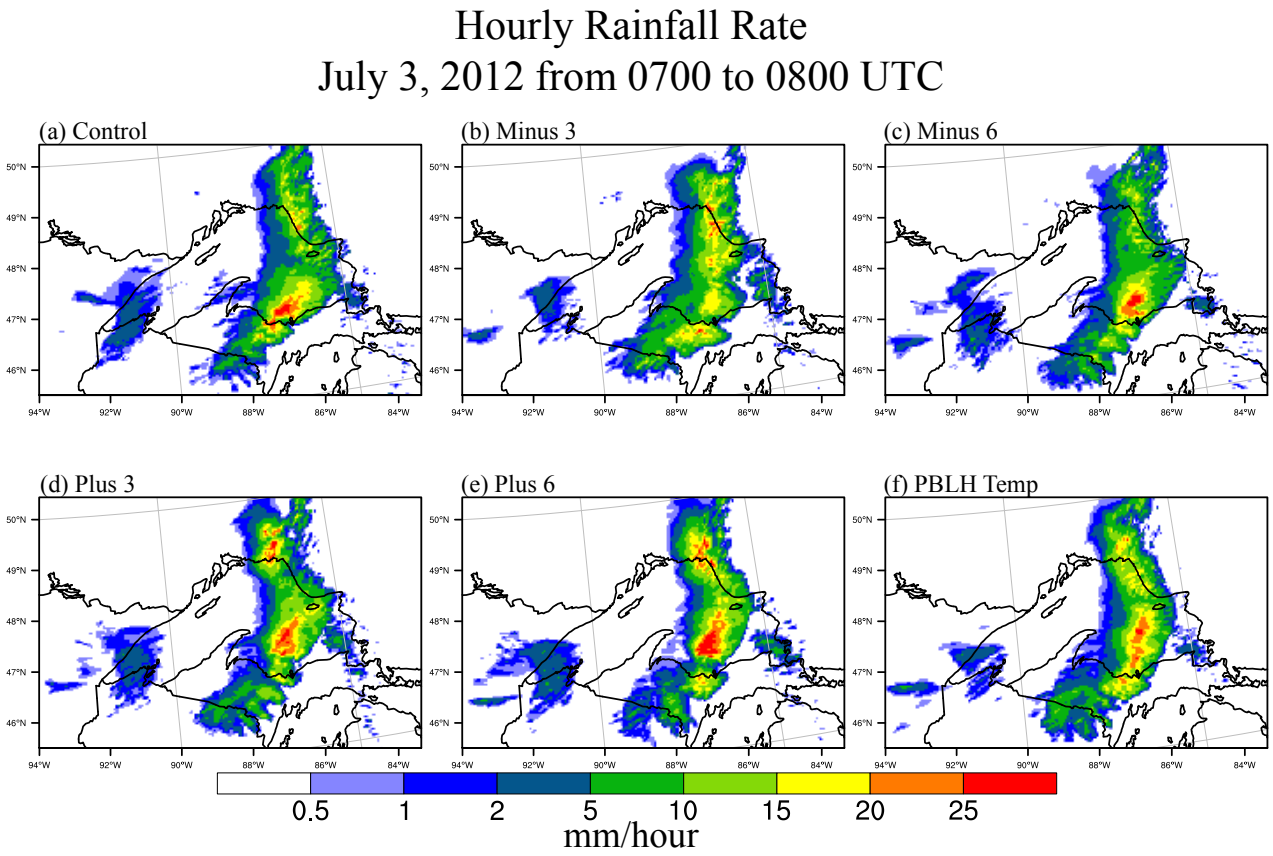

Figure 4.11. Same as Figure 4.9, except from 07 to 08 UTC on July 3, 2012.

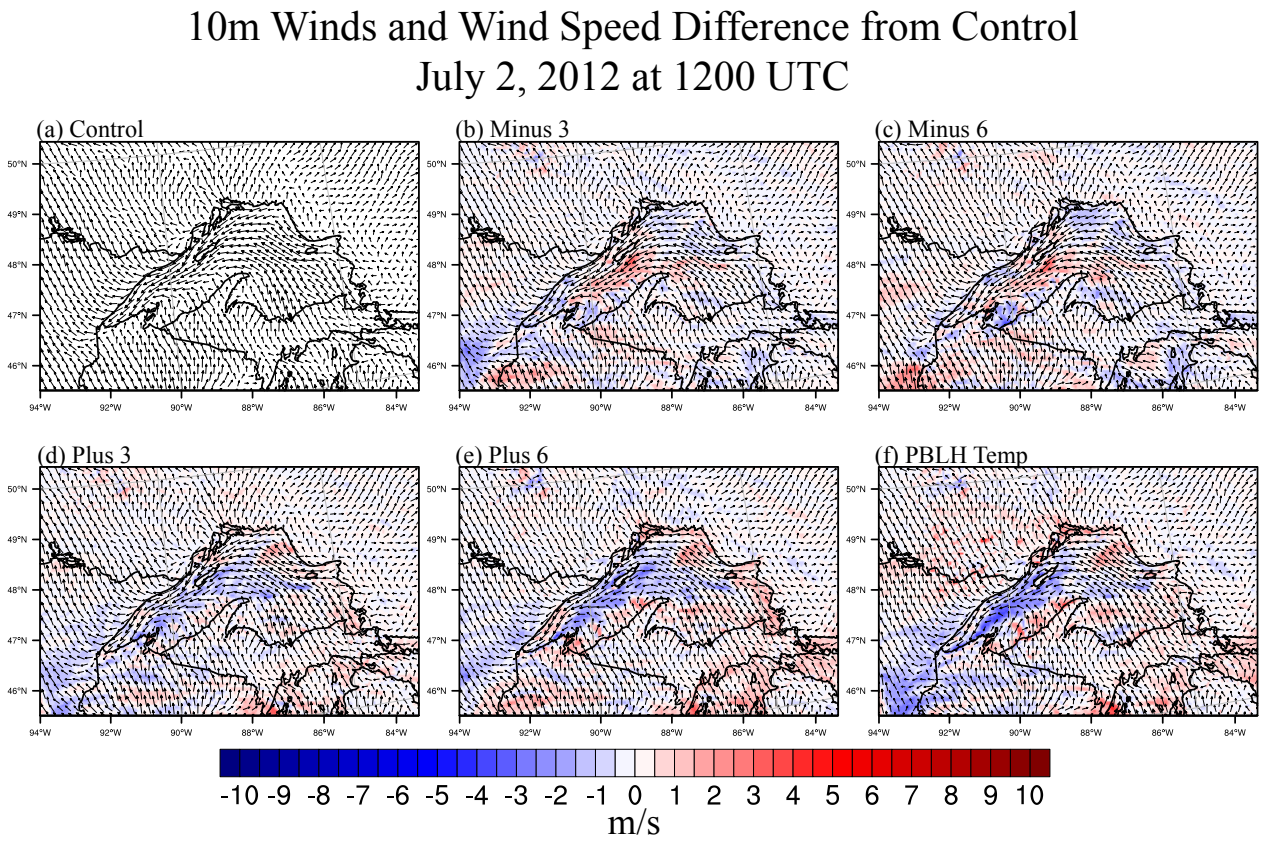

Figure 4.12. 10m wind direction at 12 UTC on July 2, 2012 for (a) Control, (b) Minus 3, (c) Minus 6, (d) Plus 3, (e) Plus 6, and (f) PBL Temp. Shaded regions in (b) through (f) are wind speed differences (m/s) from the Control case study. Positive values mean the winds are fast in the sensitivity study than the Control case study.

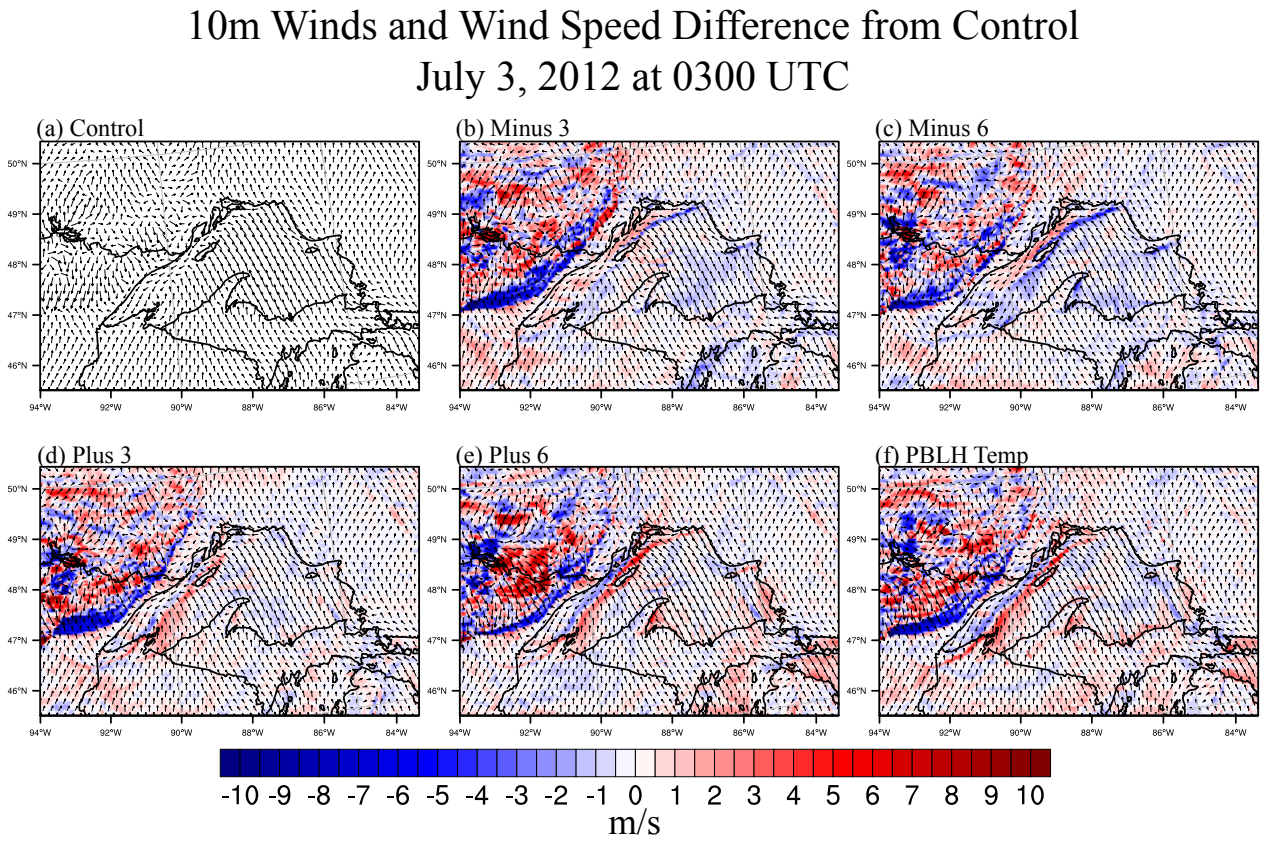

Figure 4.13. Same as Figure 4.12, except at 03 UTC on July 3, 2012.

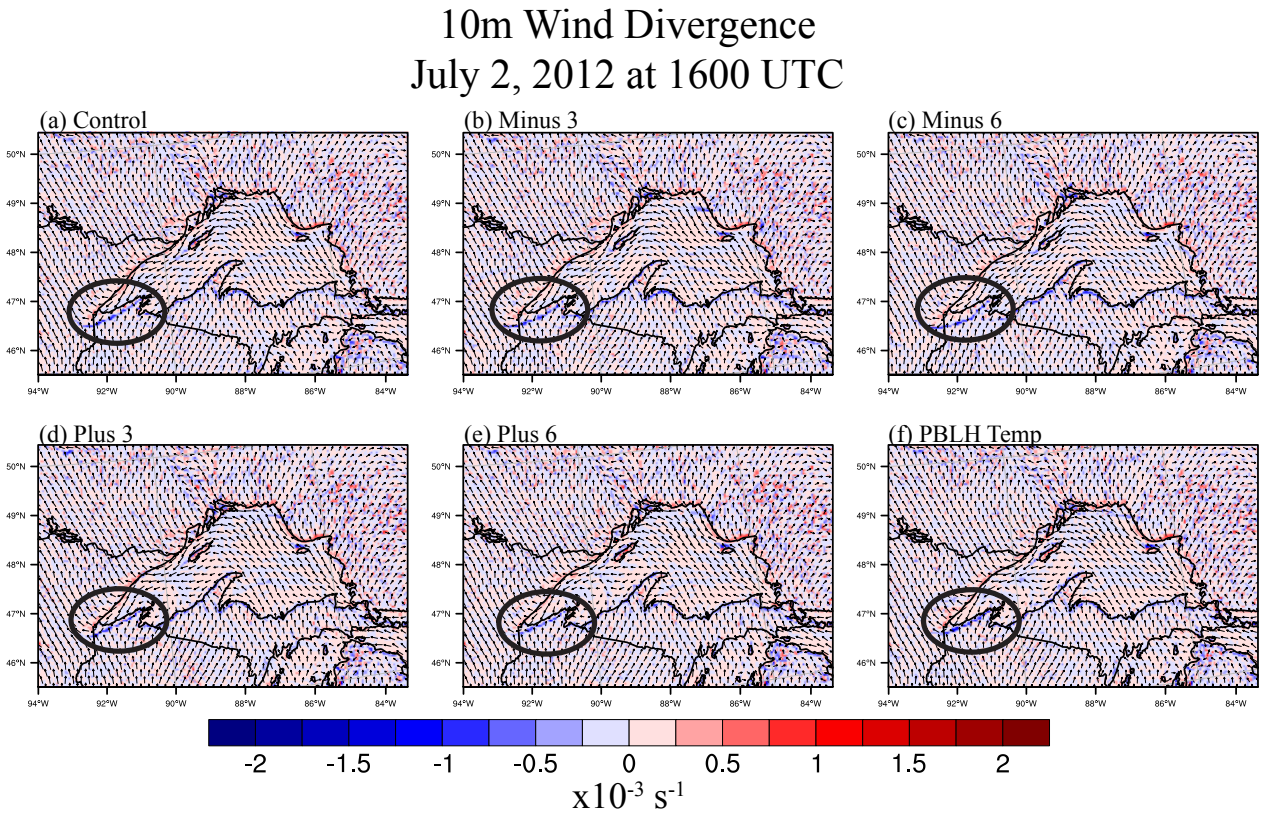

Figure 4.14. 10m wind divergence ($x10^{-3}$ s^{-1}) at 16 UTC on July 3, 2012 for (a) Control, (b) Minus 3, (c) Minus 6, (d) Plus 3, (e) Plus 6, and (f) PBL Temp. Red shading represents divergence, while blue represents convergence. Black circle represents area of convergence associated with the barrier jet over land.

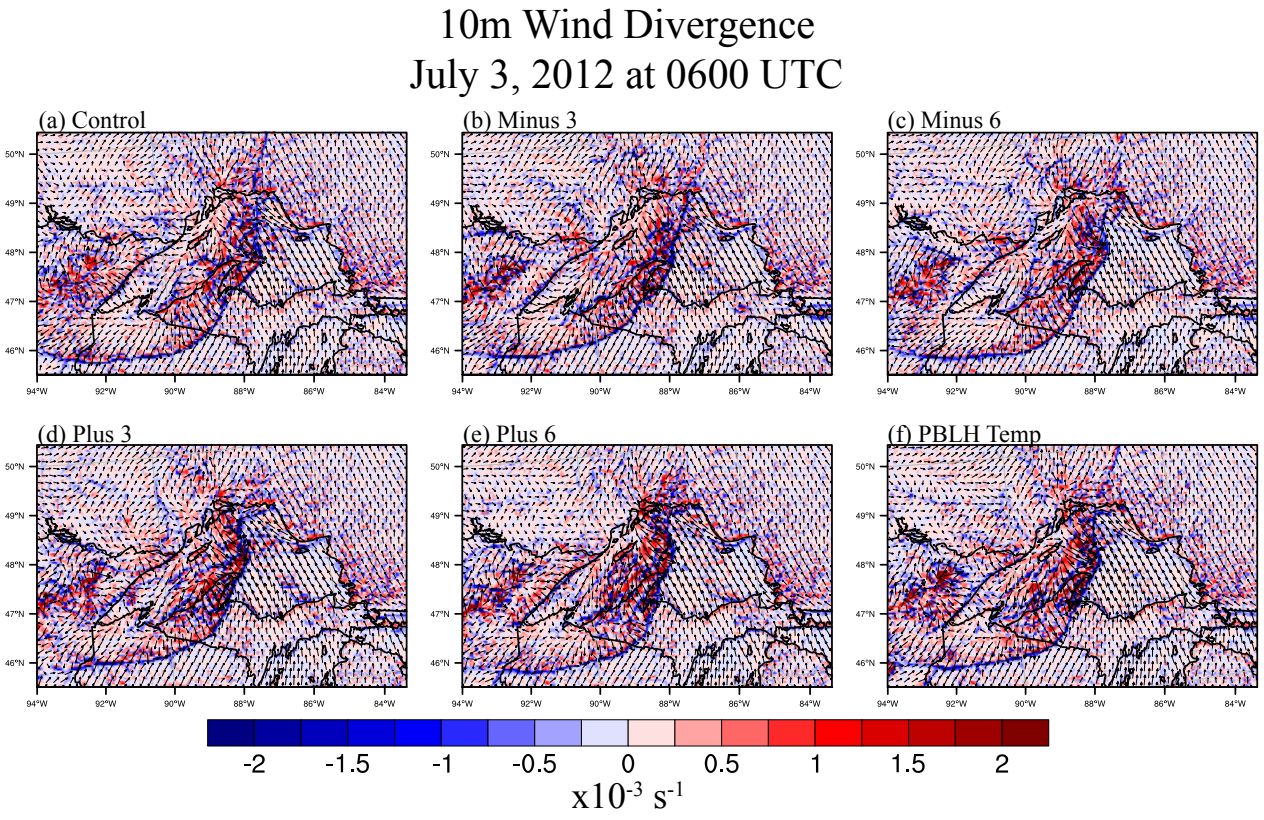

Figure 4.15. Same as Figure 4.14, except at 06 UTC on July 3, 2012.

July 1, 2012 at 1200 UTC
48.011° N 87.8634° W

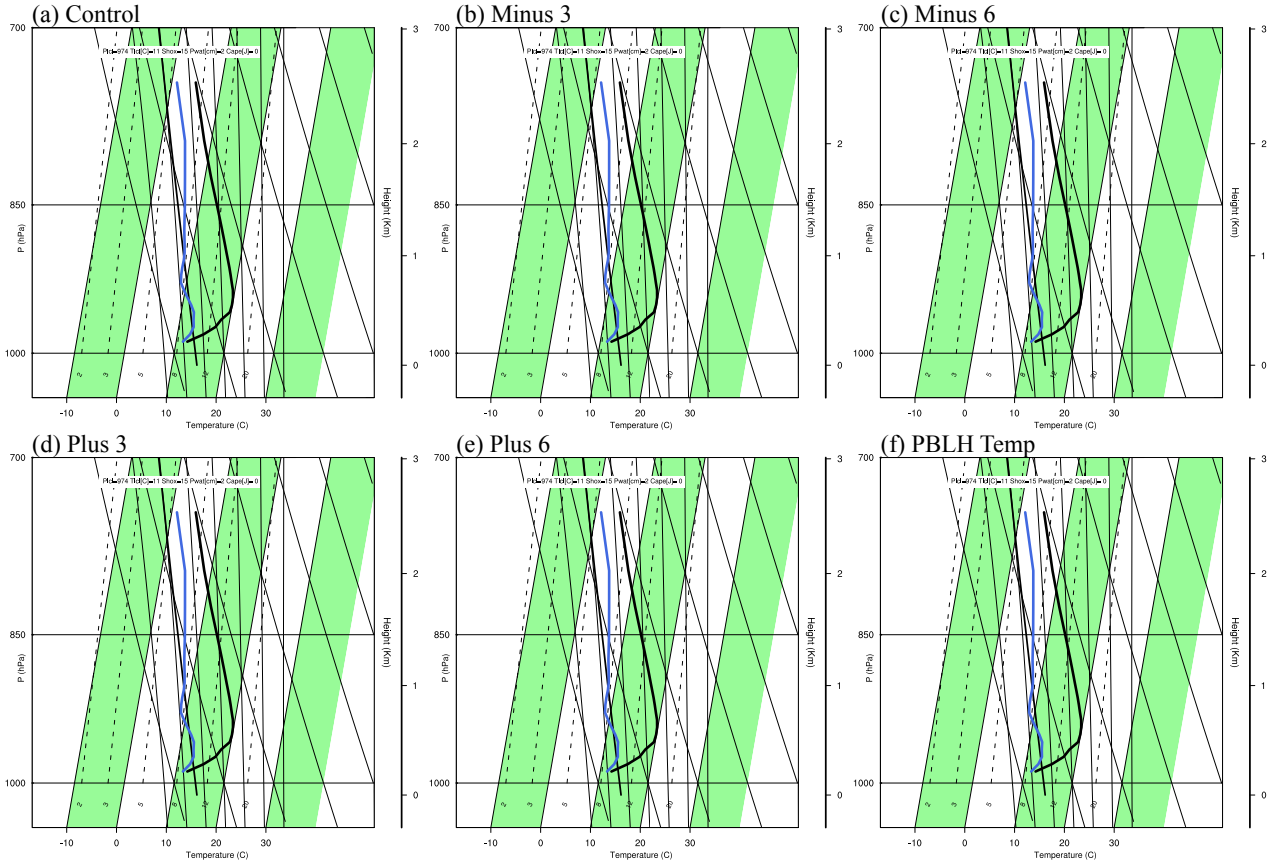

Figure 4.16. Skew-T diagrams of the lowest 3km at 12 UTC on July 1, 2012 just east of Isle Royale (48.011 degrees N, 87.8634 degrees W). (a) Control, (b) Minus 3, (c) Minus 6, (d) Plus 3, (e) Plus 6, (f) PBL Temp.

July 3, 2012 at 0200 UTC
48.011° N 87.8634° W

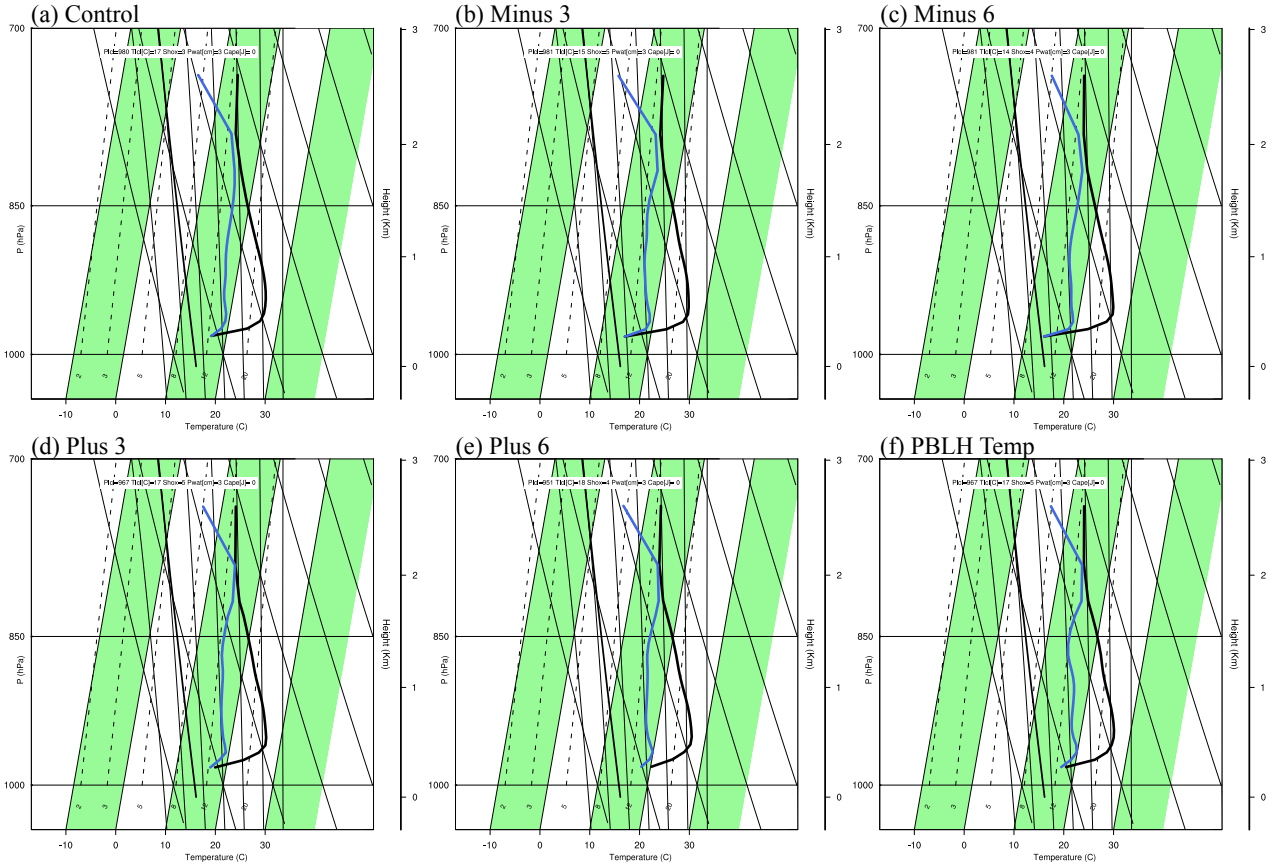

Figure 4.17. Same as Figure 4.16, but at 02 UTC on July 3, 2012.

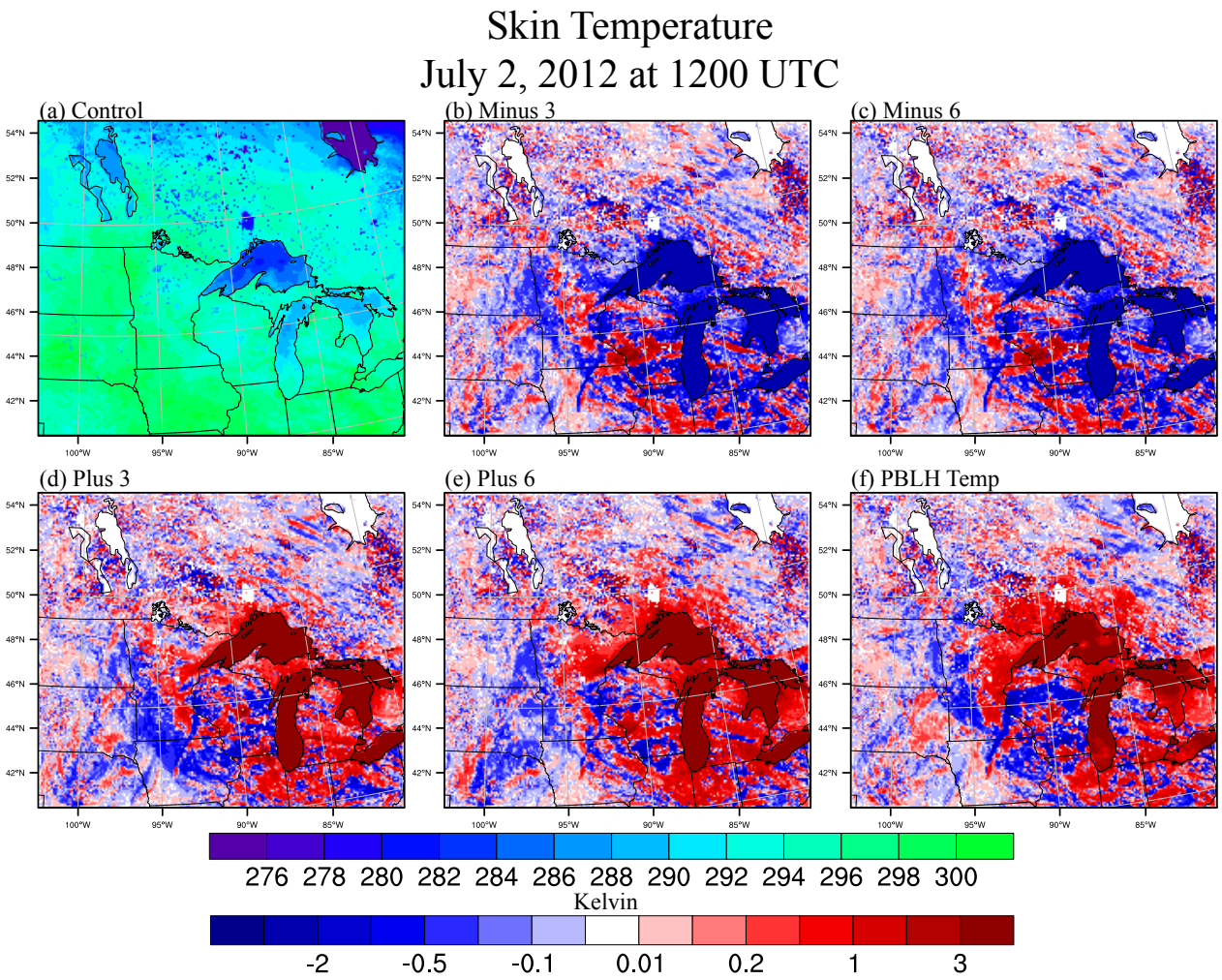

Figure 4.18. Skin temperature (Kelvin) for (a) Control and difference from Control for (b) Minus 3, (c) Minus 6, (d) Plus 3, (e) Plus 6, and (f) PBLH Temp on July 2, 2012 at 12 UTC.

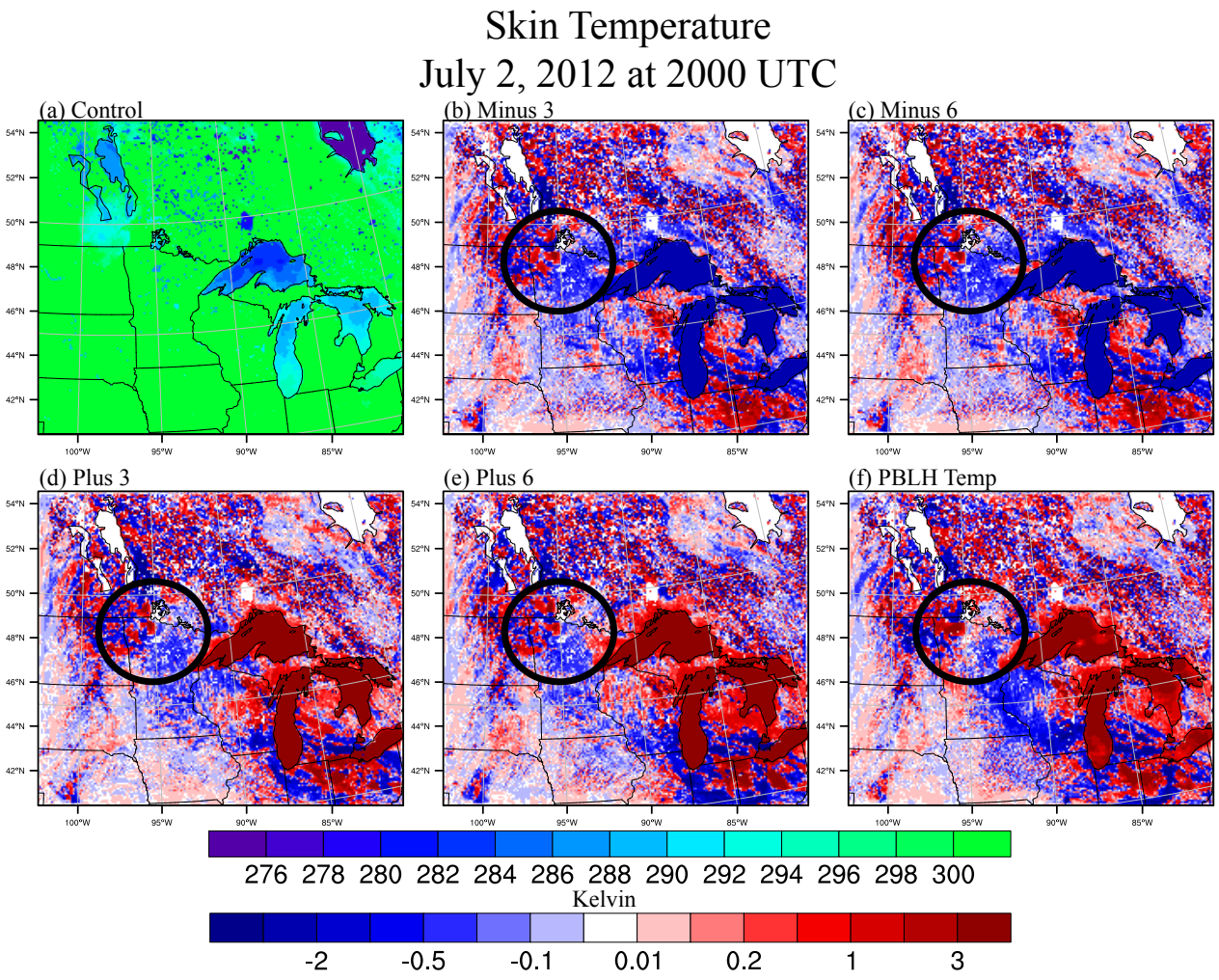

Figure 4.19. Same as Figure 4.18, except on July 2, 2012 at 20 UTC.

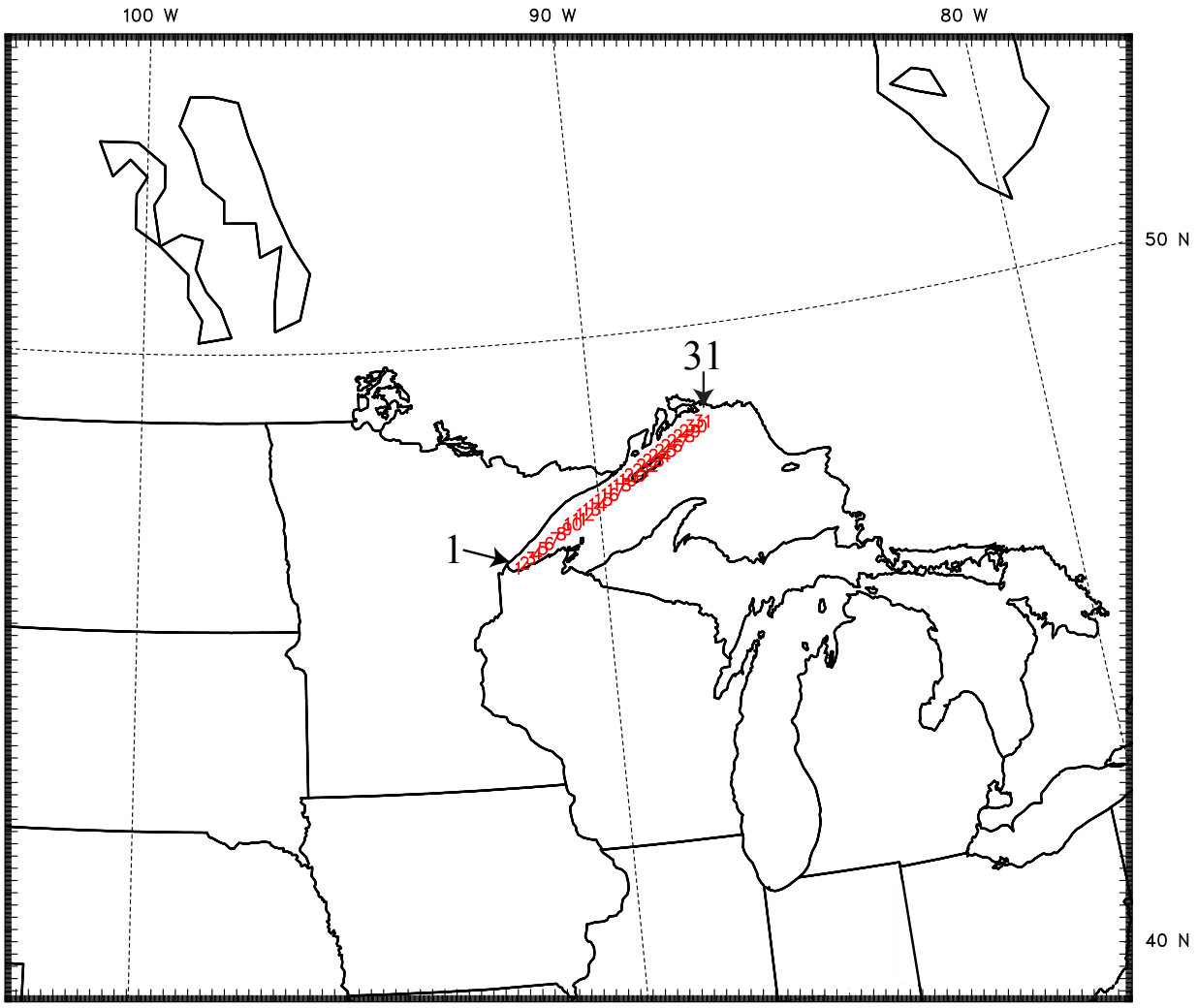

Figure 4.20. Position of parcels released at 03 UTC on July 3, 2012 used for parcel trajectory calculations.

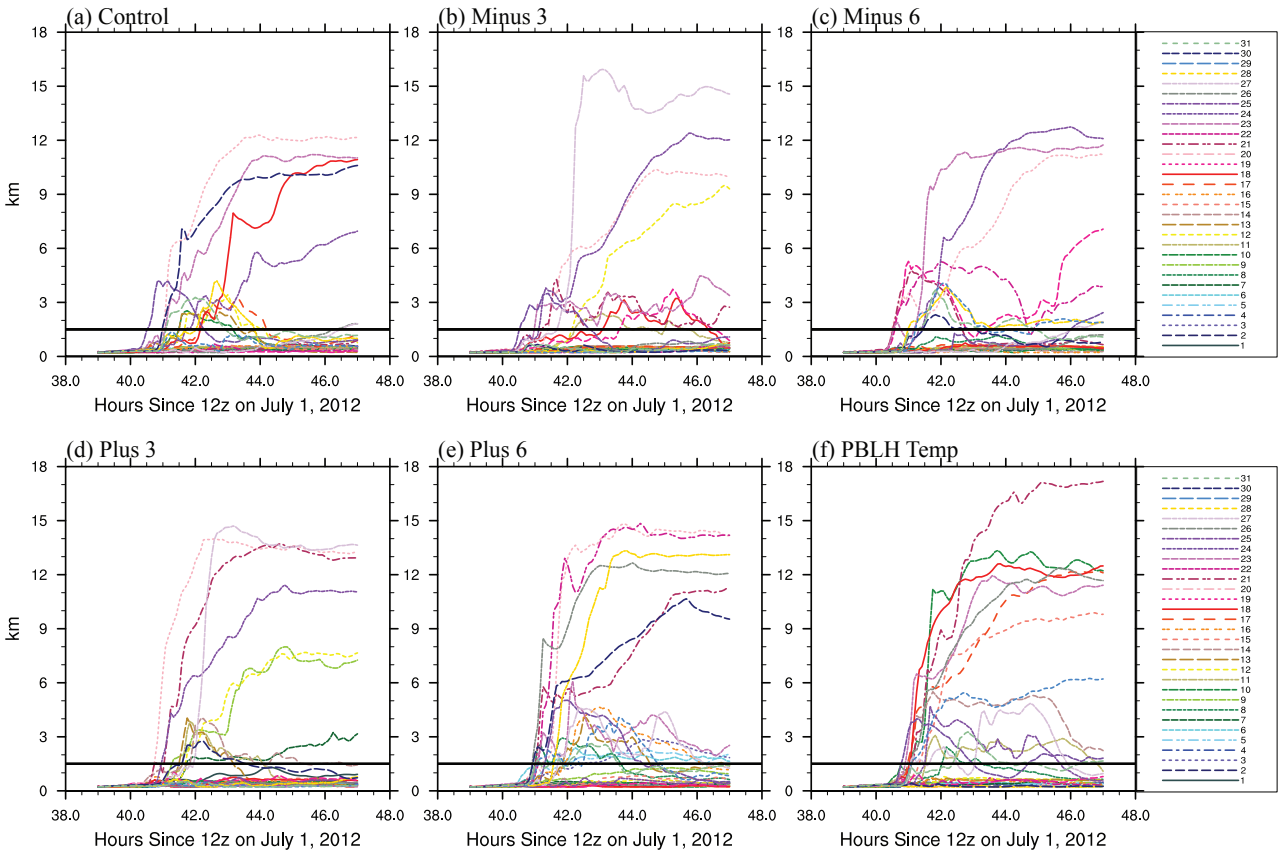

Figure 4.21. Height of the parcels (km) over time for (a) Control, (b) Minus 3, (c) Minus 6, (d) Plus 3, (e) Plus 6, and (f) PBLH Temp. Parcels are released at hour 39 (July 3 at 03 UTC) and positions are calculated until hour 47 (July 3 at 11 UTC).

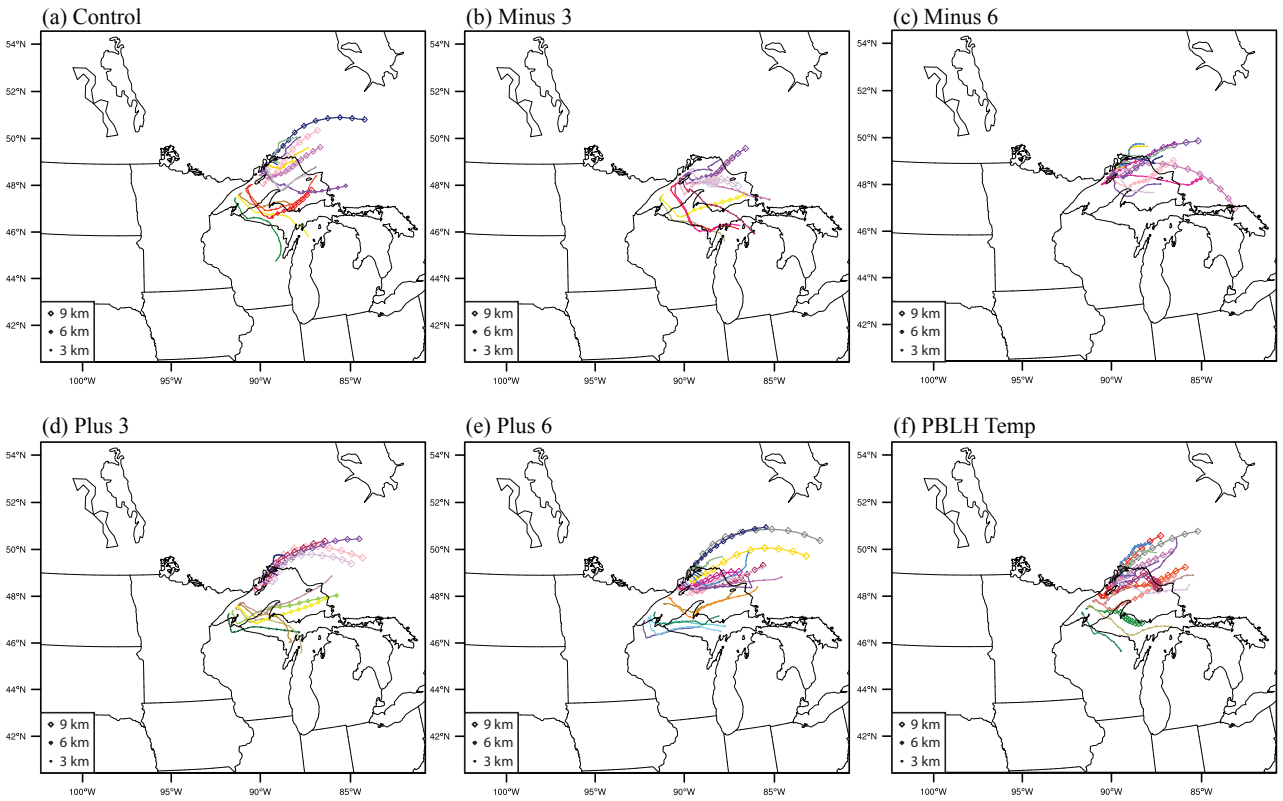

Figure 4.22. Location of parcels from July 3 at 03 UTC to 11 UTC for (a) Control, (b) Minus 3, (c) Minus 6, (d) Plus 3, (e) Plus 6, and (f) PBLH Temp. Only parcels that reach at least 1.5 km during the calculation are plotted. The size of the symbol along the path is proportional to the elevation.

CHAPTER 5. CONCLUSIONS

The attribution of weather events to changes in climate has been predominantly a statistical representation to this point. While these analyses are beneficial in illuminating the dominant forcing responsible for the change in a weather event, it does not bring to light the physical changes that a system undergoes in the future climate environment and the sensitivity of the storm system to the ingredients. By understanding the sensitivity of a storm system to different components, an understanding of the dynamics and feedbacks in the atmosphere leading to the system can be garnered. This knowledge does not only have applications to the research community, but also weather forecasters and community planners to be able to forecast and plan for extreme events.

Through studying the Great Lakes region, where lake temperatures are currently and expected to warm in the future (Austin and Colman 2007, Trumpickas et al. 2009), the changes in lake temperature and how those are communicated to atmospheric circulations and changes in precipitation have been explored.

5.1 Chapter Summaries

In Chapter 2, the role of the lake surface temperature and lake ice in winter season lake-effect snowfall was quantified. It is found that the lake ice has a critical role in generating convergence zones over ice-free portions of the lake, controlling the distribution of snowfall along the shoreline downwind of the lake. The most intense snowfall was distributed further downwind when lake temperature is increased, increasing the overall amount of accumulation. It was also reiterated from previous

studies that the complex interactions with topography downwind of the lakes have a significant influence on the placement and intensity.

In Chapter 3, a springtime case study of convective initiation parallel to Lake Michigan, which visually had similar characteristics to a lake breeze, was associated with the passing of an upper level PV feature. Through removing the lake surface, the convection still initiated over the former lake surface, showing that the lake is not the primary source for convective initiation but can influence the placement of convection. Changing the lake surface temperature did not significantly change the placement or timing of the convection, but did have a role in modifying the intensity in certain areas.

Chapter 4 explored a MCS passing over Lake Superior and the influence of the lake temperature on the system. Through a series of both positive and negative lake temperature alterations, it was found that in most cases the overall accumulated rainfall increased. This increase was due to varying degrees of mechanical forcing created by the barrier jet along the northern shore of Lake Superior and changes in the thermodynamics of the near-surface air. The structure of the storm as it passed over the lake was subject to alterations due to change in the environment ahead of the MCS and around the lake.

5.2 General Conclusions

Through the simulations, it is found that the warm season influence of the lake might be minimal compared to the influence from cold season. In the cases presented here in Chapters 3 and 4, these warm season cases shows little influence in terms of placement and precipitation intensity with changes in lake temperature. In both cases, the larger scale environment appears to play a larger influence on the system than the lakes. In the wintertime (Chapter 2), the lakes do have a significant influence on the systems,

especially when the lake surface properties are changed. A large reason for this is that in the winter, the lake is a primary driver of lake-effect snow. Without the lake, the snowfall would not exist, as is seen when the lake is covered with ice. In the summer months, the synoptic scale influences are the primary drivers, with minor adjustments made by the lake environment.

Kristovich (2009), when explaining an overview of climate sensitivities in the Great Lakes, made the claim that the signal from the lakes in the cold season is much stronger than the warm season for weather events, but warm season case studies were not as well investigated as cold season. Bryan et al. (2015) concluded that the local feedback between the lakes and atmosphere are important for the local hydroclimate. From this study, it is found that on weather time scales during the warm season, the lakes have little influence on the direction creation of precipitation for the events studied. This does not mean that these changes could not have a larger influence on climate timescales, where a consistent increase in rainfall from single events could lead to changes in the local climate.

The events presented in this dissertation are still single weather events; so applying the conclusions made from each study to climate timescales would exceed the scope of the data. These results do hint at the potential influence from the lakes to create more intense precipitation events during the cold season, while controlling the distribution of precipitation in the warm season. Resolving these features may be important to improving climate simulations across the region. The results also allow establish a baseline and framework to test future events in order to explore the direct role the lakes have in a particular event. It should be noted that the sensitivity of these systems to

changes in initial atmospheric conditions was not tested, so the strength and robustness of these studies are not fully realized at this time.

5.3 Future Work

Further simulations into similar events as the ones presented in this dissertation are needed to gain a complete view of the overall role of the lake and to test the repeatability of the variations found in the distribution of precipitation and changes in dynamical circulations. These simulations could help to solidify the conclusions drawn and give a better understanding of projected precipitation changes over the region in a future climate.

While the studies presented cover a wide variety of weather types in the Great Lakes, there are still several weather features that need to be studied to understand their sensitivity to lake temperature. One of the most important systems left untested is the passing of an extratropical cyclone during the winter and the role of the lake temperature has on the dynamics of the system. While studies have looked at the aggregate influence of the lake surface on the passing of these systems in the Great Lakes region (Sousounis and Fritsch 1994), they have not looked at the direct role the lake temperature has on them. Future simulations with altered lake surface temperature could help to illuminate the role of the lake on enhancing precipitating structures within the system.

Future studies are also needed to create climatologies of several features in the region. First, more exploration is needed to show the frequency of storms initiated off of Lake Michigan due to lake breezes and those due to PV passing over the lake. This could aid forecasters in the region identify key characteristics to identifying when and where the convection may take place off of the lake. Second, a climatology of the barrier jet over

Lake Superior is needed to determine the influence of this feature has to the west of Lake Superior and the role it plays in distribution of rainfall and temperatures over this region.

APPENDICES

APPENDIX A. LAKE TEMPERATURE MODIFICATION

To modify the lake surface temperature, the initial conditions are first generated for the case study through the WRF Preprocessor System (WPS). The program creates the initial model grid configuration and land surface characteristics to be used by WRF. It then horizontally interpolates the initial atmospheric conditions onto this grid without any vertical interpolation. Vertical interpolation is handled in the "real.exe" program within the WRF system.

The NetCDF files generated by the completion of the WPS program are then modified to adjust the lake surface temperature. First, a region defined by latitude and longitude is created over the entire Great Lakes region (Chapters 2 and 3) or specific lakes (Chapter 4). Next, the land mask generated by WPS is used to find the Cartesian coordinates of all water points located within the selected region. If the conditions are met that a specific grid point is located in the region and is a water point, then the skin temperature of this point is adjusted. If not, then no modifications are made to the skin temperature at this location. The new skin temperature field replaces the field in the files generated from WPS. This new skin temperature is used to initialize the lake surface temperature in WRF.

It should be noted that this technique does modify all resolved water points within the specified region.

APPENDIX B. REMOVAL OF LAKE MICHIGAN

To remove Lake Michigan from the simulation the land surface created in the files created from the completion of the WRF Preprocessing System (WPS). A region was selected around Lake Michigan (41.586 to 46.124 degrees N, 88.07 to 84.7 degrees W) to remove the water grid points. The following fields were altered to create the new landmass:

1.) Soil moisture for the four soil layers was created for the new landmass using a three-grid spacing average of the values to the west of the selected region around the lake. For each y-value, the average of the three-grid spaces to the west of the region are applied to water points within the region. If the soil moisture fractional average was greater than a critical (0.4), this value was replaced by the previous row's average. This eliminated the influence from inland lakes to the west of the region, which has soil moisture percentages of 1.0, resulting in abnormally high averaged values.

2.) Soil temperature for the four soil layers was also initialized using a three-grid spacing average to the west of the latitude/longitude grid box for each row. The average temperature at each soil depth was compared to the previous rows value to eliminate discontinuities in the north-south direction. A critical difference of 1 Kelvin was used for the surface soil temperatures, .7 Kelvin for surface to 10 cm, .5 Kelvin for 10 to 40cm, 1 Kelvin for 40 to 100 cm, and 1 Kelvin for 100 to 200 cm.

3.) Other surface values were changed to the average value of the three grid points to the west of the latitude/longitude box around the lake. These included: albedo, greenness fraction, and canopy water.

4.) The following values were adjusted over the former lake surface to be representative of the region to the west of Lake Michigan: land mask, land use index, slope category, and soil type category.

Values were visually inspected to make sure that there were no discontinuities or erroneous values.

The western shore was chosen to represent the new landmass due to the strong west to east temperature gradient for this case. Values along the western shore were more representative of the background state of the atmosphere at this time, with warmer temperatures to the east of the lake.

APPENDIX C. CHANGE IN ETA LEVEL CREATION

A feature was discovered in the default vertical coordinate calculation of WRF v3.4.1 where the first six layers were predetermined to represent the full planetary boundary layer (PBL). This meant that the height of the first six levels would be constant, no matter the total number of vertical levels requested. The remaining requested levels were distributed above the PBL, with a tighter vertical spacing just above the top of the PBL. This code was modified to remove the specification and allow for a fraction of the total number of vertical levels requested to be explicitly set within the approximate PBL. The code did explicitly set three layers at the top of the PBL to gradually transition vertical grid spacing to coarser resolution in the free troposphere, which was found to aid in a smoother transition in the vertical grid spacing near the top of the PBL compared to when it was not used.

Eta level calculations began with a base of 19 interface levels (Z_w) between 1 (surface) and 0 (top of modeled atmosphere). Initial mass coordinates (Z_u) are then created exactly half way between adjacent interface levels. The following equation was used to create the initial temperature profile:

$$T_h = \max\left(210, T_0 + 50 \ln\left(\frac{p_h}{p_0}\right)\right) \quad \text{(C.1)}$$

Where T_0 is the base temperature (290 Kelvin), p_h is the pressure at the current height, and p_0 is the surface pressure. Equation C.1 uses the maximum value between the calculated temperature and 210 as an error check to keep temperatures from falling too low.

This background temperature profile is used to calculate the potential temperature and in turn the density at each mass coordinate. The density is then used to populate the grid with more than the original 19 vertical coordinates.

$$Z_{w,k+1} = Z_{w,k} - \frac{g\Delta z}{100 * \rho_k(p_0 - p_{top})} \quad \text{(C.2)}$$

In Equation C.2, g is the gravitational acceleration, Δz is the overall change in height per level, ρ_k is the density at level k, and p_{top} is the atmospheric pressure for the top of the model domain. Equation C.3 was altered to allow for the inclusion of a fraction of the total number of vertical levels (n) to be within be within the PBL, where n_{PBL} is the number of levels within the PBL.

$$\Delta z = \begin{cases} \frac{Z_{top} - Z_{PBL}}{n - n_{PBL}} & for\ z > Z_{PBL} \\ \frac{Z_{PBL}}{n_{PBL}} & for\ z \leq Z_{PBL} \end{cases} \quad \text{(C.3)}$$

The first n_{PBL} levels were calculated using Equation C.2. The next n-n_{PBL}-3 levels were also calculated using the same method. The final three levels were added above the PBL using a series of weighted values from previously calculated levels (Equations C.4-C.6).

$$Z_{w,n_{PBL}+1} = .75 * Z_{w,n_{PBL}} + .25 * Z_{w,n_{PBL}+4} \quad \text{(C.4)}$$

$$Z_{w,n_{PBL}+2} = .50 * Z_{w,n_{PBL}} + .50 * Z_{w,n_{PBL}+4} \quad \text{(C.5)}$$

$$Z_{w,n_{PBL}+3} = .25 * Z_{w,n_{PBL}} + .75 * Z_{w,n_{PBL}+4} \quad \text{(C.6)}$$

APPENDIX D. WRF PHYSICS TESTING

With the number of physics schemes available in the model setup, both literature reviews and sensitivity studies were conducted for the control simulation of each case study. The following sections are divided into cold and warm season testing due to the differences in the processes associated with each season.

D.1. Cold Season

For the simulations attempted in Chapter 2, a literature review was conducted to evaluate the schemes used by previous modeling efforts. LaPlante and Leins (2008) and Shi et al. (2010) used WRF to simulate convection over Lake Erie using the Thompson microphysics scheme and the Mellor-Yamada-Janjic planetary boundary layer scheme. The authors found this configuration to produce drier and more realistic results.

D.2. Warm Season

For the May 2003 case study (Chapter 3), the microphysics and planetary boundary layer schemes were tested on a 25km grid. The Morrison and WSM6 microphysics schemes were tested against the Mellor-Yamada-Janjic and ACM2 planetary boundary layer scheme. It was found that the use of Morrison microphysics and Mellor-Yamada-Janjic produced better timing and placement of the larger system on the coarser grid. The YSU scheme was used for the higher-resolution domains due to the nonlocal closure within the scheme, which is advocated for this resolution (Ching et al. 2014, Cohen et al. 2015).

Testing of the WRF 4-D Data Assimilation (FDDA) was attempted for the 10km domain of the May 2003 case study. Analysis nudging was used with the NARR data above approximately 700mb, allowing for features in the PBL to evolve naturally. Nudging was attempted every 3 and 6 hours, with minimal differences in the large-scale flow between the two simulations and the control simulation.

400m horizontal grid spacing was also attempted for the May 2003 case. The model physics were identical to the 2km domain, with changes to the dynamical core options. The diffusion option, "diff_opt", was changed to full diffusion (diff_opt = 2). 3d TKE was also used (km_opt = 2). This option goes against recommendations of the WRF documentation, since a PBL scheme was still being used to handle vertical turbulent flows, but was recommended to use from the WRF developers (H. Morrison, personal communication, Oct. 15, 2013). This domain setup was abandoned due to the high cost of running the simulations and the lack of new information about the system it appeared to provide compared to the 2km domain.

For the July 2012 case study (Chapter 4), the physics options from the previous case study were used, with a change in the cumulus scheme on the 10km domain. Changes in initialization time was compared between 12 UTC on July 1st and 00 UTC on July 2nd. Initialization on July 1st at 12 UTC was found to improve the time the storm first reached the shore while keeping the intensity closer to radar observations while over the lake.

REFERENCES

American Meteorological Society, cited 2016: Climate. Glossary of Meteorology. [Available online at http://glossary.ametsoc.org/wiki/Climate].

American Meteorological Society, cited 2016: Weather. Glossary of Meteorology. [Available online at http://glossary.ametsoc.org/wiki/Weather].

Angel, J. R., and S. A. Isard, 1997: An Observational Study of the Influence of the Great Lakes on the Speed and Intensity of Passing Cyclones. *Mon. Wea. Rev.*, **125**, 2228-2237.

Arritt, R. W., 1987: The Effect of Water Surface Temperature on Lake Breezes and Thermal Internal Boundary Layer. *Boundary-Layer Meteor.,* **40**, 101-125.

Assel, R., K. Cronk, and D. Norton, 2003: Recent Trends in Laurentian Great Lakes Ice Cover. *Climatic Change,* **57**, 185-204.

Assel, R. A., 2005: Classification of Annual Great Lakes Ice Cycles: Winters of 1973-2002. *J. Climate*, **18**, 4895-4905.

Austin, J. A., and S. M. Colman, 2007: Lake Superior Summer Water Temperatures are Increasing More Rapidly than Regional Air Temperatures: A Positive Ice-Albedo Feedback. *Geophys. Res. Lett.,* **34,** L06604..

Ballentine, R. J., A. J. Stamm, E. F. Chermack, G. P. Byrd, and D. Schleede, 1998: Mescoscale Model Simulation of the 4-5 January 1995 Lake-Effect Snowstorm. *Wea. Forecasting*, **13**, 893-920.

Bard, L., and D. A. R. Kristovich, 2012: Trend Reversal in Lake Michigan Contribution to Snowfall. *J. Applied Meteor.,* **51**, 2038-2046.

Barrett, B. S., R. D. Garreaud, and M. Falvey, 2009: Effect of Andes Cordillera on Precipitation from a Midlatitude Cold Front. *Mon. Wea. Rev.*, **137**, 3092-3109.

Biggs, G. W., and M. E. Graves, 1962: A Lake Breeze Index. *J. Applied Meteor.,* **1**, 474-480.

Blake, E. S., T. B. Kimberlain, R. J. Berg, J. P. Cangialosi, J. L. Bevenn II, 2013: Tropical Cyclone Report: Hurricane Sandy (AL182012), 157 pp. Accessed 5 May 2016. [Available online at http://www.nhc.noaa.gov/data/tcr/AL182012_Sandy.pdf]

Brook, J. R., P. A. Makar, D. M. L. Sills, K. L. Hayden, R. McLaren, 2013: Exploring the Nature of Air Quality over Southwestern Ontario: Main Findings from the Border Air Quality and Meteorology Study. *Atmos. Chem. Phys.*, **13**, 10461-10482.

Bryan, A. M., A. L. Steiner, and D. J. Posselt, 2015: Regional Modeling of Surface-Atmosphere Interactions and their Impacts on Great Lakes Hydroclimate. *J. Geophys. Res. Atmos.*, **120**, 1044-1064.

Burnett, A. W., M. E. Kirby, H. T. Mullins, and W. P. Patterson, 2003: Increasing Great Lake-Effect Snowfall during the Twentieth Century: A Regional Response to Global Warming? *J. Climate*, **16**, 3535-3543.

Chandik, J. F., and W. A. Lyons, 1971: Thunderstorms and the Lake Breeze Front. *Preprints 7th Conf. Severe Local Storms*, Kansas City, MO, Amer. Meteor. Soc., 218-225.

Ching, J., R. Rotunno, M. LeMone, A. Martilli, B. Kosovic, P. A. Jimenez, 2014: Convectively Induced Secondary Circulations in Fine-Grid Mesoscale Numerical Weather Prediction Models. *Mon. Wea. Rev.*, **142**, 3284-3302.

Christidis N, P. A. Stott, A. Scaife, A. Arribas, G. S. Jones, D. Copsey, J. R. Knight, and W. J. Tennant, 2013: A New HadGEM3-A Based System for Attribution of Weather and Climate-Related Extreme Events. *J. Climate*, **26**, 2756– 2783.

Cordeira, J. M., and N. F. Laird, 2008: The Influence of Ice Cover on Two Lake-Effect Snow Events over Lake Erie. *Mon. Wea. Rev.*, **139,** 2747-2763.

Cotton, W. R., G. D. Alexander, R. Hertenstein, R. L. Walko, R. L. McAnelly, and M. Nicholls, 1995: Cloud venting – A review and some new global annual estimates. *Earth-Sci. Rev.*, **39**, 169-206.

Cohen, A. E., S. M. Cavallo, M. C. Coniglio, H. E. Brooks, 2015: A Review of Planetary Boundary Layer Parameterization Schemes and Their Sensitivity in Simulating Southeastern U.S. Cold Season Severe Weather Environments. *Wea. Forecasting,* **30**, 591-612.

Crosman, E. T., and J. D. Horel, 2012: Idealized Large-Eddy Simulations of Sea and Lake Breezes: Sensitivity to Lake Diameter, Heat Flux and Stability. *Boundary-Layer Meteor.*, **144**, 309-328.

Desai, A. R., J. A. Austin, V. Bennington, and G. A. McKinley, 2009: Stronger Winds over a Large Lake in Response to Weakening Air-to-Lake Temperature Gradient. *Nature Geosci.*, **2**, 855-858.

Durran, D. R., 2000: Comments on "The Differentiation Between Grid Spacing and Resolution and their Application to Numerical Modeling." *Bull. Amer. Meteor. Soc.*, **81**, 2478.

Eichenlaub, V. L., 1970: Lake effect Snowfall to the Lee of the Great Lakes: Its Role in Michigan. *Bull. Amer. Meteor. Soc.*, **51**, 403-412.

Eichenlaub, V. L., 1979: Weather and Climate of the Great Lakes Region. University of Notre Dame Press, 335 pp.

Francis, J. A., and S. J. Vavrus, 2015: Evience for a Wavier Jet Stream in Response to Rapid Arctic Warming. *Environ. Res. Lett.*, **10**, 014005.

Gallus Jr., W. A., and M. Segal, 1999: Cold Front Acceleration over Lake Michigan. *Wea. Forecasting*, **14**, 771-781.

Gerbush, M. R., D. A. R. Kristovich, and N. F. Laird, 2008: Mesoscale Boundary Layer and Heat Flux Variations over Pack Ice-Covered Lake Erie. *J. App. Meteor. Climatol.,* **47**, 668-683.

Graham, R., M. Bentley, J. Sparks, B. Dukesherer, and J. Evans, 2003: Lower Michigan MCS Climatology: Trends, Pattern Types, and Marine Layer Impacts. *Preprints 22nd Conference on Severe Local Storms*, Hyannis, MA, Amer. Meteor. Soc.

Grasso, L. D., 2000: The Differentiation Between Grid Spacing and Resolution and their Application to Numerical Modeling. *Bull. Amer. Meteor. Soc.*, **81**, 579–580.

Grover, E. K., and P. J. Sousounis, 2002: The Influence of Large-Scale Flow on Fall Precipitation Systems in the Great Lakes Basin. *J. Climate*, **15**, 1943-1956.

Gula, J., and W. R. Peltier, 2012: Dynamical Downscaling over the Great Lakes Basin of North American Using the WRF Regional Climate Model: The Impact of the Great Lakes System on Regional Greenhouse Warming. *J. Climate*, **25**, 7723-7743.

Hannart, A., J. Pearl, F. E. L. Otto, P. Naveau, and M. Ghil, 2016: Causal Counterfactual Theory for the Attribution of Weather and Climate Related Events. *Bull. Amer. Meteor. Soc.*, **97**, 99-110.

Hjelmfelt, M. R., and R. R. Braham, 1983: Numerical Simulation of the Airflow over Lake Michigan for a Major Lake-Effect Snow Event. *Mon. Wea. Rev.*, **111**, 205-219.

Hjelmhelt, M. R., 1992: Orographic Effects in Simulated Lake-Effect Snowstorms over Lake Michigan. *Mon. Wea. Rev.*, **120**, 373-377.

Holroyd, E. W., 1971: Lake-effect cloud bands as seen from weather satellites. *J. Atmos. Sci.*, **28**, 1165-1170.

Hong, S.-Y., Y. Noh, and J. Dudhia, 2006: A New Vertical Diffusion Package with an Explicit Treatment of Entrainment Processes. *Mon. Wea. Rev.*, **134**, 2318-2341.

Houze, R. A., Jr., 2004: Mesoscale Convective Systems. *Rev. Geophys.,* **42**, RG4003.

James, R. P., P. M. Markowski, and J. M. Fritsch, 2006: Bow Echo Sensitivity to Ambient Moisture and Cold Pool Strength. *Mon. Wea. Rev.*, **134**, 950-964.

Johns, R. H., and W. D. Hirt, 1987: Derechos: Widespread Convectively Induced Windstorms. *Wea. Forecasting*, **2**, 32-49.

Keen, C.S., and W.A. Lyons, 1978: Lake/land Brreze Circulations on the Western Shore of Lake Michigan. *J. Appl. Meteor.*, **17**, 1843-1855.

Kelly, R. D., 1986: Mesoscale frequencies and seasonal snowfalls for different types of Lake Michigan snow storms. *J. Appl. Meteor.*, **25**, 308-312.

Kershner, K., 2012: "Did Global Warming cause Hurricane Sandy?" Accessed 5 May 2016 [Available online at http://science.howstuffworks.com/nature/natural-disasters/global-warming-cause-hurricane-sandy.htm].

King, P.W.S, M. J. Leduc, D. M. L. Sills, N. R. Donaldson, D. R. Hudak, P. Joe, and B. P. Murphy, 2003: Lake Breezes in Southern Ontario and Their Relation to Tornado Climatology. *Wea. Forecasting*, **18**, 795-807.

Kristovich, D. A. R., 2009: *Climate Sensitivity of Great Lakes-Generated Weather Systems*. In *Climatology, Variability, and Change in the Midwest*, S. C. Pryor, Editor. Indiana University Press, 236-246.

Kristovich, D. A. R., and N. F. Laird, 1998: Observations of widespread lake-effect cloudiness: Influences of LST and upwind conditions. *Wea. Forecasting*, **13**, 811-821.

Kristovich, D. A. R., N. F. Laird, M. R. Hjelmfelt, R. G. Derickson, and K. A. Cooper, 1999: Transitions in boundary layer meso-γ convective structures: An observational case study. *Mon. Wea. Rev.*, **127**, 2895-2909.

Kristovich, D. A. R., N. F. Laird, and M. R. Hjelmfelt, 2003a: Convection evolution across Lake Michigan during a widespread lake-effect snow event. *Mon. Wea. Rev.*, **131**, 643-655.

Kristovich, D. A. R., R. E. LaPlante, N. F. Laird, and W. Kubina, 2003b: Are Thunderstorms that Form Along Lake Breezes More Intense? *Reprint 2003 Midwest Regional Conference on Extreme and Hazardous Weather*, Champaign, IL, Amer. Meteor. Soc.

Kunkel, K. E., N. E. Westcott, and D. A. R. Kristovich, 2002: Assessment of Potential Effects of Climate Change on Heavy Lake-Effect Snowstorms near Lake Erie. *J. Great Lakes Res.*, **28**, 521-536.

Kunkel, K. E., L. Ensor, M. Palecki, D. Easterling, D. Robinson, K. G. Hubbard, and K. Redmond, 2009: A New Look at Lake-Effect Snowfall Trends in the Laurentian

Great Lakes using a Temporally Homogeneous Data Set. *J. Great Lakes Res.*, **35**, 23-29.

Laird, N. F., 1999: Observation of Coexisting Mesoscale Lake-Effect Vortices over the Western Great Lakes. *Mon. Wea. Rev.*, **127**, 1137-1141.

Laird, N. F., D. A. R. Kristovich, X. Liang, R. W. Arritt, K. Labas, 2001: Lake Michigan Lake Breezes: Climatology, Local Forcing, and Synoptic Environment. *J. Applied Meteor.,* **40**, 409-424.

Laird, N. F., D. A. R. Kristovich, and J. E. Walsh, 2003a: Idealized Model Simulations Examining the Mesoscale Structure of Winter Lake-Effect Circulations. *Mon. Wea. Rev.*, **131**, 206-221.

Laird, N. F., J. E. Walsh, and D. A. R. Kristovich, 2003b: Model Simulations Examining the Relationship of Lake-Effect Morphology to Lake Shape, Wind Direction, and Wind Speed. *Mon. Wea. Rev.,* **131**, 2102-2111.

Laird, N. F., and D. A. R. Kristovich, 2004: Comparison of Observations with Idealized Model Results for a Method to Resolve Winter Lake-Effect Mesoscale Morphology. *Mon. Wea. Rev.*, **132**, 1093-1103.

LaPlante, R., and D. Leins, 2008: Simulating LES with the WRF: Sensitivity to model configuration and Great Lakes water temperature. *Great Lakes Operational Meteorology Workshop 2008*, Ann Arbor, MI.

Liu, A. Q., G. W. K. Moore, K. Tsuboki, and I. A. Renfrew, 2004: A High-Resolution Simulation of Convective Roll Clouds during a Cold-Air Outbreak. *Geophys. Res. Lett.,* **31**.

Liu, A. Q., G. W. K. Moore, K. Tsuboki, and I. A. Renfrew, 2006: The Effect of the Sea-Ice Zone on the Development of Boundary-Layer Roll Clouds During Cold Air Outbreaks. *Boundary-Layer Meteor.*, **118**, 557-581.

Loescher, K. A., G. S. Young, B. A. Colle, and N. S. Winstead, 2006: Climatology of Barrier Jets along the Alaskan Coast. Part I: Spatial and Temporal Distributions. *Mon. Wea. Rev.*, **134**, 437-453.

Lofgren, B. M., 1997: Simulated Effects of Idealized Laurentian Great Lakes on Regional and Large-Scale Climate. *J. Climate*, **10**, 2847-2858.

Lyons, W. A., 1966: Some Effects of Lake Michigan Upon Squall Lines and Summertime Convection. *Great Lakes Res. Div.*, **15**, 259-273.

Lyons, W. A., 1972: The Climatology and Prediction of the Chicago Lake Breeze. *J. Applied Meteor..,* **11**, 1259-1270.

Lyons, W. A., and L. E. Olsson, 1972: Mesoscale Air Pollution Transport in the Chicago Lake Breeze. *J. Air Pollut. Control Assoc.,* **22**, 876-881.

Martin, J. E., 2006: Mid-Latitude Atmospheric Dynamics: A First Course. Hoboken, NJ, USA: Wiley. Accessed December 28, 2015. ProQuest ebrary. 281-282.

Mann, G. E., R. B. Wagenmaker, and P. J. Sousounis, 2002: The Influence of Multiple Lake Interactions upon Lake-Effect Storms. *Mon. Wea. Rev.*, **130**, 1510-1530.

Mesinger, F., and Coauthors, 2006: North American Regional Reanalysis. *Bull. Amer. Meteor. Soc.*, **87**, 343-360.

Metz, N. D., 2011: Persistence and Dissipation of Lake Michigan-Crossing Mesoscale Convective Systems. Thesis, Dept. of Atmospheric and Environmental Sciences, University of Albany, 260 pp.

Miller, S. T. K., B. D. Keim, R. W. Talbot, H. Mao, 2003: Sea Breeze: Structure, Forecasting, and Impacts. *Rev. Geophys.*, **41**, 3.

Moroz, W. J., and E. W. Hewson, 1966: The Mesoscale Interaction of a Lake Breeze and Low Level Outflow from a Thuderstorm. *J. Appl. Meteor.*, **5**, 148-155.

National Academies of Sciences, Engineering, and Medicine, 2016: *Attribution of Extreme Weather Events in the Context of Climate Change*. Washington, DC: The National Academies Press. 133 pp.

NOAA/Great Lakes Environmental Research Lab (GLERL), 1980: Great Lakes Shoreline Data. NOAA/GLERL. [Available online at http://www.glerl.noaa.gov/data/char/glshoreline.html]. Accessed July 2016.

NOAA/National Centers for Environmental Information, 1995: NEXRAD Data Archive. NOAA/National Centers for Environmental Information. [Available online at http://www.ncdc.noaa.gov/nexradinv]. Accessed June 2013.

NOAA/National Data Buoy Center (NDBC), 1981: Buoy Data Archive. NOAA/National Data Buoy Center. [Available online at http://www.ndbc.noaa.gov]. Accessed June 2013 and February 2016.

NOAA/National Ice Center, 1995: Great Lakes Ice Analysis Products. NOAA/National Ice Center. [Available online at http://www.natice.noaa.gov/products/great_lakes.html]. Accessed August 2011.

NOAA/Storm Prediction Center (SPC), 1999: Storm Reports Archive. NOAA/Storm Prediction Center. [Available online at http://www.spc.noaa.gov/archive]. Accessed March 2014 and July 2015.

Niziol, T. A., 1987: Operational Forecasting of Lake-Effect Snowfall in Western and Central New York. *Wea. Forecasting*, **2**, 310-321.

Niziol, T. A., W. R. Snyder, and J. S. Waldstreicher, 1995: Winter Weather Forecasting throughout the Eastern United States. Part IV: Lake Effect Snow. *Wea. Forecasting*, **10**, 61-77.

Notaro, M., A. Zarrin, S. Vavrus, and V. Bennington, 2013: Simulation of heavy lake-effect snowstorms across the Great Lakes basin by RegCM4: Synoptic climatology and variability. *Mon. Wea. Rev.*,**141**, 1990-2014.

Pall, P., T. Aina, D. A., Stone, P. A. Stott, T. Nozawa, A. G. J. Hilberts, D. Lohmann, and M. R. Allen, 2011: Anthropogenic Greenhouse Gas Contribution to Flood Risk in England and Wales in Autumn 2000. *Nature*, **470**, 382-385.

Parker, M. D., 2008: Response of Simulated Squall Lines to Low-Level Cooling. *J. Atmos. Sci.*, **65**, 1323-1341.

Reynolds, D. W., and A. S. Dennis, 1986: A Review of the Sierra Cooperative Pilot Project. *Bull. Amer. Meteor. Soc.*, **67**, 513-523.

Rodriguez, Y., D. A. R. Kristovich, and M. R. Hjelmfelt, 2007: Lake-to-Lake Cloud Bands: Frequencies and Locations. *Mon. Wea. Rev.*, **135**, 4202–4213.

Rotunno, R., J. B. Klemp, and M. L. Weisman, 1988: A Theory for Strong, Long-Lived Squall Lines. *J. Atmos. Sci.*, **45**, 463-485.

Rutledge, G. K., J. Alpert, and W. Ebuisaki, 2006: NOMADS: A Climate and Weather Model Archive at the National Oceanic and Atmospheric Administration. *Bull. Amer. Meteor. Soc.*, **87**, 327-341. Accessed January 2011, June 2013, and September 2015.

Ryznar, E., and J.S. Touma, 1981: Characteristics of True Lake Breezes Along the Eastern Shore of Lake Michigan. *Atmos. Environ.*, **15**, 1201-1205.

S.-Y. Hong, Y. Noh, and J. Dudhia, 2006: A New Vertical Diffusion Package with Explicit Treatment of Entrainment Processes. *Mon. Wea. Rev.*, **134**, 2318–2341.

Schoenberger, L. M., 1986: Mesoscale Features of the Michigan Land Breeze using PAM II Temperature Data. *Wea. Forecasting*, **1**, 127–135.

Schultz, D. M., 1999: Lake-Effect Snowstorms in Northern Utah and Western New York with and without Lightning. *Wea. Forecasting*, **14**, 1023–1031.

Scott, R. W., and F. A. Huff, 1996: Impacts of the Great Lakes on Regional Climate Conditions. *J. Great Lakes Res.,* **22**, 845-863.

Sepic, J., and A. B. Rabinovich, 2014: Meteotsunami in the Great Lakes and on the Atlantic Coast of the United States Generated by the ‘‘Derecho’’ of June 29–30, 2012. *Natural Hazards*, **74**, 74-107.

Shi, J. J., and Coauthors, 2010: WRF Simulations of the 20-22 January 2007 Snow events over Eastern Canada: Comparison with In Situ and Satellite Observations. *J. App. Meteor. Climatol.*, **49**, 2246-2266.

Skamarock, W. C., and Coauthors, 2008: A description of the Advanced Research WRF version 3. NCAR Tech. Note TN-475+STR, 113 pp. [Available online at http://www2.mmm.ucar.edu/wrf/users/docs/arw_v3.pdf]

Smith, B.B., 2001: Development of a Lake Breeze Forecast Methodology for Northern Michigan. *Nat. Wea. Digest,* **25**, 47-52.

Sousounis, P. J., and G. E. Mann, 2000: Lake-Aggregate Mesoscale Disturbances. Part V: Impacts on Lake-Effect Precipitation. *Mon. Wea. Rev.*, **128**, 728-745.

Sousounis, P. J., and J. M. Fritsch, 1994: Lake-Aggregate Mesoscale Disturbances. Part II: A Case Study of the Effects on Regional and Synoptic-Scale Weather Systems. *Bull. Amer. Meteor. Soc.*, **75**, 1793-1811.

Sousounis, P., and E. K. Grover, 2002: Potential Future Weather Patterns over the Great Lakes Region. *J. Great Lakes Res.*, **28**, 496-520.

Stoelinga, M. T., 2009: RIP version 4.5. National Center for Atmospheric Research.

Stott, P. A., N. Christidis, F. E. L. Otto, Y. Sun, J.-P. Vanderlinden, G. J. van Oldenborgh, R. Vautard, H. von Storch, P. Walton, P. Yiou, and F. W. Zwiers, 2015: Attribution of Extreme Weather and Climate-Related Events. *WIREs Climate Change*, **7**, 23-41.

Stull, R., 2015: Regional Winds. *Practical Meteorology: An Algebra-based Survey of Atmospheric Science*. Univ. of British Columbia. 645-686.

Szeto, K. K., and H.-R. Cho, 1994: A Numerical Investigation of Squall Lines. Part II: The Mechanics of Evolution. *J. Atmos. Sci.*, **51**, 425-433.

Theeuwes, N. E., G. J. Steeneveld, F. Krikken, and A. A. M. Holtslag, 2010: Mesoscale Modeling of Lake-Effect Snow over Lake Erie – Sensitivity to Convection, Microphysics and Lake Water Temperature. *Adv. Sci. Res.*, **4**, 15-22.

Trenberth, K. E., 2012: Framing the way to Relate Climate Extremes to Climate Change. *Climatic Change*, **115**, 283-290.

Trumpickas, J., B. J. Shuter, C. K. Minns, 2009: Forecasting Impacts of Climate Change on Great Lakes Surface Water Temperatures. *J. Great Lakes Res.*, **35,** 454-463.

US Environmental Protection Agency, and Government of Canada, 1995: The Great Lakes: An Environmental Atlas and Resource Book. Great Lakes National Program Office: US Environmental Protection Agency, 51 pp.

Vavrus, S., J. E. Walsh, W. L. Chapman, and D. Portis, 2006: The Behavior of Extreme Cold Air Outbreaks Under Greenhouse Warming. *Int. J. Climatol.*, **26**, 1133-1147.

Vavrus, S., M. Notaro, and A. Zarrin, 2013: The Role of Ice Cover in Heavy Lake-Effect Snowstorms over the Great Lakes Basin as Simulated by RegCM4. *Mon. Wea. Rev.*, **141**, 148-165.

Vogel, C., J. D. Epstein, T.J. Pignataro, 2014: "Toughing it out as concerns shift." *The Buffalo News* 23 Nov. 2014. Accessed 5 May 2016. [Available online at http://www.buffalonews.com/city-region/winter/toughing-it-out-as-concerns-shift-20141123].

Walsh, J.E., A. S. Phillips, D. H. Portis, and W. L. Chapman, 2001: Extreme Cold Outbreaks in the United States and Europe, 1948-99. *J. of Climate*, **14**, 2642-2658.

Wiggin, B. L., 1950: Great snows of the Great Lakes. *Weatherwise*, **3**, 123-126.

Wilson, P. H., 2008: Warm-Season Lake-/Sea-Breeze Severe Weather in the Northeast. Thesis, Dept. of Earth and Atmospheric Sciences, University of Albany, 128 pp.

Workoff, T. E., D. A. R. Kristovich, N. F. Laird, R. LaPlante, D. Leins, 2012: Influence of the Lake Erie Overlake Boundary Layer on Deep Convective Storm Evolution. *Wea. Forecasting,* **27**, 1279-1289.

Wright, D. M., D. J. Posselt, and A. L. Steiner, 2013: Sensitivity of Lake-Effect Snowfall to Lake Ice Cover and Temperature in the Great Lakes Region. *Mon. Wea. Rev.*, **141**, 670-689. ©American Meteorological Society. Used with permission.

Wright, D. M., 2015: "Was this storm caused by climate change?" How the Great Lakes can help to connect climate change with daily weather events. *Down to Earth, Physics Today*. [Available online at http://scitation.aip.org/content/aip/magazine/physicstoday/news/10.1063/PT.5.4017]

Zhao, L., S.-Y. Wang, J. Jin, and A. J. Clarke, 2015: Weather Research and Forecasting Model Simulations of a Rare Springtime Bow Echo near the Great Salt Lake, USA. *Meteor. Appl.*, **22**, 301-313.

Zremski, J., 2014: "Winter Weather Weirdness May Be Just Beginning." *The Buffalo News* 22 Nov. 2014. Accessed 5 May 2016. [Available online at http://www.buffalonews.com/city-region/weather/winter-weather-weirdness-may-be-just-beginning-20141122].

Zulauf, M. A., and S. K. Krueger, 2003: Two-dimensional Cloud-Resolving Modeling of the Atmospheric Effects of Arctic Leads Based upon Midwinter Conditions at the Surface Heat Budget of the Arctic Ocean Ice Camp. *J. Geophys. Res.*, **108**, 4312.